AN EXPERIMENTAL STUDY WITH SIMPLE

INSTRUMENTATION FOR LARGE FIRES

By

MICHAEL HOLT NASH
//

Bachelor of Science

Oklahoma State University

Stillwater, Oklahoma

1970

Submitted to the Faculty of the
Graduate College of the
Oklahoma State University
in partial fulfillment of
the requirements for
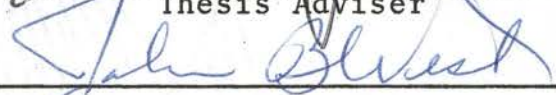the Degree of
MASTER OF SCIENCE
July, 1972

AN EXPERIMENTAL STUDY WITH SIMPLE

INSTRUMENTATION FOR LARGE FIRES

Thesis Approved:

_____
Thesis Adviser

_____

_____
Dean of the Graduate College

837075

ii

ACKNOWLEDGMENT

TABLE OF CONTENTS

LIST OF TABLES

LIST OF FIGURES

vii

NOMENCLATURE

A	area, ft^2
C	composition
Cp	specific heat, $BTU/lb_m ft$
E	activation energy, cal/gm mole
f	function
H	height, ft
h	heat transfer coefficient, $BTU/ft^2 hr\,^{\circ}F$
K	temperature dependent term
k_o	frequency factor
1	length of rod, ft
M	mass, lb_m
M_b	mass of liquid evaporated during test, lb_m
M_i	initial mass, lb_m
Q	rate of heat gain from the surroundings, BTU/hr
Q_e	heat of evaporation, BTU
Q_t	total heat flow, BTU
Q_v	heat flow due only to the unconfined fire, BTU
Q_1, Q_2, Q_3	heat flow defined in equation 17, BTU
q	heat flow per unit area, BTU/ft^2
R	radius, ft

T	temperature, $^{\circ}F$
T_b	liquid boiling point, $^{\circ}F$
T_f	melting temperature, $^{\circ}F$
T_i	initial temperature, $^{\circ}F$
T_o	average oven temperature, $^{\circ}F$
T_p	uniform temperature of the plate, $^{\circ}F$
T_∞	temperature at an infinite distance, $^{\circ}F$
t	thickness, ft
V	total volume, ft^3
V_i	initial volume, ft^3
V_1	volume of liquid vaporized, ft^3
W_m	weight of the metal container, lb
x,y	dimensions of the plate surface, ft
z	plate thickness, ft

Greek Symbols

η_a	heat absorption efficiency defined by equation 4
η_v	vaporization efficiency defined by equation 2
θ	time, min
λ_b	latent heat of vaporization, BTU/lb_m
λ_f	latent heat of fusion, BTU/lb_m
ρ	density, lb_m/ft^3

Subscripts

a	average
h	quartz heating lamp
i	inside
1	liquid
m	metal
o	outside
s	surroundings

Miscellaneous

d	differential operator
Δ	increment, interval spacing

CHAPTER I

INTRODUCTION

Unconfined fires are notably difficult to instrument
for temperature and heat flux measurements. Sensors must
be durable in the hot environment, and recorders or tele-
metering equipment also must be well protected or located
at a safe distance from the fires. Even the wiring for
such apparatus must be protected, usually by burying it in
the ground. Open or unconfined fires, due to their large
extent and nonhomogeneous nature and the strong effects of
even slight winds, necessitate the use of many sensing
units to get reasonably representative data. In the past,
expensive and precise data measuring equipment was suggested
for characterizing these large, unconfined fires. One
example which is still being used is a test field instru-
mented with a large array of thermocouple installations.
The thermocouples are connected to an electronic recorder
and are used to measure the transient temperatures inside
fires. However, the main purpose for gathering the data
is to obtain a better general understanding of large-scale
fires and not necessarily precise data. Therefore, due to

1

the continued interest shown by governmental and industrial agencies, further development of small inexpensive passive heat flux sensing and recording devices was felt necessary.

The purpose of this continued study is to further analyze, design, construct, and test some of the simple and inexpensive instrumentation suggested by McCoy.(11) Of particular significance in this study was the construction, field testing, and analysis of the fusible-rod integrated-heat flux meter and the evaporative dosimeter. Both of these devices are used to measure the total amount of heat absorbed by a surface in a fire. This study also included laboratory testing of temperature sensitive compounds, which are presumed to indicate by a change in color when the temperature of a surface has attained or exceeded a predetermined value. Construction of all these devices was based on cost, ruggedness, reliability, and thermal properties of the materials. Perhaps a more important construction consideration, however, was that the devices must be easy to install, read, and interpret.

Due to the lack of sufficient time, final testing of the redesigned devices was not completely carried out but information obtained warrants continued investigation.

CHAPTER II

THE EVAPORATIVE DOSIMETER

Vaporization of a pure liquid, like the melting of a pure solid, usually takes place at a specific temperature with an accompanying heat effect. Therefore, the vaporization of a liquid lends itself to the design of instruments which record the total heat absorbed by a surface at a given temperature. The 100 ml aluminum evaporative dosimeter, which is fundamentally a vented liquid container, is shown in Figure 1. Before being exposed to a test fire, the dosimeters are painted black with India ink and filled with a known amount of liquid. After the test, the instruments are retrieved and the amount of liquid evaporated is given by the difference between the initial measured amount and the amount remaining after the test. If some of the liquid was vaporized during the test, then the total amount of heat absorbed by the instrument can be calculated. However, a liquid may evaporate considerably before and after a fire to confound the amount driven off by the fire itself. Therefore, control dosimeters are necessary at various points in the test field to give a measure of the evaporation due to conditions other than the fire.
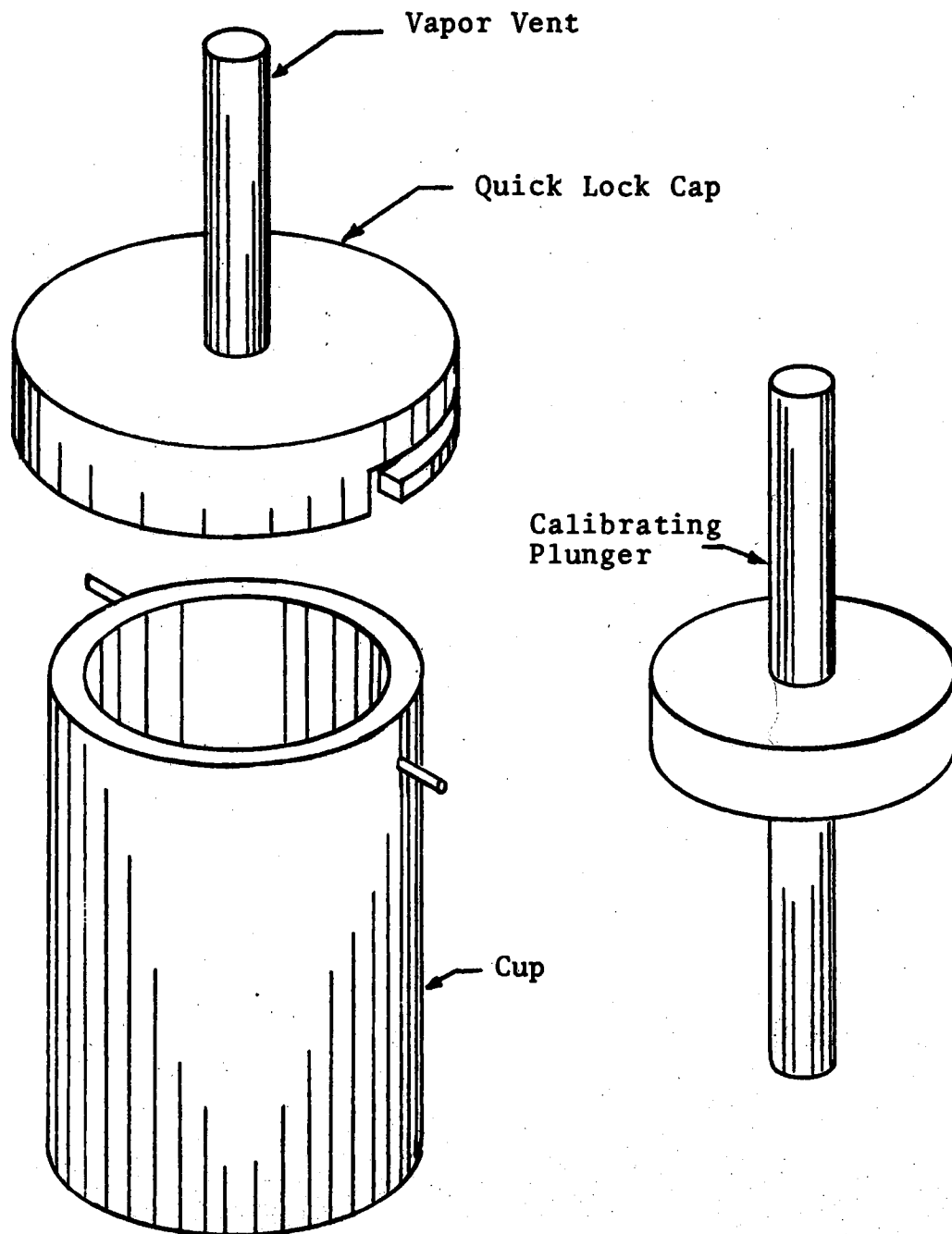
Figure 1. 100 ml Aluminum Evaporative Dosimeter

To facilitate the filling of the dosimeter with a known amount of liquid, a calibration plunger is used. The cup is initially filled to the brim with a moderately low boiling point liquid, such as carbon tetrachloride or water. The calibrating plunger is then inserted vertically until it hits the bottom of the cup. This plunger displaces excess liquid so that exactly 100 ml remains. The plunger is removed and the vent cap is locked in place. The dosimeter is then mounted in the bracket for the test.

The mathematical derivations used to analyze the data given by the dosimeter are given by McCoy. Assuming the specific heats and the heat of vaporization are constant, and assuming that some liquid is vaporized, the total heat absorbed by the dosimeter is

$$Q_t = (M_m Cp_m + M_{il} Cp_l)(T_b - T_i) + \lambda_b M_b \qquad (1)$$

where

M_m = mass of the metal container

M_{il} = initial mass of the liquid

Cp_m = specific heat of the metal

Cp_l = specific heat of the liquid

T_b = the boiling point of the liquid

T_i = the initial atmospheric temperature conditions

λ_b = the latent heat of vaporization of the liquid

M_b = the mass of the liquid evaporated during the test.

The particular liquid used in the test is determined by the characteristics of the fires being tested. Since

the particular fires of interest are of short duration
and reach temperatures up to 1000° to 1200°F, carbon
tetrachloride was chosen as the test liquid. To determine
the best test liquid for fires with other characteristics,
McCoy gives an analysis and a method for determining vapor-
ization efficiencies. The vaporization efficiency η_v used
by McCoy is defined as the ratio of the heat absorbed,
which causes a measurable loss of liquid, to the total
heat absorbed.

$$\eta_v = \frac{\lambda_b M_b}{(M_m Cp_m + M_{il} Cp_l)(T_b - T_i) + \lambda_b M_b} \qquad (2)$$

Thus by knowing the duration of the fire and the expected
temperatures to be reached, one can use these vaporization
efficiencies as a method for choosing the most suitable
test fluid.

Two dosimeter designs were tested, a small one for
low intensity fires and a larger one for more intense fires.
The dosimeters were made from 1 inch OD copper tubing and
2 1/4 inch OD aluminum pipe. Both of these metals have a
high thermal conductivity which insures that only small
temperature gradients exist in the walls of the dosimeter.
From the mathematical analysis done by McCoy, the best
design is probably the one with the height equal to the
diameter. Therefore, a 100 ml aluminum dosimeter having
inside and outside diameters of 2 inches and 2 1/4 inches
respectively and an inside and outside height of 2 1/2

inches and 2 11/16 inches respectively was designed. The
dosimeter was held in place by a C-clamp as shown in Figure
2.

Depending on the initial temperatures, the measurable
rates of heat absorbed per unit area for the 100 ml
aluminum dosimeter range from 150 to 1590 BTU/ft^2 for water
as the test liquid and from 40 to 274 BTU/ft^2 for carbon
tetrachloride. However, the need to measure lower values
of total heat absorbed per unit area necessitated a second
design which gave a larger area to volume ratio. The new
design was a 25 ml copper dosimeter made from standard
1 inch OD tubing. A new suspension system as shown in
Figures 3 and 4 was also designed. The notches in the
hanging rack of the new system prevented the dosimeter
from being upset or knocked to the ground. Also, this new
system was less bulky and did away with the need for a
C-clamp to hold the dosimeter in place. One should note
that detailed drawings for these new dosimeter designs
appear in Appendix A.

Depending on the initial atmospheric conditions, the
measurable rate of heat absorption per unit area for this
25 ml dosimeter varied from 24 to 156 BTU/ft^2 for carbon
tetrachloride as the test liquid and from 90 to 900 BTU/ft^2
for water as the test liquid. Since the ranges of the
total heat absorbed per unit area overlap for these dosi-
meters, both designs can be used on locations to measure
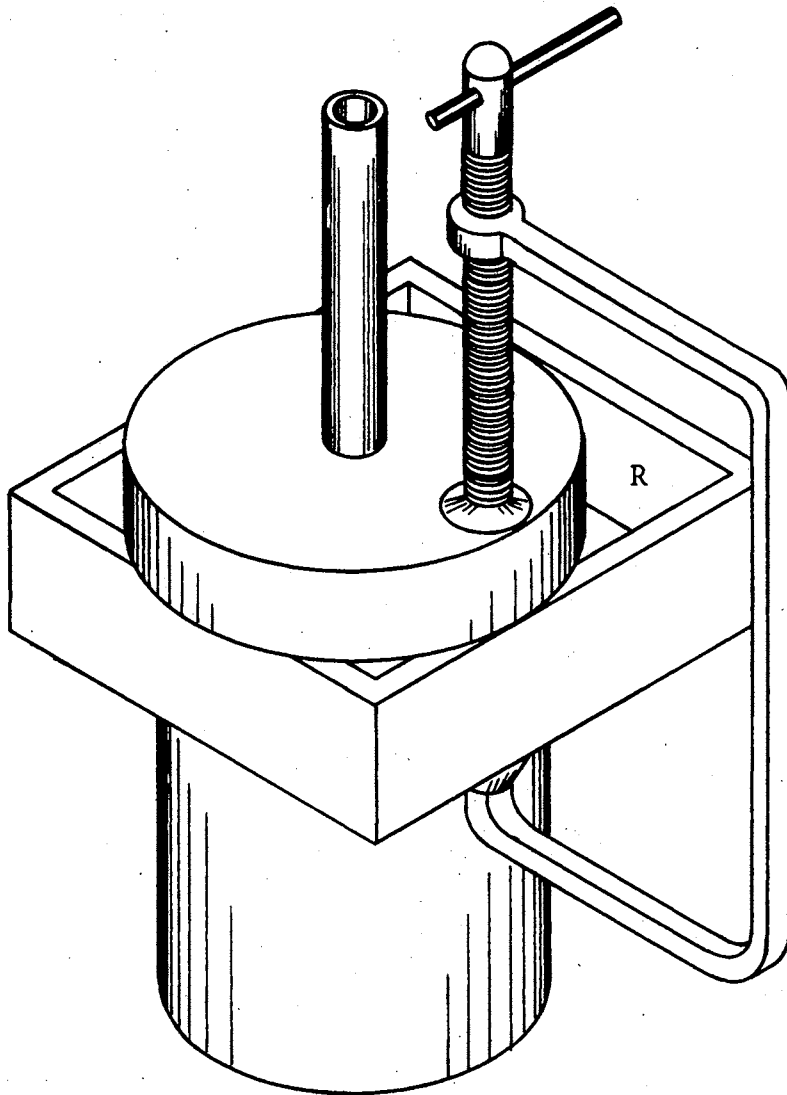
Note: Dosimeter supporting mount is
        attached to wall via a bolt
        through Face R

Figure 2.   Mounting of 100 ml
            Aluminum Evaporative
            Dosimeter

Vapor Vent

Quick Lock Cap

Calibration
Bar

Dual Cap Lock
and Suspension
Mechanism

Cup
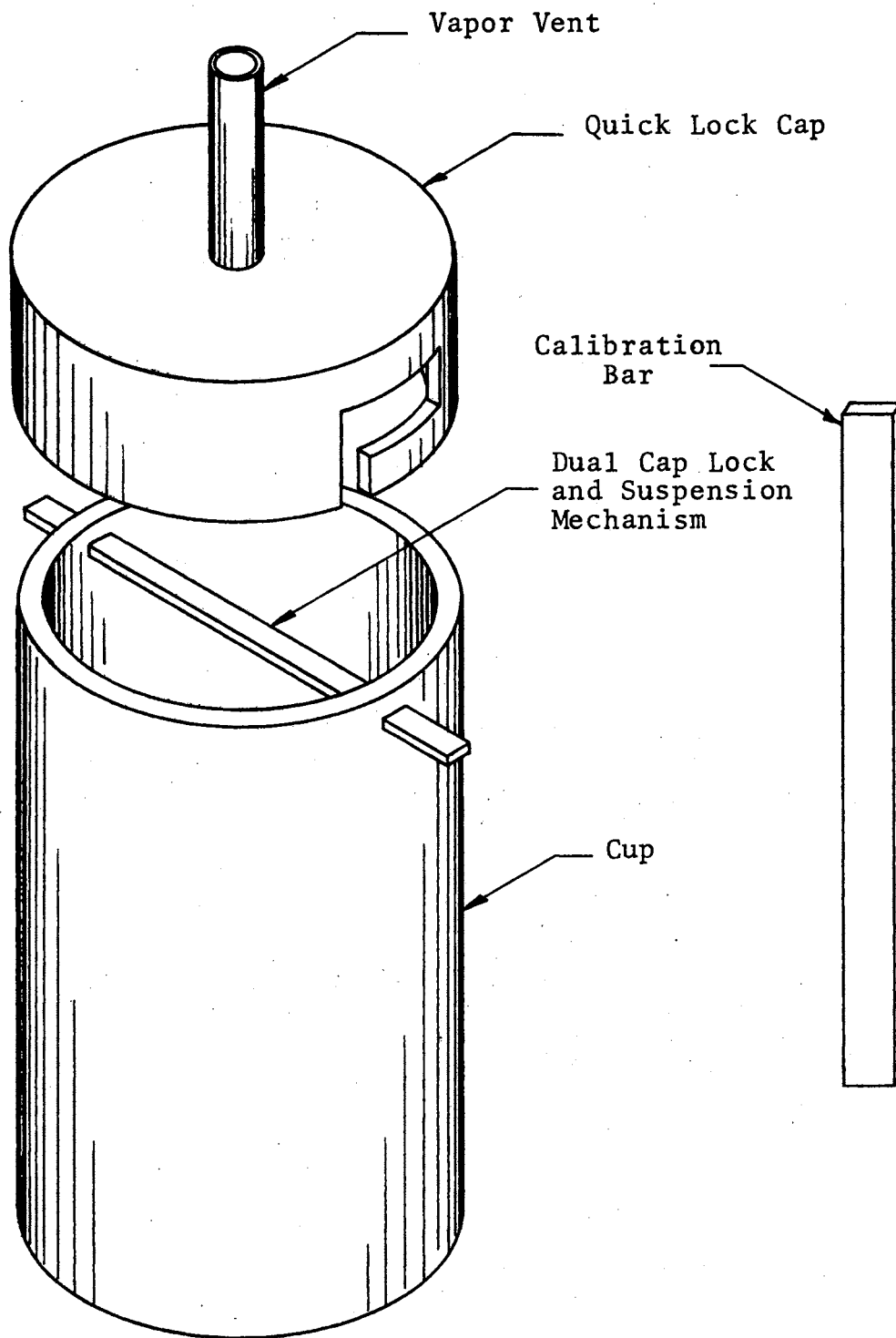
Figure 3. New Design for the 25 ml Evaporative
Dosimeter
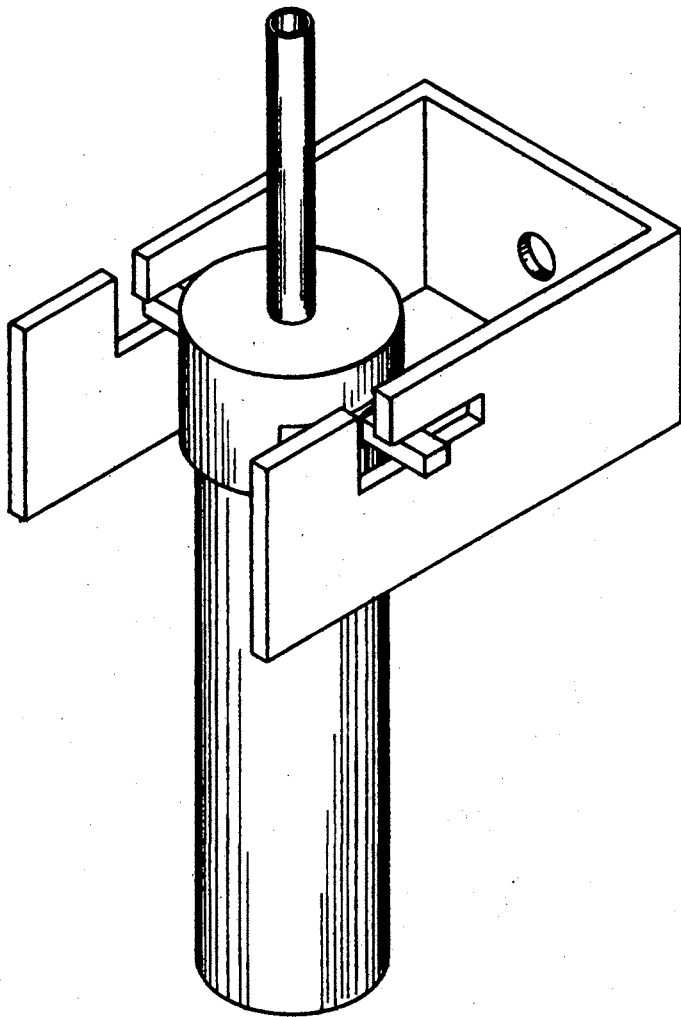
Figure 4.   New Hanging Rack Design
            for the Evaporative
            Dosimeter

all expected rates of total heat absorbed per unit area
and to determine reproducibility in those areas of overlap.

Like the fusible-rod integrated-heat flux meter, the
evaporative dosimeter can be used to map the hot and
relatively cold areas in an unconfined fire. Using several
different liquids in identical meters, qualitative infor-
mation on the total heat absorbed by surfaces at various
temperatures throughout the fire and the average heat flux
on these surfaces can be obtained.

Correct Interpretation of Results

To analyze correctly the information obtained from
a test utilizing the evaporative dosimeter, a statistical
number of control dosimeters are necessary on the test
range. The evaporation from the control devices will be
influenced by only the atmospheric conditions on the test
range and not at all by the fire. These control devices
must contain the same type and amount of liquid as the
dosimeters being tested. To show the significance of the
above procedure an example is worked below.

Example 1. A test copper dosimeter, which is identical to
the one for which Figure 4 was drawn, was filled with 25
ml of carbon tetrachloride at 26.7°C (80°F). Likewise,
two control copper dosimeters were filled with 25 ml of
carbon tetrachloride at 26.7°C and set out in the environ-
ment but not in the test area. The test dosimeter was then

exposed to an unconfined fire. After the test, 10 ml of carbon tetrachloride had been vaporized. Also, after the test, a measure of the average volume of the two control dosimeters indicated that 1 ml of carbon tetrachloride had evaporated due to the atmospheric conditions only. Calculate the total heat absorbed by the dosimeter.

Given: Cp_1 = .201 cal/g$^{\circ}$C

Cp_m = .09305 cal/g$^{\circ}$C

λ_1 = 46.42 cal/g

W_m = 76.312 g

T_b = 76.8°C

ρ_1 = 1.595 g/cc

where Cp_1 and Cp_m, λ_1, W_m, T_b, and ρ_1 are the specific heats of carbon tetrachloride and copper respectively, the latent heat of vaporization of carbon tetrachloride, the average weight of the copper dosimeter, the boiling point of carbon tetrachloride, and the density of carbon tetrachloride.

The physical properties for carbon tetrachloride and copper were taken from references.(8, 9, 12)

The total heat absorbed to vaporize a given volume V_1 is given by

$$Q_t = (W_m Cp_m + \rho_1 V_{i1} Cp_1)(T_b - T_i) + \rho_1 V_1 \lambda_1 \qquad (3)$$

Therefore, the total heat necessary to vaporize 10 ml of carbon tetrachloride is

$$Q_t = 1498 \text{ cal}$$

Also the total heat necessary to evaporate 1 ml of carbon tetrachloride is

$$Q_e = \rho_1 V_1 \lambda_1 = 74 \text{ cal}$$

Thus, the total heat absorbed solely from the fire is

$$Q_v = Q_t - Q_e = 1424 \text{ cal} = 5.65 \text{ BTU}$$

The same calculations can be made by using Figure 10, and noting that for 9 ml of carbon tetrachloride evaporated, the total heat absorbed is 5.65 BTU. Thus, if the control devices had not been used, the error caused by not knowing the real amount vaporized solely by the fire would have been

$$\text{Error} = \frac{(1498 - 1424) \text{ cal}}{1424 \text{ cal}} \times 100\% = 5.2\%$$

The calculations and assumptions made to establish Figures 5 to 12 are included in Appendix A. Using the dimensions for the 100 ml aluminum dosimeter given in Appendix A, Figures 5 to 8 can be used to analyze dosimeter data collected when water and carbon tetrachloride are the test liquids. Likewise, for the 25 ml copper dosimeter, Figures 9 to 12 can be used when water and
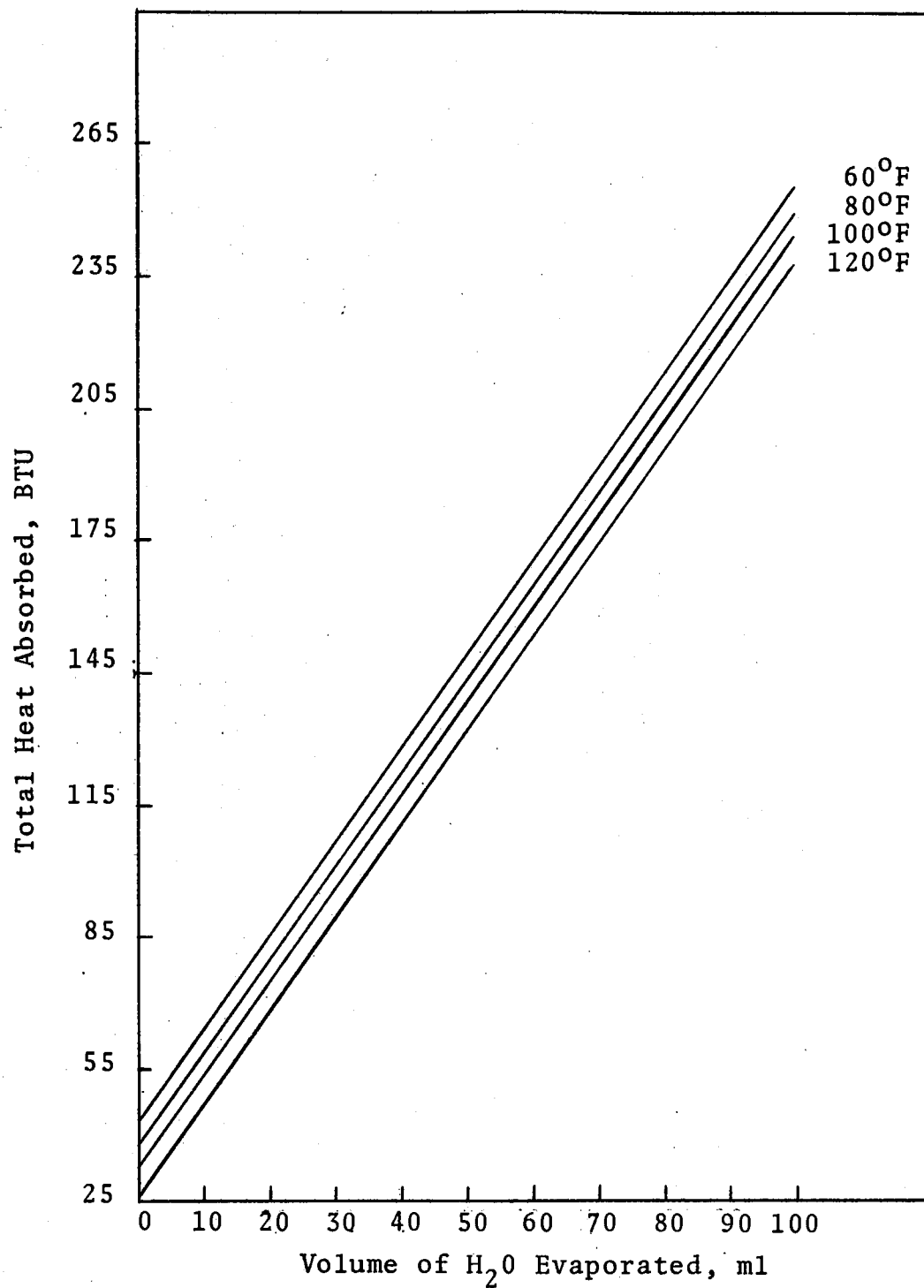
Figure 5. Total Heat Absorbed by the Aluminum
            Dosimeter Containing 100 ml of
            Water
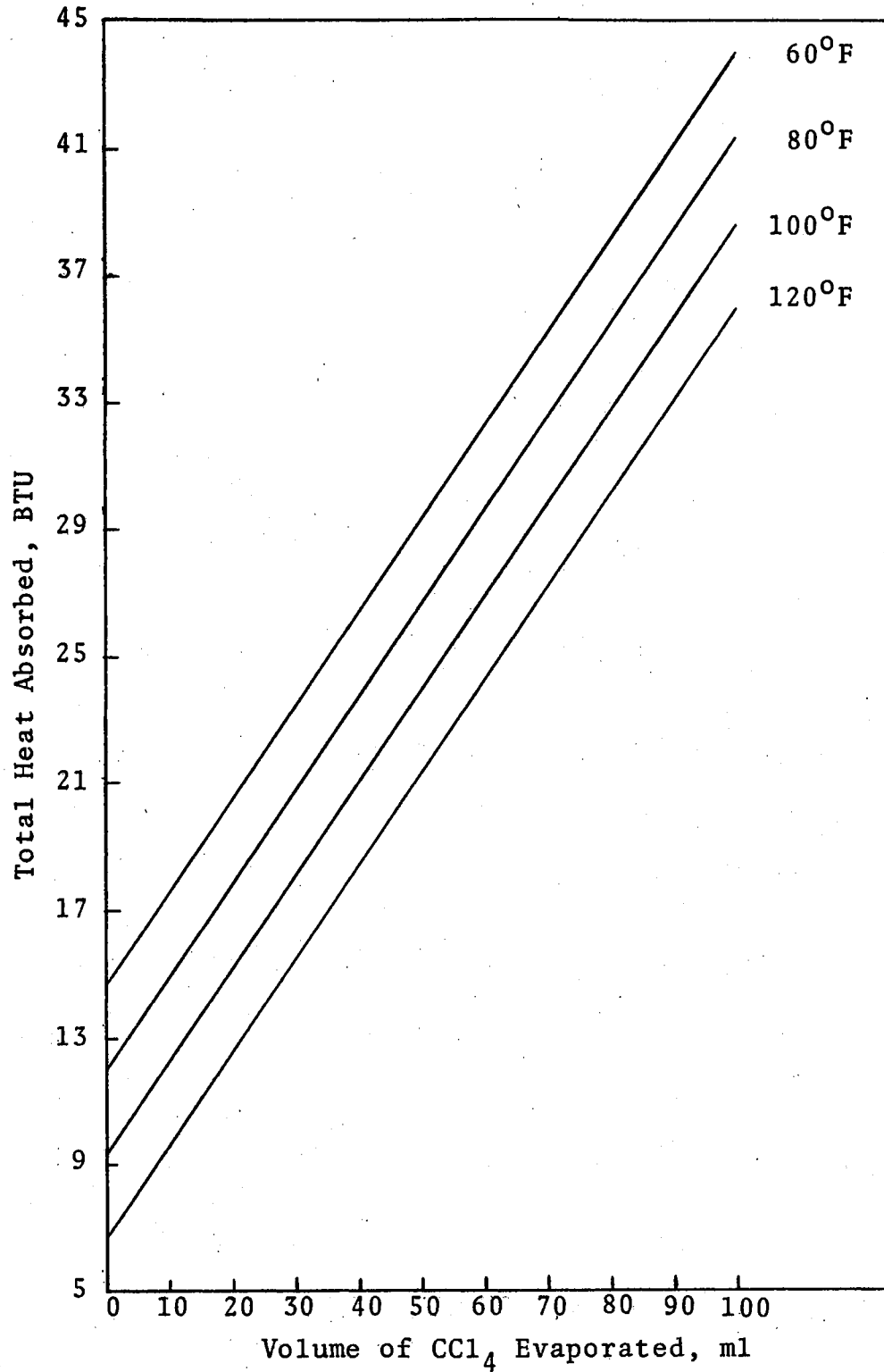
Figure 6. Total Heat Absorbed by the Aluminum
Dosimeter Containing 100 ml of
Carbon Tetrachloride
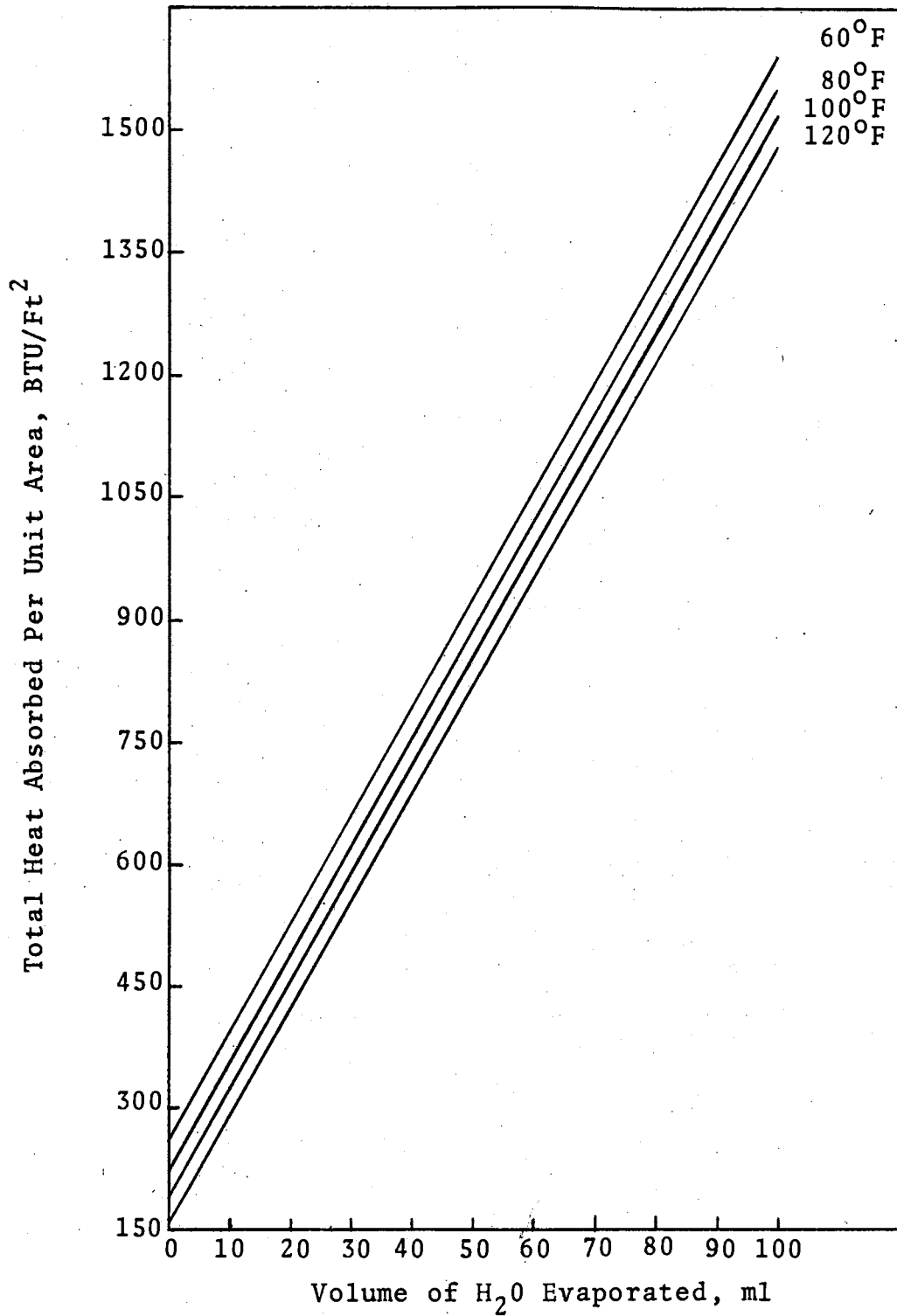
Figure 7. Total Heat Absorbed Per Unit Area
for the Aluminum Dosimeter
Containing 100 ml of Water
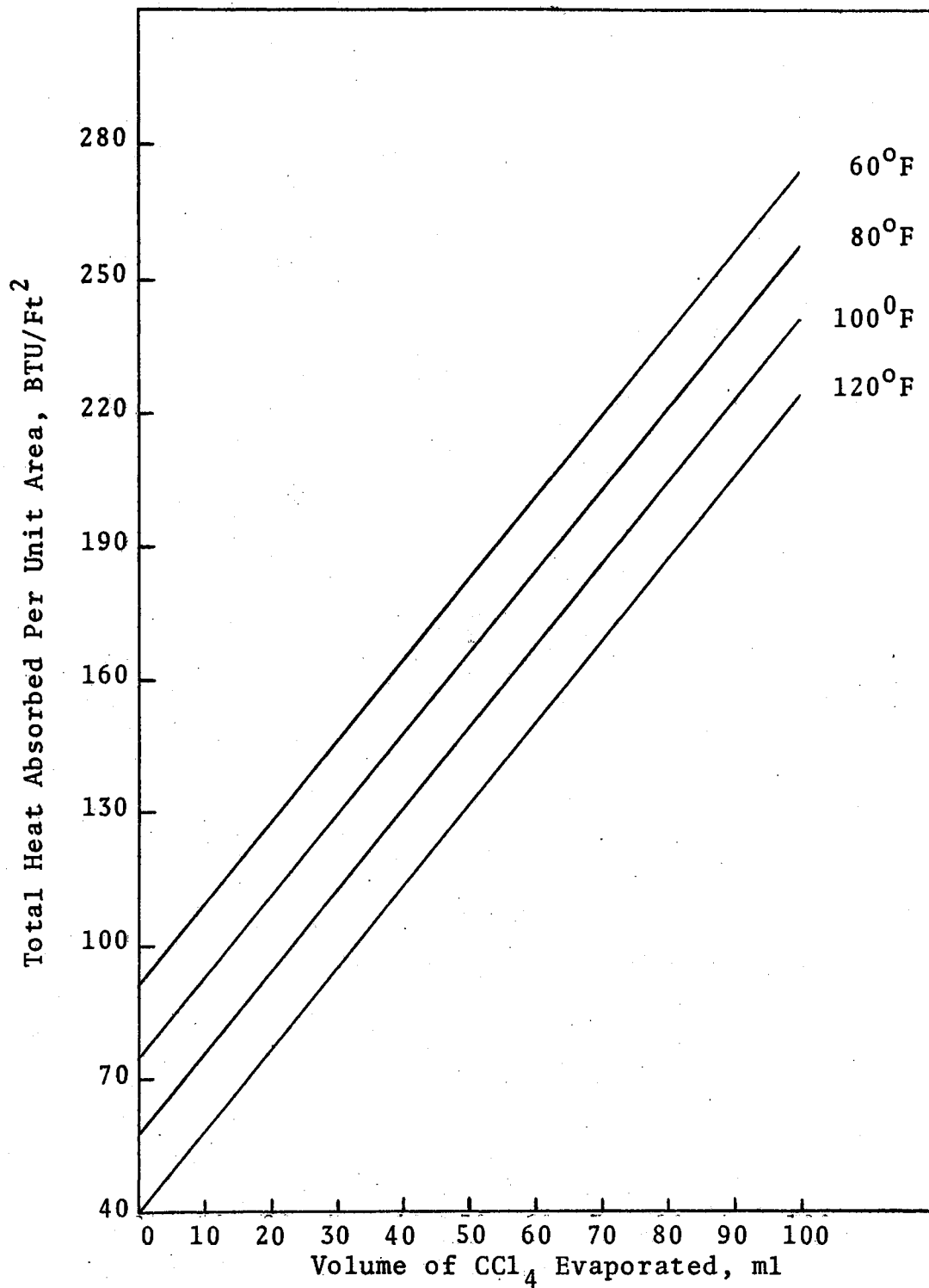
Figure 8.   Total Heat Absorbed Per Unit Area
for the Aluminum Dosimeter
Containing 100 ml of Carbon
Tetrachloride
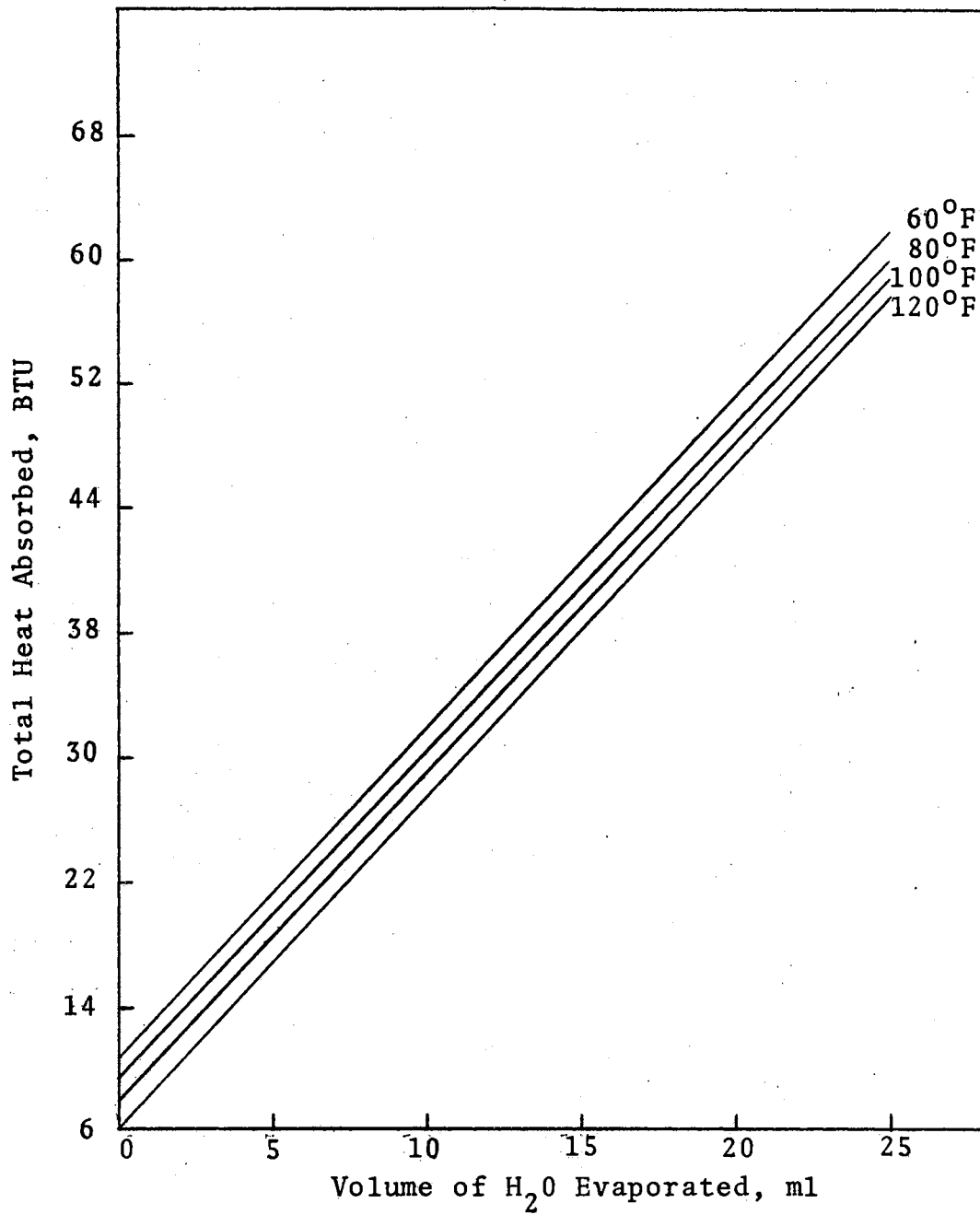
Figure 9. Total Heat Absorbed by the Copper
Dosimeter Containing 25 ml of Water
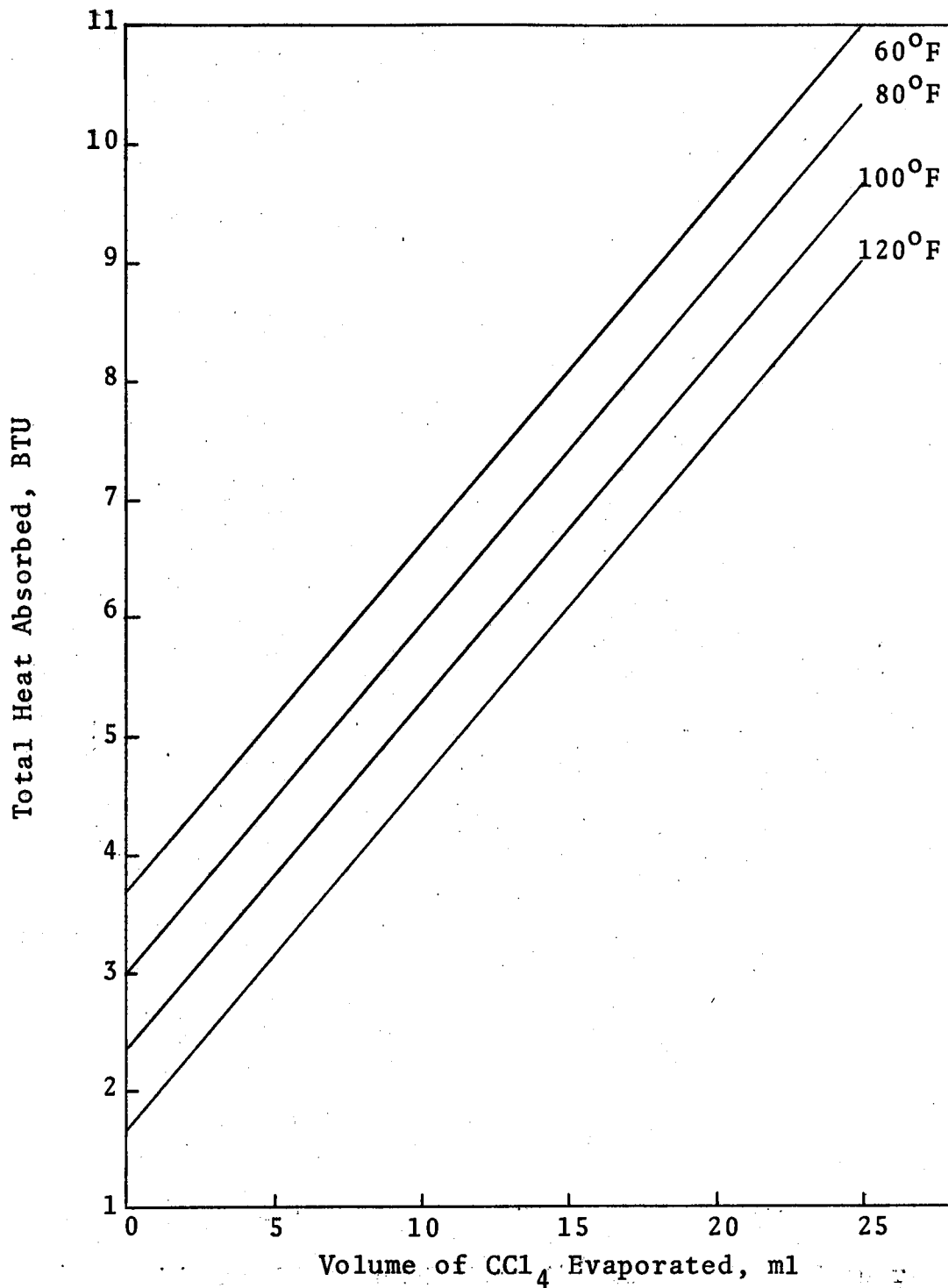
Figure 10. Total Heat Absorbed by the Copper
Dosimeter Containing 25 ml of
Carbon Tetrachloride
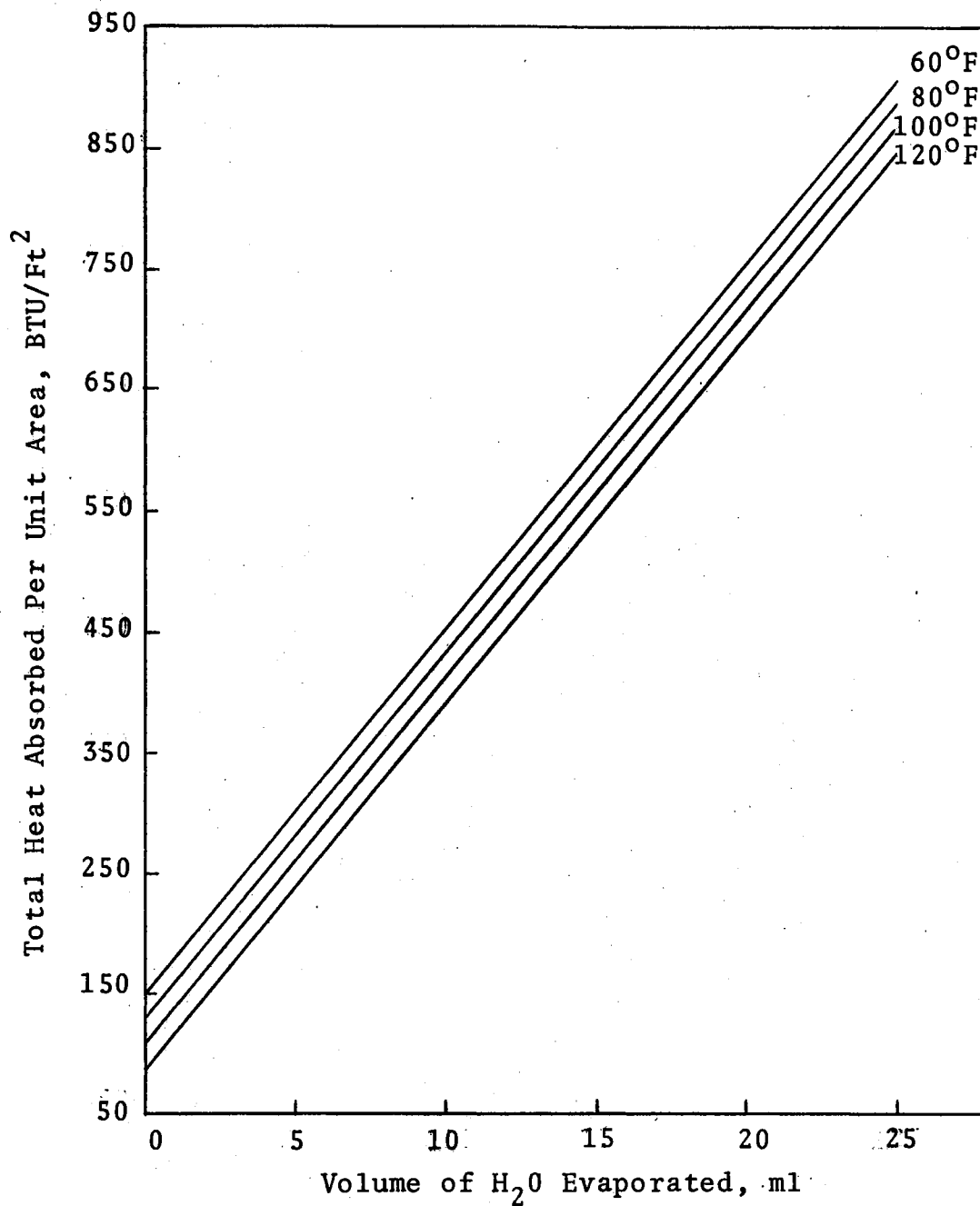
Figure 11. Total Heat Absorbed Per Unit Area for
the Copper Dosimeter Containing 25
ml of Water
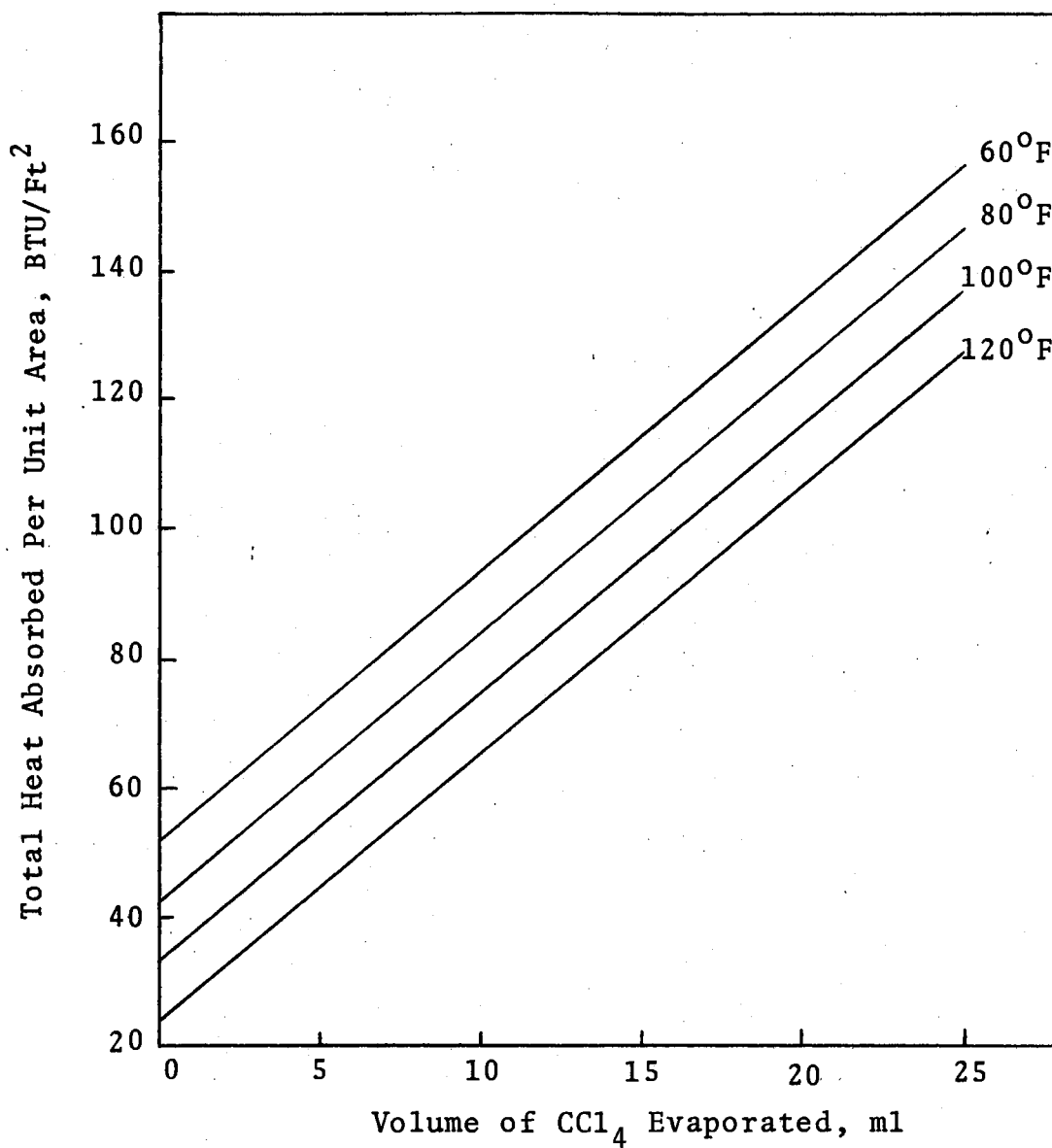
Figure 12.   Total Heat Absorbed Per Unit Area for
the Copper Dosimeter Containing 25
ml of Carbon Tetrachloride

carbon tetrachloride are the test liquids. Also included in Appendix A are graphs using calories as the units for measurement of heat.

Testing and Results

Both the 25 ml and 100 ml dosimeters were in tests analyzing fuel fires at the Naval Weapons Center, China Lake, California. These dosimeters were placed in the proximity of an expensive thermocouple installation in order that comparisons of the recorded data could be made. During the actual testing period the dosimeters seemed to work as expected. At this time, however, the data reduction from the more elaborate testing apparatus has not been received; thus the necessary analysis of the test data has not been completed.

Recommendations

During periods of high heat flux, rapid vaporization may cause liquid entrainment to occur. If escaping vapors do carry the liquid droplets through the vapor vent, the dosimeter will register too high a liquid loss. Therefore, tests should be initiated to determine the level of flux at which liquid entrainment occurs. If this flux is expected in the unconfined test fires, then I recommend that as a method of reducing liquid entrainment, a small metal baffle be placed just below the inside opening of the vapor vent.

In order to determine what mechanical designs for the
dosimeter would be most effective, McCoy did a detailed
mathematical analysis to determine the heat absorption
efficiency of various dosimeter configurations. The heat
absorption efficiency, as defined by McCoy, is the ratio
of the total heat absorbed by the dosimeter, after the
working fluid has been heated to its boiling point, T_b,
to the total heat which would be absorbed by the dosimeter
if the entire exposed surface were at T_b. The efficiency
may be written as

$$\eta_a = \frac{\int_0^{A_m}(T_s - T_m)\,dA}{(T_s - T_b)A_m} \tag{4}$$

where A_m, T_s, and T_m are the total exposed metal surface
area, the temperature of the surroundings and the temp-
erature of the metal, respectively.

One should note that the temperature distribution over
the surface of the dosimeter must be calculated before
Equation (4) can be integrated. Thus, for convenience, the
dosimeter was divided into three domains and various
assumptions, the details of which will not be discussed
here, were made by McCoy in his derivation. It is felt
that simulated testing to determine the actual in-fire
efficiency for various feasible dosimeter configurations
should be done in order that the mathematical derivations
and calculations made by McCoy can be verified. If an

approximation of the in-fire efficiency can be determined,
then the accuracy with which the instrument is used will be
increased.

CHAPTER III

FUSIBLE-ROD INTEGRATED-HEAT FLUX METER

Experimental Apparatus

The melt stick dosimeter shown in Figure 13 and in detailed drawings in Appendix B was designed to measure the total amount of heat absorbed by a surface during an unconfined fire. The simple instrument is basically a copper disk upon which the heat is absorbed, and a fusible 2-naphthol rod which melts at $122^{\circ}C$ thus removing the heat absorbed by the metal plate. Shortly after the copper plate has reached this melting point temperature, the 2-naphthol rod begins to melt on the interface between the rod and the copper disk. This melting acts as a heat sink and keeps the temperature of the copper disk at or near the melting temperature of the fusible rod. As the melted 2-naphthol runs into the insulated metal catch tank, a metal plunger and compression spring push new material to the heated surface. The insulated material catch tank is attached below the copper disk and the exhaust opening in the fusible rod guiding tube. This metal catch tank serves also as part of the heat shield to prevent the fusible rod
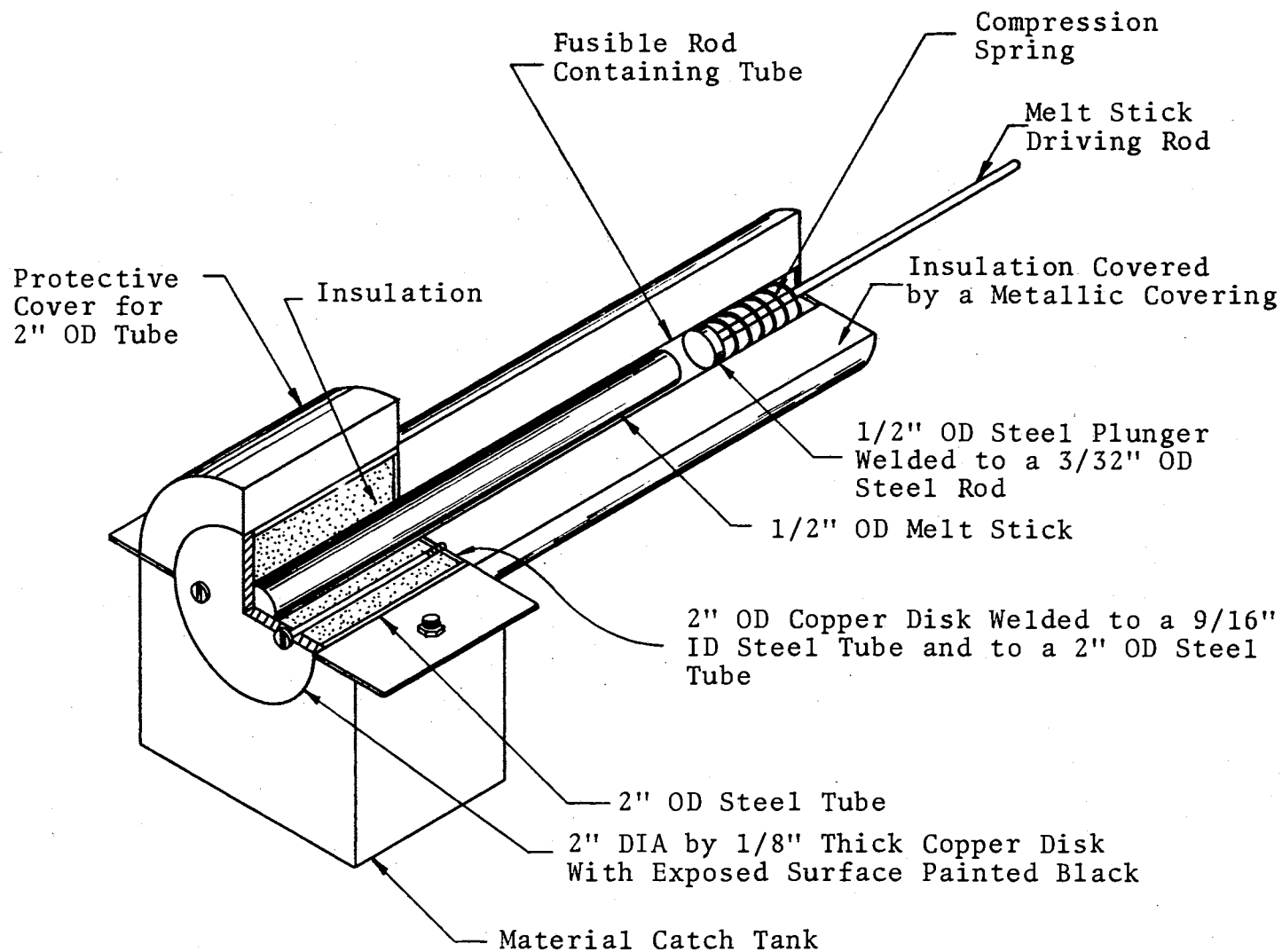
Figure 13. Fusible-Rod Integrated-Heat Flux Meter

Labels in figure:
- Fusible Rod Containing Tube
- Compression Spring
- Melt Stick Driving Rod
- Protective Cover for 2" OD Tube
- Insulation
- Insulation Covered by a Metallic Covering
- 1/2" OD Steel Plunger Welded to a 3/32" OD Steel Rod
- 1/2" OD Melt Stick
- 2" OD Copper Disk Welded to a 9/16" ID Steel Tube and to a 2" OD Steel Tube
- 2" OD Steel Tube
- 2" DIA by 1/8" Thick Copper Disk With Exposed Surface Painted Black
- Material Catch Tank

from being heated from a source other than through the
copper disk as well as preventing the melted material from
vaporizing or burning.

The length of the steel rod extending out of the
surrounding insulation is used to measure the amount of
2-naphthol rod that is consumed during a test. Before the
test, the exposed length of the protruding rod is measured.
After the test has been conducted, the exposed length of
the rod is again measured. The difference between the two
measurements is the length of the fusible rod which has
been melted.

In order to minimize temperature gradients in the
metal disk, the disk was made of copper which has a high
thermal conductivity. The following criteria were used for
choosing the material for the fusible rod. The fusible
rod (1) must be made from a material with a low thermal
conductivity so that the heat lost to conduction down the
rod may be neglected; (2) must have a small melting range,
preferably less than $1^{\circ}C$, and melt near $100^{\circ}C$ to better
facilitate heat absorption measurements; (3) must not be
hazardous to touch or inhale, so that special care in
handling will not be necessary; and (4) must not vaporize
easily, decompose when heated, or be extremely flammable
thus necessitating special designs. Therefore, the fusible
rods were made of 2-naphthol and beeswax. The thermal
conductivity of 2-naphthol is 0.139 BTU/ft-hr-$^{\circ}F$, and the
melting range is 122-122.7$^{\circ}C$. 2-Naphthol is not hazardous

or extremely flammable, but does vaporize slightly when heavily heated in an open area. The thermal conductivity of beeswax is .0202 BTU/ft-hr-^{o}F and the melting range is 62-65°C. Beeswax is definitely not hazardous nor flammable and does not vaporize easily. However, beeswax is difficult to form into rods because of its adhesive properties and difficult to maintain in a rod-like form because of its ability to soften before melting.

An instrument should be designed to have a high ratio for metal disk radius to fusible rod radius. Using a steady state Bessel equation, a mathematical evaluation to determine the heat absorption efficiency of the exposed surface was done by McCoy. The results presented by McCoy indicated that the efficiency of the exposed metal surface is clearly seen to decrease with any increase in the heat transfer to that surface and with any increase in the radius of that surface. However, at low values of the heat transfer coefficient, which are expected in this experiment, very little heat absorption efficiency is lost in a metal disk made of small thicknesses of high thermal conductivity metals, regardless of the diameter of the metal disk. Therefore, to insure large fusible rod length changes in the operating equipment, the initial design utilized a 1/2 inch diameter fusible rod with a 2 inch diameter by 1/8 inch thick copper disk.

Development of Rod Molding Technique

The instrumentation used to mold the 6 inch long, 1/2 inch O.D. 2-naphthol rods is shown in Figure 14. The apparatus consisted of an 11 inch piece of 5/8 inch I.D. thin-walled electrical conduit, which was wrapped with a 1/2 inch Briskeat heating tape. Inside the conduit was an 11 inch piece of 9/16 inch O.D. Pyres glass tubing. The glass tubing was plugged with a cork stopper on the bottom to prevent the molten liquid from escaping. A Powerstat made by the Superior Electric Company was the heat controlling device used to melt the Reagent grade 2-naphthol crystals.

The wrapped conduit was connected to the ringstand by two ring clamps. The Pyrex glass tubing was inserted into the conduit and was supported on the bottom by a flat plate connected to the ringstand. Due to the expansion properties of the liquid 2-naphthol, the glass tubing was initially filled with about 6 inches of 2-naphthol crystals. The Powerstat was then set on 60 to melt the crystals. Intermittently, crystals were added until the entire glass tube was filled with liquid 2-naphthol.

In earlier trial experimentation on resolidifying techniques, it was discovered that if all the liquid were to cool at the same time, a pin hole would form in the middle of the rod and thus prevent the formation of a solid 6 inch long rod. To prevent the occurrence of a pin hole, the above molding technique was modified. By leaving the
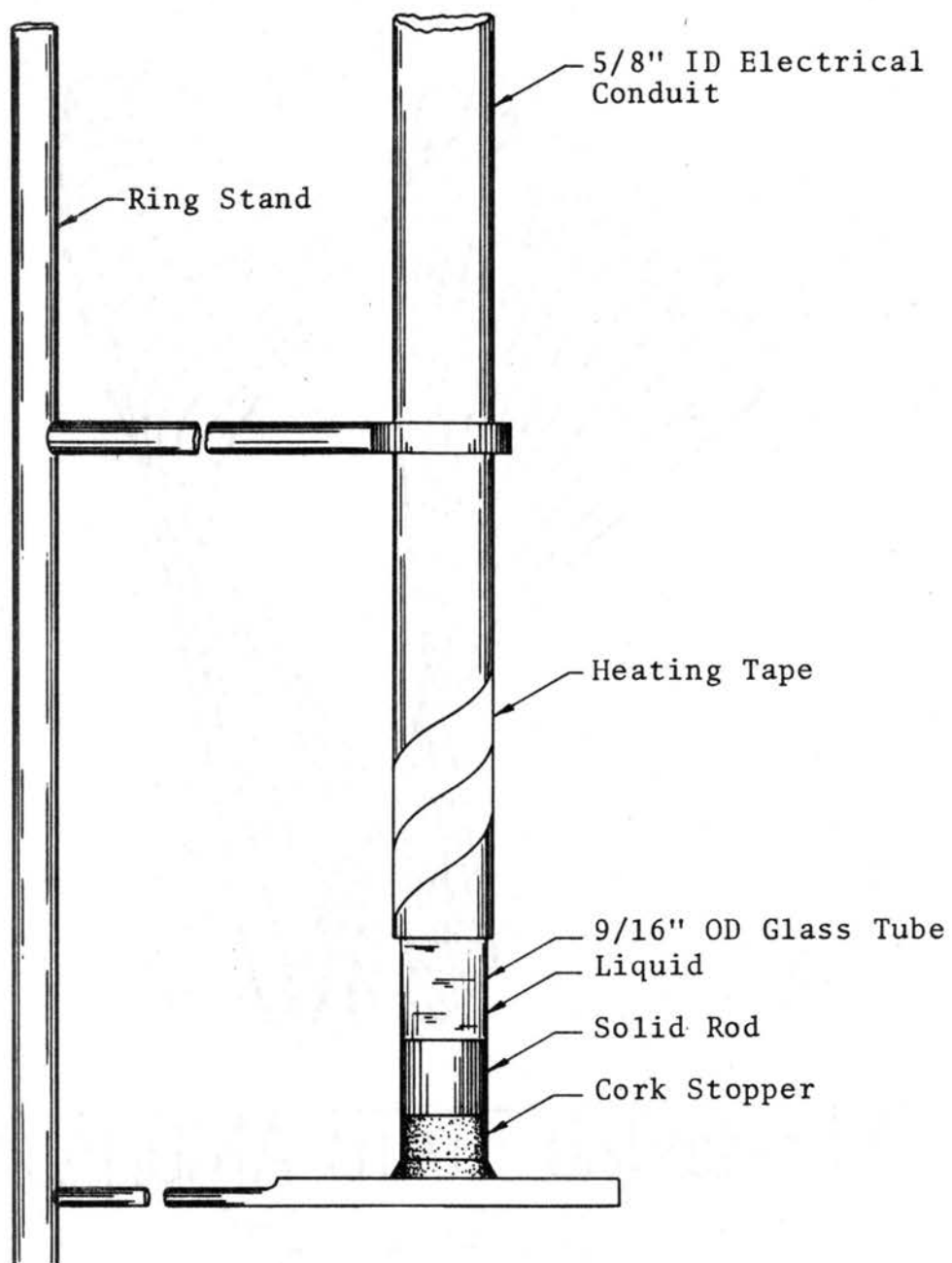
Figure 14. Schematic Diagram of Rod
Molding Apparatus

Powerstat setting just above the melting point of the liquid and lowering the glass tubing 1 inch out of the wrapped conduit, a solid 1 inch rod would be formed as the liquid cooled. Then by repeating this method on 1 inch intervals the 6 inch by 1/2 inch O.D. rod could be formed. To facilitate the removal of the rod from the glass tubing without breaking the rod, the glass tubing was placed in the refrigerator for 3 hours. The low temperature caused the solid rod to further contract and thus be drawn away from the sides of the glass tubing. Then using a 5/16 inch steel rod, the 2-naphthol rods could be removed from the glass tube. The usual product of this method was an 8 inch solid rod which had to be cut down to the required size.

During this operation, if the excess 2-naphthol had not been overheated to the point of color transition or possible thermal decomposition, the scrap rod could again be melted and used in the next rod.

Experimentation with the Melt Stick Dosimeter

An early test of the dosimeter indicated that only about 1/10th of the heat absorbed by the copper disk was transferred to the melt stick. This heat loss indicated that heat sinks of large magnitude were present and that redesign might be necessary. Review of the design indicated that the heat losses might be caused by the steel screws connecting the copper disk to the dosimeter and by the steel support cylinder where the edges of the copper disk

touch. One should also note that losses caused by possible reradiation and convection effects are inevitable and should not be charged against the design. Therefore, Warren K. Smith, of the Naval Weapons Center, China Lake, California, (13) performed two tests to give an indication of the magnitudes of the thermal losses to the supporting metal structures in the melt stick dosimeter.

Experimental Procedure

A #36 gauge chromel-alumel thermocouple was attached to the back of the copper disk about mid-radius by means of staking the wires into two small holes drilled 1/8 inch apart. The instrumented copper disk was blackened with India ink and set flush into a shallow recess in an asbestos block. The recess was made purposely with an irregular bottom to further limit thermal contact with the copper disk. The power setting for the quartz infrared heating lamps was determined by a preliminary test using a Hy-Cal calorimeter of the Gardon Gauge water-cooled type. Using an ice bath for the thermocouple reference junction and a heat flux of 1.0 cal/cm^2sec, temperature vs. time curves were recorded on a Hewlett-Packard x-y-y' Recorder with the x-axis used as the time base.

After the test with only the copper disk on the asbestos block, the disk was re-blackened with India ink and assembled on the dosimeter apparatus in the regular manner except that the 2-naphthol rod was omitted; the steel rod used for melt

measurements was not allowed to touch the copper disk.
The heating and cooling sequence were then performed again
at 1.0 cal/cm^{2}sec. The results of both of these tests are
shown in Figure 15.

Analysis of Results

The calculations to determine the losses of heat in
the dosimeter were done on an instantaneous heat flux basis.
For the test with the copper disk recessed in the asbestos,
the underlying assumptions were that all the heat not
absorbed by the copper disk was heat lost to convection and
reradiation and that there is no temperature gradient in
the copper; thus the temperature measured was the surface
temperature of the disk.

The rate of total heat output per unit area for the
quartz infrared heating lamp was easily calculated by
multiplying 1.0 cal/cm^{2}sec by the time interval in question.
The rate of heat absorbed per unit area by the copper disk
can be calculated using the instantaneous changes of
temperature with time as shown in Figure 15. The instantan-
eous rate of net heat gain from the surrounding for $\Theta > 0$ is
given by

$$Q = \rho VCp \frac{\Delta T}{\Delta \Theta} = \rho tACp \frac{\Delta T}{\Delta \Theta} \tag{5}$$

where Cp, ρ, V, t, and A are the specific heat, density,
total volume, disk thickness, and surface area of the disk;
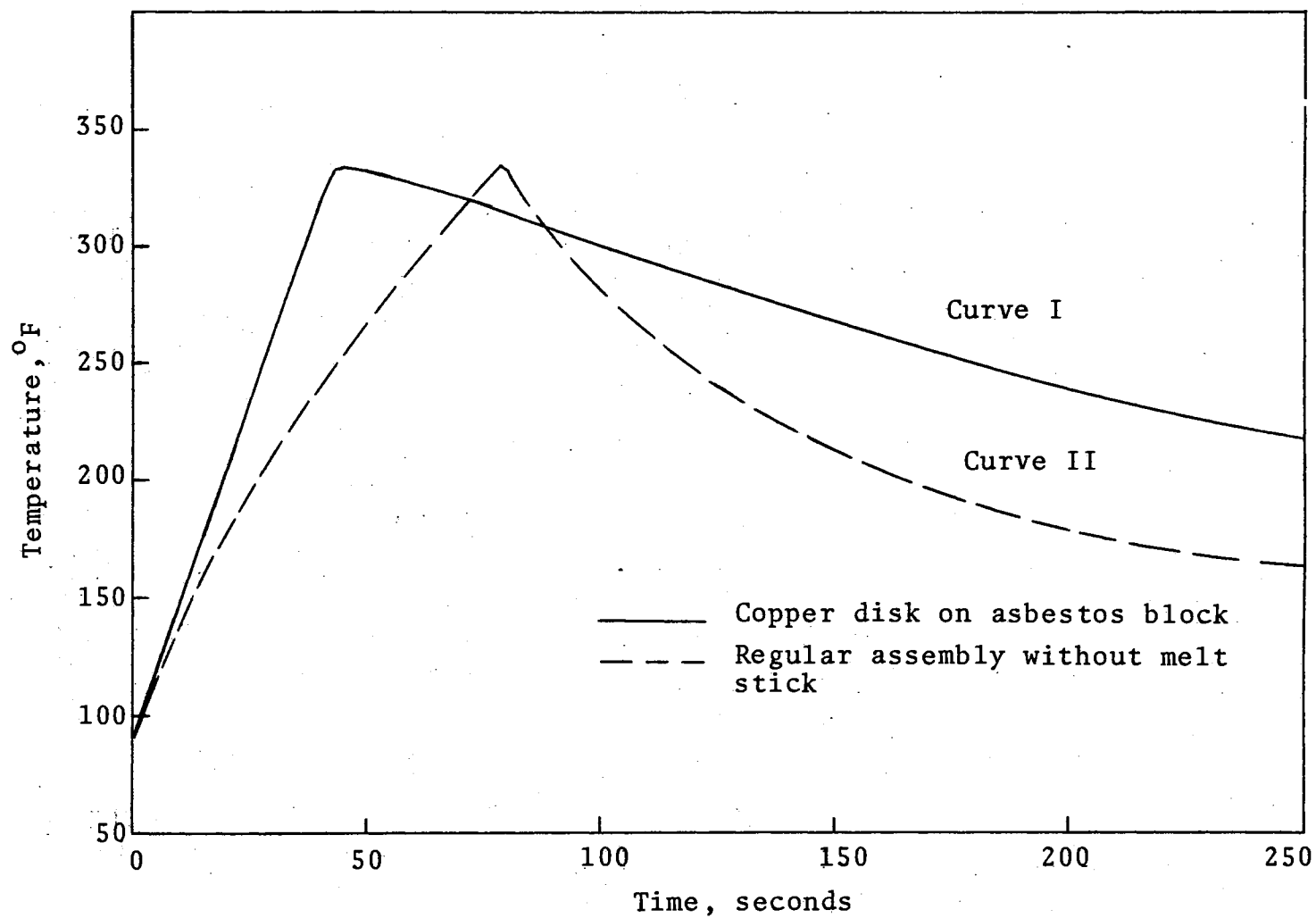
Figure 15. Indicated Thermal Losses in Melt Stick Dosimeter

ΔT is the temperature change of the disk and Δθ is the
time interval over which this temperature change occurred.
To determine the total heat gained per unit area for a
given time interval the above equation becomes

$$(Q/A)\Delta\theta = \rho t Cp\Delta T \qquad (6)$$

Using the following values for the copper disk,

   t = .3175 cm

   ρ = 8.89 g/cm^3

   Cp = .094 cal/gram $^\circ$C

the equation becomes

$$(Q/A)\Delta\theta = (.2653 \ \Delta T^\circ C)cal/cm^2 = q_{ab} \qquad (7)$$

One should note that Figure 15 is a plot of temperature in
$^\circ$F vs. time and that the conversion factor $\Delta T^\circ C = \Delta T^\circ F/1.8$
must be used.

Calculations were made using the above equation, and
the difference between the total heat output per unit area
of the quartz heating lamp and the calculated rate of heat
absorbed per unit area by the copper disk was assumed heat
lost to convection and reradiation. These calculations
are shown on Table VII in Appendix B for time intervals
of 2.5 sec for Curve I of Figure 15.

Figure 16 shows the relationship of the total heat
per unit area lost to convection for each time interval vs.
the average surface temperature. Using Figure 16 and
assuming that at T_s (average surface temperature) the heat
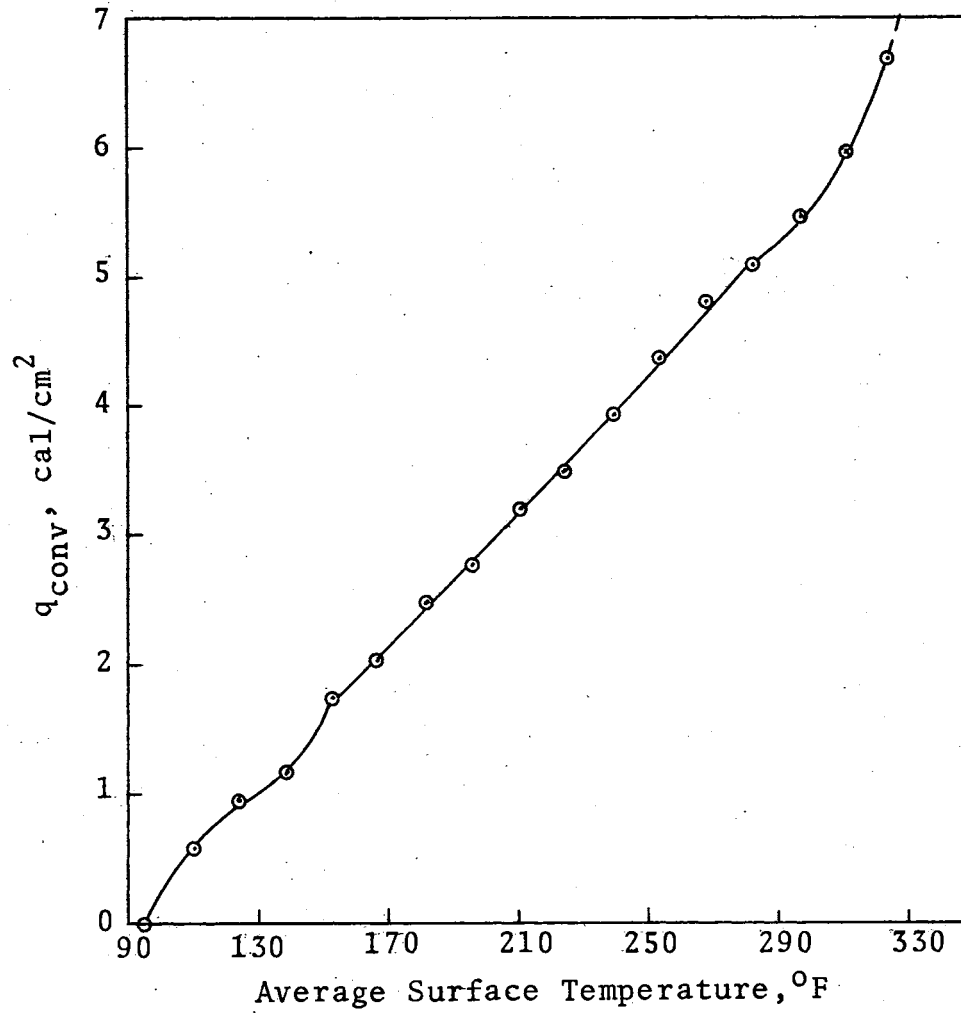
Figure 16.   Total Heat Per Unit Area Lost to
            Convection for the Copper Disk
            on the Asbestos Block

36

lost due to convection and reradiation are the same for the
dosimeter assembly as they are for the copper disk on the
asbestos block, the heat balance equation for the regular
dosimeter assembly becomes

$$q_h = q_{ab} + q_{conv} + q_{cond} \tag{8}$$

where q_h, q_{ab}, q_{conv}, q_{cond} are, for a given time interval,
the rate of heat output per unit area for the quartz heating
lamp, the rate of heat absorbed per unit area by the disk,
the rate of heat per unit area lost to convection and rerad-
iation, and the rate of heat per unit area lost by conduction
to the disk supporting structure.

Using the same procedures to calculate q_h and q_{ab} as
before and using Figure 16 for q_{conv}, q_{cond} can be found by
the difference. Tabulated values of these calculations for
time intervals of 2.5 sec are contained in Table VIII and
IX in Appendix B for Curve II of Figure 15. If the total
rate of heat transfer lost per unit area is assumed to be
the sum of the q_{conv} and q_{cond} terms, it can be seen that
the total rate of heat lost per unit area ranges from 23.5%
of the total rate of heat output per unit area for the
quartz lamp at 5 sec to 53% at 75 sec. However, of this
total loss, the rate of heat per unit area lost to conduction
into the disk support structure accounts for 54% of the total
lost at 5 sec to 83% at 75 sec. Therefore, by eliminating
the heat losses due to conduction, the total heat lost can be

reduced to 11.8% of the total rate of heat output per unit area for the quartz lamp at 5 sec and to about 9% at 75 sec.

In analyzing the cooling curves to determine the heat transfer coefficient of air for the cooling copper on the asbestos block, the following assumptions were made: (1) Assume that no conduction into the asbestos block takes place; (2) Assume that T_∞ for air is $87^\circ F$; (3) Assume that the surface temperature is equal to the average temperature of the given time interval.

The rate of heat loss by the hot copper disk can be expressed by Equations (5) and (6) and the heat absorbed by the air is shown to be

$$Q = hA(T_s - T_\infty) \tag{9}$$

where h, A, T_s, and T_∞ are the unit surface heat transfer coefficient, the surface area of the disk, the surface temperature of the disk, and the temperature at an infinite distance from the disk. Utilizing the assumption that there is no conduction, then the heat per unit area given up by the disk is equal to the heat per unit area absorbed by the air via convection. Equating these terms

$$\rho t Cp \frac{\Delta T}{\Delta \Theta} = h(T_s - T_\infty) \tag{10}$$

Therefore

$$h = \frac{\rho t Cp(\Delta T/\Delta \Theta)}{T_s - T_\infty} \tag{11}$$

Using the following physical properties and dimensions,

ρ = 555 lb/ft^3

Cp = .094 BTU/lb $^{\circ}$F

t = .0104 ft

the equation becomes

$$h = 1956.375 \left(\frac{\Delta T^{\circ}F/\Delta\theta sec}{(T_s - T_{\infty})^{\circ}F} \right) \frac{BTU}{hr\ ft^2\ ^{\circ}F} \qquad (12)$$

For the cooling part of Curve I for the copper disk on the asbestos block, the calculations are shown in Table X in Appendix B and indicate that the convective and reradiation loss coefficient corresponds to a nearly constant heat transfer coefficient of 6.17 BTU/hrft^2°F. The relative size and near constancy of the value suggest that a circulation fan to prevent the quartz heating lamps from over heating was going while the tests were being run and this resulted in a forced convection process rather than natural convection.

Utilizing the same assumptions, the calculations were made for the cooling curve for test II, regular dosimeter assembly. Table XI in Appendix B shows the results which indicate that at high temperatures the heat transfer coefficient is nearly 4 times that calculated earlier while after 170 seconds (2.84 minutes) the coefficient is about normal for forced convection. This large difference suggests that a large amount of the heat lost during cooling is lost to conduction to the metal supporting structure.

To calculate the total heat flux lost due to conduction during cooling, the following assumptions were made: (1) Assume that the heat liberated during cooling of the copper disk in the regular dosimeter assembly is due to convection and conduction only; (2) Assume that the flux of heat can be expressed as a function of convection and conduction; (3) Assume that the heat transfer coefficient for forced convection is constant and is equal to the average of the values obtained for the copper disk on the asbestos block.

Therefore, combining earlier calculations,

$$\text{Cooling Flux} = \text{Convection Flux} + \text{Conduction Flux} \quad (13)$$

$$Q/A = (Q/A)_{conv} + (Q/A)_{cond} \quad (14)$$

$$\rho t C p \frac{T_2 - T_1}{\Delta\theta} = h_a(T_s - T_\infty) + (Q/A)_{cond} \quad (15)$$

where T_2 and T_1, T_s, and h_a are the temperature values for the $\Delta\theta$ time interval on the cooling curve of the regular assembly, the average of the temperature in the $\Delta\theta$ time interval, and the average heat transfer coefficient for forced convection. From earlier calculations the above equations become

$$(Q/A)_{cond} = 1956.375 \left(\frac{(T_2-T_1)^{\circ}F}{\Delta\theta \text{ sec}}\right) - 6.17((T_s-87)^{\circ}F) \frac{BTU}{hr \text{ } ft^2} \quad (16)$$

Summary of these calculations are included in Table XII in Appendix B where the $(T_2-T_1)/\Delta\theta$ ratios and (T_s-T_∞) calculations are taken from Table XI in Appendix B.

These calculations suggest that the magnitude of the
losses for conduction during cooling vary from 74% of the
total heat liberated at high surface temperatures to about
3% at low surface temperatures. Therefore, since these
conduction losses are still prevalent during cooling, the
assumption by McCoy that the excess heat stored in the metal
disk is rapidly conducted to the fusible rod is incorrect
and the calculation used to estimate the length of fusible
rod consumed during a test of an "ideal" instrument would be
invalid.

Recommendations and Update of Design

The above tests indicate that indeed conduction losses
are the major problem of the presently designed melt stick
dosimeter. However, if the steel screws, which hold the
copper disk in place, are replaced and the steel cylinder,
which the copper disk rests against, is modified, the
conduction losses could be greatly reduced. Figure 17
shows a recommended method of improving the present design.
The steel screws have been replaced by two small steel
plates which act like fingers to hold the copper disk in
place. The top plate can be adjusted to apply the necessary
pressure to hold the disk. The steel cylinder, as shown in
the cutaway of Figure 17, has been reduced in height and an
asbestos insulation spool with a 3/16 inch lip has been
inserted. The lip on the asbestos spool will lie between
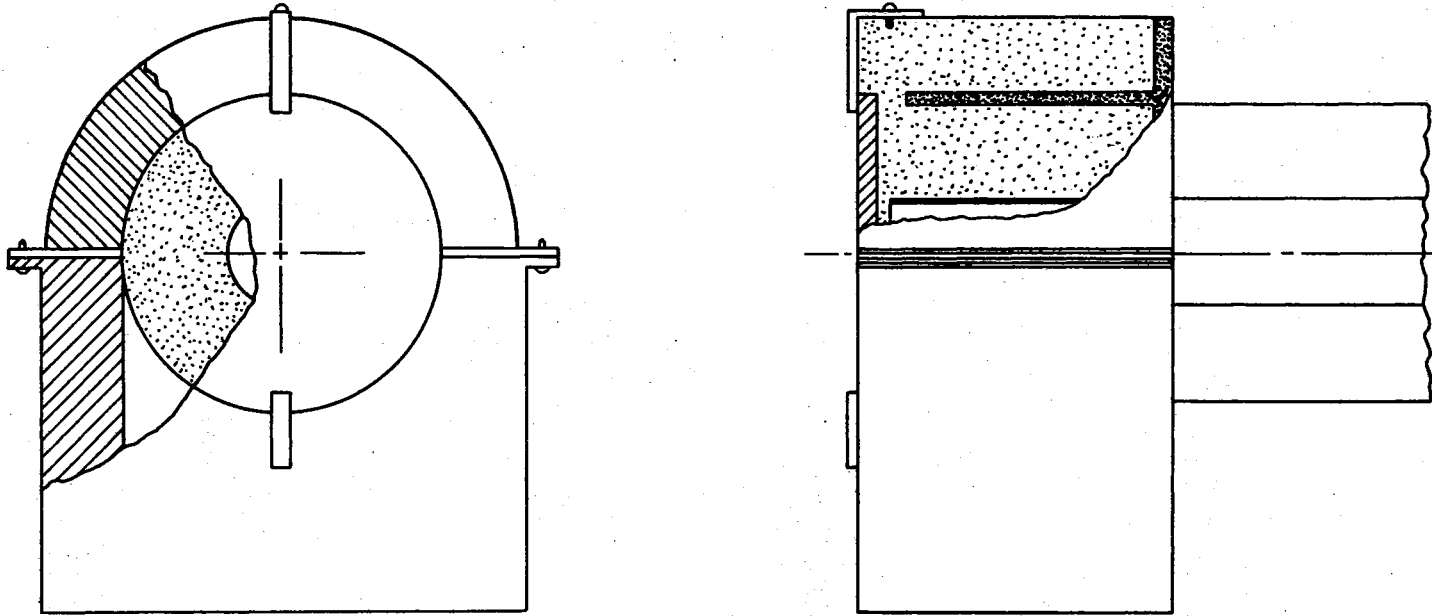
Figure 17.   Views of the Redesigned Fusible-Rod Integrated-Heat Flux
            Meter

the copper disk and the steel support cylinder, thus preventing heat transfer to the support cylinder.

Thus, these redesign improvements were made and tests similar to those described earlier were run by Warren K. Smith.(14) Curve I of Figure 18 indicates the heat up and cooling experienced by the copper disk on an asbestos block when the heat flux is 1.0 cal/cm^{2}sec. Under this same heat flux, Curve II indicates the heat up and cooling experienced by the copper disk in the empty melt stick dosimeter. These curves indicate that during heat ups to the same temperature the controllable heat sinks have been removed. However, when the melt stick dosimeter is loaded with the 2-naphthol rod and tested, Figure 19 indicates that all the problems have not been solved. Curves I and II of Figure 19 are calibration curves for a heat flux of 2 cal/cm^{2}sec and 1 cal/cm^{2}sec, respectively, from the heat source. For a heat flux of 2 cal/cm^{2}sec, Curves III and IV are results of actual runs with the rod in place. Also, for a heat flux of 1 cal/cm^{2}sec, Curve V is the result of an actual run with the rod in place. Additional results of these tests are shown in Table I.

To determine the reason for the discrepancy in the results, further tests in the same set up were run except that this time the length of the melt stick was monitored throughout the run. The results of two of these type of tests are shown in Table II.
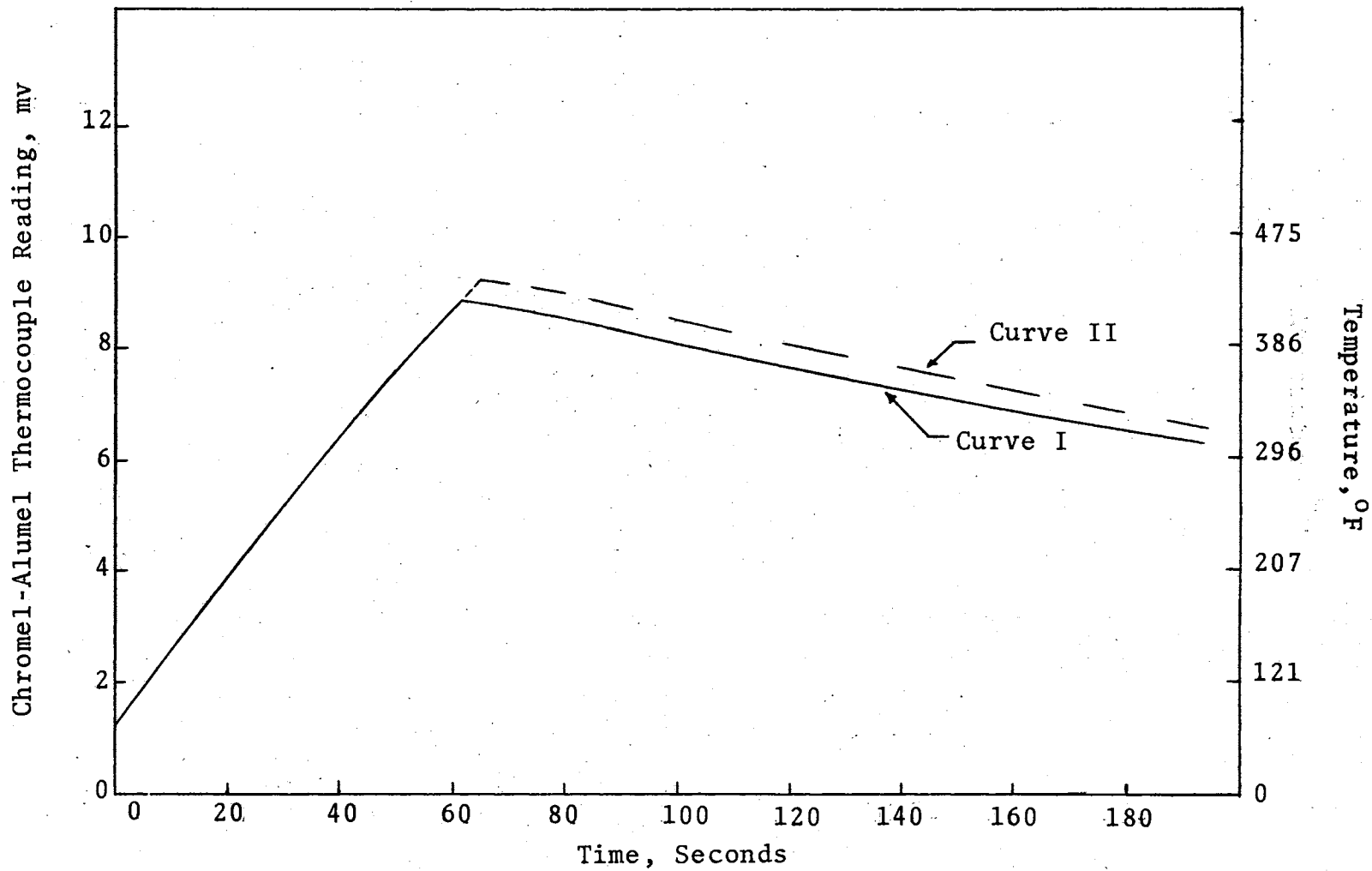
Figure 18.   Thermal Loss Test for Redesigned Melt Stick Dosimeter
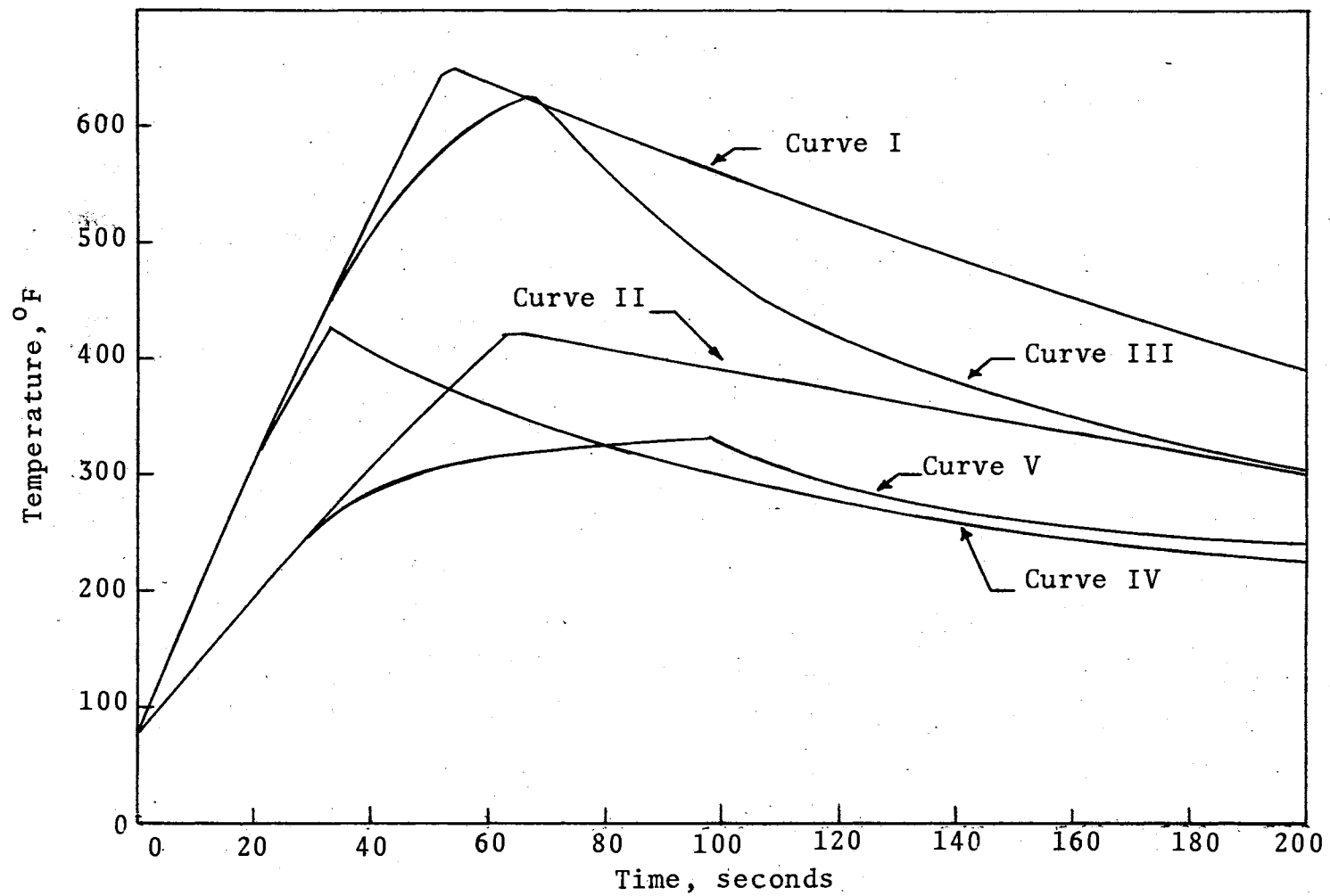
Figure 19. Melt Stick Dosimeter Test with Melt Stick

TABLE I

RESULTS OF TESTS RUN ON THE REDESIGNED
MELT STICK DOSIMETER

Length of Rod Melted in	Heat absorbed to melt this length* BTU	Heat Flux from source cal/cm^{2}sec	Heating Period sec	Heat generated by source BTU
3.69	5.8	1	98	7.87
1.13	3.2	2	33	5.3
2.87	5	2	68	10.92

* Taken from Figure 20 with 75°F as basis.

TABLE II

RESULTS OF MONITORED MELT STICK DOSIMETER TESTS
RUN ON THE REDESIGNED DOSIMETER

Heat flux = 1 cal/cm^{2}sec   Final temperature = 540°F
Heating time = 154 sec   Total heat generated
Initial temperature = 65°F   by source = 12.38 BTU

Time	Change in Time, $\Delta\theta$	Change in length of rod, ΔL	$\Delta L/\Delta\theta$
sec	sec	inches	in/sec
0			
85	85	.5	.0059
110	25	.5	.02
140	30	.4	.0133
170	30	.6	.02
230	60	.4	.0067
330	100	.7	.007

Heat flux = 2 cal/cm^{2}sec   Final temperature = 580°F
Heating time = 51 sec   Total heat generated
Initial temperature = 150°F   by source = 8.2 BTU

Time	Change in Time, $\Delta\theta$	Change in length of rod, ΔL	$\Delta L/\Delta\theta$
sec	sec	inches	in/sec
0			
35	35	.20	.0057
48	13	.20	.0154
66	18	.25	.0139
91	25	.25	.01
151	60	.50	.0083
208	57	.25	.0044

One should note from these tables that the problem
of heat loss is caused by the liquid 2-naphthol not draining
into the material catch tank quickly enough. Table I
indicates that for high fluxes over long periods of time,
a great deal of heat is lost because the viscosity of the
fluid prevents rapid draining of the liquid 2-naphthol.
Another point which should be noted is that given the
conditions for the 2 cal/cm^{2}sec test in Table II, it is
necessary for 5.7 inches of 2-naphthol to melt. Thus,
given that the melting occurs over the 208 second period
then the average ratio of $\Delta L/\Delta\Theta$ must be .02 inches/second
which is a great deal above that actually achieved.
Therefore, continued investigation to find another material
from which fusible rods can be made is necessary.

Proper Interpretation of Dosimeter Test Results

As the rod melts, the remaining portion of the rod is
moved toward the heated metal surface. This procedure may
be visualized as a heat source moving along a stationary
rod. Assuming that the physical properties of the fusible
rod are independent of temperatures and that the initial
atmospheric conditions are known, calculations can be
made to show the dependence of the length of the fusible
rod on the maximum heat which is presupposed to be absorbed
on the exposed metal surface. Figure 20 shows the amount of
heat required to melt various lengths of 1/2 inch diameter
2-naphthol rods at various initial conditions.
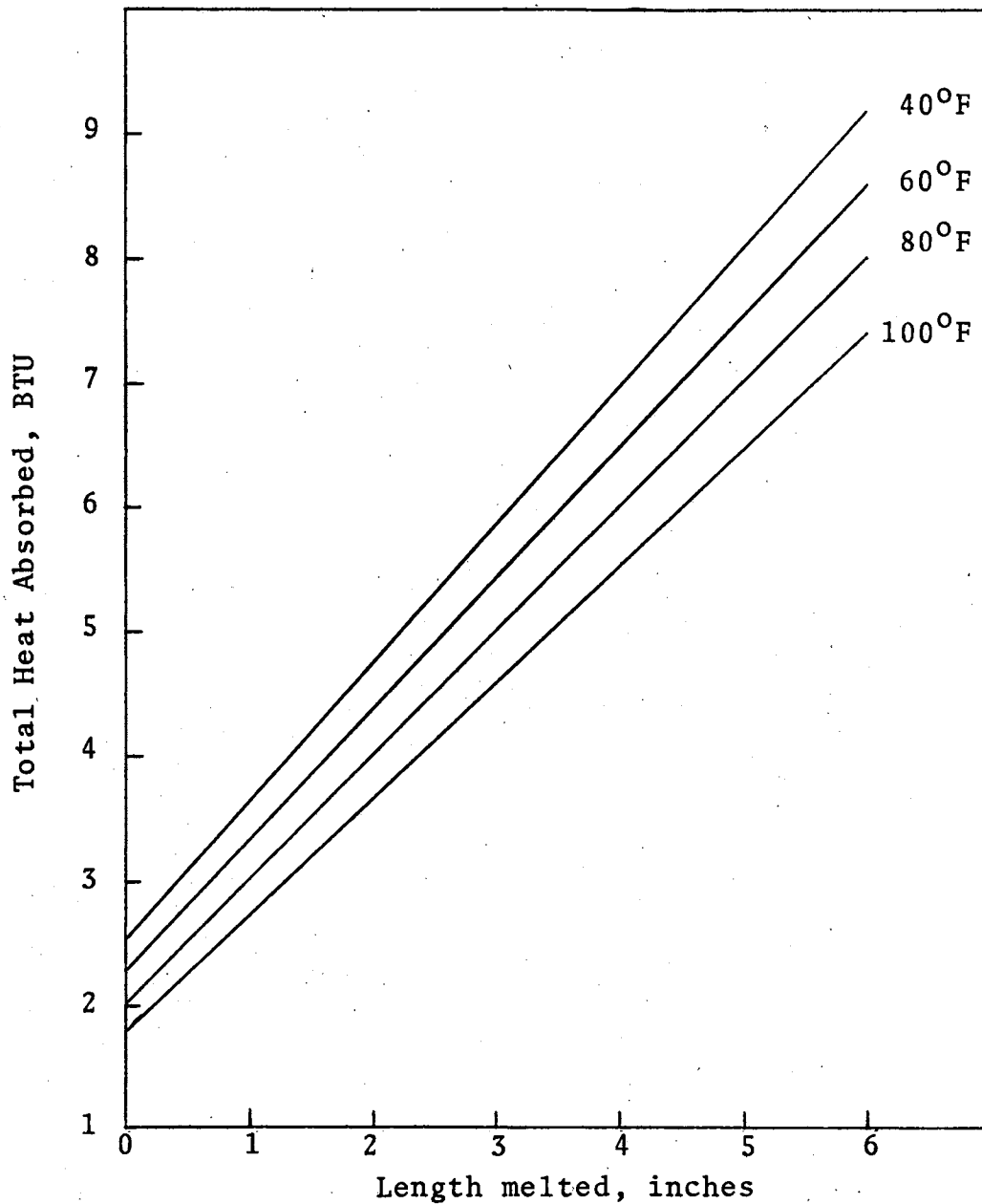
Figure 20. Heat Required to Melt a Given Length
of a 1/2 inch Diameter 2-naphthol
Fusible Rod at Various Initial
Atmospheric Temperatures

Using the following average thermo-physical properties,

Cp = Specific heat of copper = .094 BTU/lb ^{o}F

ρ = Density of copper = 555 lb/ft^3

Cp = Specific heat of 2-naphthol = .345 BTU/lb^{o}F

ρ = Density of 2-naphthol = 76 lb/ft^3

λ_f = Heat of fusion of 2-naphthol = 56.4 BTU/lb

T_m = Melting temperature of 2-naphthol = 122°C = 251.6^{o}F

for a 2 inch diameter by 1/8 inch thick copper disk and a
1/2 inch 2-naphthol rod, the total heat absorbed by the
dosimeter can be determined. The heat balance equation is

$$Q_t = Q_1 + Q_2 + Q_3 \qquad (17)$$

where Q_1, Q_2, and Q_3 are the total heat necessary to raise
the copper disk to the melting temperature of 2-naphthol,
the total heat necessary to raise a given length of 2-naphthol
to its melting temperature, and the total heat necessary to
melt a given length of a 2-naphthol rod. If the specific
heats are constant the equation becomes

$$Q_t = (\rho V Cp \Delta T)_{disk} + (\rho Al Cp \Delta t + \rho Al \lambda_f)_{rod} \qquad (18)$$

$$Q_t = (\rho \pi R^2 t Cp (T_f - T_i))_{disk} + (\rho \pi R^2 l (Cp (T_f - T_i) + \lambda_f))_{rod} \qquad (19)$$

Substituting in the given values, the total heat absorbed
is given by

$$Q_t = .01184 (T_f - T_i) + 1 (.0357 (T_f - T_i) + 5.84) \quad BTU \qquad (20)$$

where T_f, T_i, and l are the melt temperature of 2-naphthol, the initial atmospheric temperature conditions, and the length of 2-naphthol rod melted during the experiment.

CHAPTER IV

TESTING AND ANALYSIS OF TEMPERATURE SENSITIVE PAINTS

Purpose and Objective

The purpose of testing temperature sensitive paints is
to determine if these paints could be a feasible type of
instrumentation for the measurement of the thermal properties
of large fires. These paints would be used most obviously
as maximum temperature indicators, but might have applica-
tion as heat absorption indicators if used in connection
with thermal capacitance devices.

These paints are advertised to indicate by a sharp,
clear, irreversible change of color when the temperature of
a surface has attained or exceeded a predetermined value,
so that information on the temperature of an entire surface
is given at a glance. These indicators can be applied
directly to a solid object either when it is cold and about
to be heated or when it is already hot.

Temperature is indicated by a chemical reaction, where
a molecule of gas, such as ammonia, carbon dioxide, or
water vapor is driven off the basic stock (colorful salts
of metals like nickel, cobalt, or chromium), thus changing
its color. The change is usually permanent after the object

cools. An exception occurs when the gas is water vapor, in which case it may slowly reabsorb this gas from the air and revert to the original color.

Although the color change is theorized to be mainly dependent on the temperature attained, the length of time to which the paint is exposed to that temperature also has some effect. For this reason, the immediate past temperature history of the indicator will influence the exact point at which it will change color. The paints are usually rated for a specific temperature over a certain time period, for instance, $140^{O}F$ in 30 minutes. This means that if held at a constant $140^{O}F$ the color change will occur in 30 minutes. If the color change occurred in less than 30 minutes, the average temperature during that period had been higher than $140^{O}F$ and vice versa. On such an indicator, if the temperature does not exceed $130^{O}F$, the change will never occur. The confidence interval of the paints is estimated as $\pm$ $10^{O}F$ and therefore the paint is considered stable below the confidence interval.

Figure 21 shows typical time-temperature relationships for two different paints, as given in the advertising literature. In the examples shown, the temperature at which color change occurs is quite critical when exposure time is short. For lower exposure temperatures, the change-over will occur in a longer time.

The primary objectives of this testing were to attempt to reproduce temperature vs. time plots supplied by the
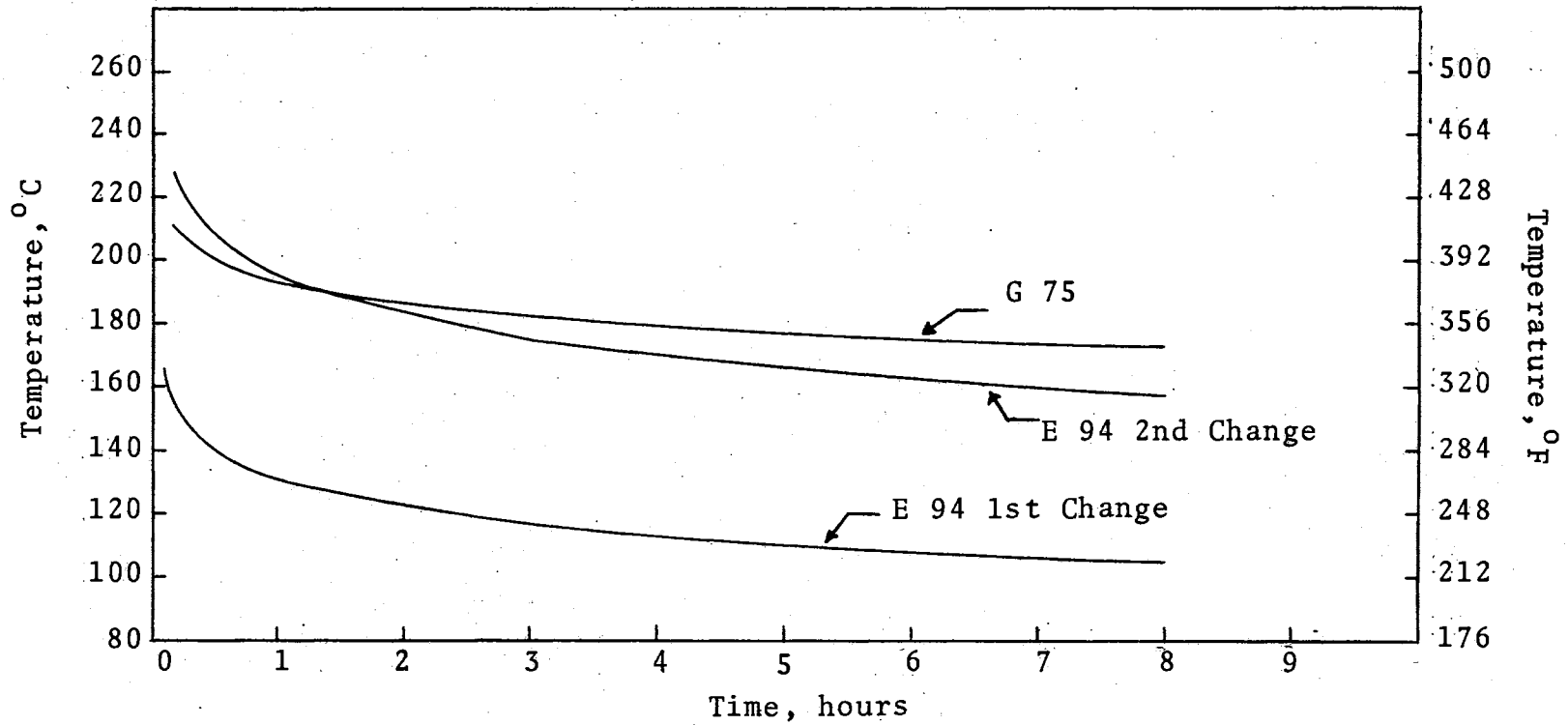
Figure 21.   Time-Temperature Relationship for Two Temperature Sensitive
Paints

manufacturer and to determine the kinetics of the color change in order that predictions of the thermal properties of large fires could be made for times less than the standard exposure time of the paints.

Experimental Apparatus and Procedure

The experiments were conducted on the Tempil Corporation Thermindex E-94 temperature indicating paint. Since all Thermindex paints have been standardized on an exposure period of 10 minutes, the first color change transition temperature for E-94 is 155°C as shown in Figure 21. All experiments on this paint were performed in a Blue M Electric Company Stabil Therm oven. The oven's temperature regulating instrumentation was checked using a calibrated tungsten-tungsten/26% rhenium thermocouple. The thermocouple was introduced through the thermometer well on top of the oven and was held approximately at the level in the oven at which the paint would be tested. The temperature regulating instrumentation performed within the accuracy of reading the potentiometer.

The simple device shown in Figure 22 was used to test the paints in the oven. The 1/16 inch steel plate upon which the paint was placed had three iron-constantan thermocouples imbedded on the top side. To reduce the possible errors caused by radiation effects of the heating coils in the oven, the steel plate was enclosed in a hollow steel box, hereafter called the shield. The air is free to

Thermocouple Wires
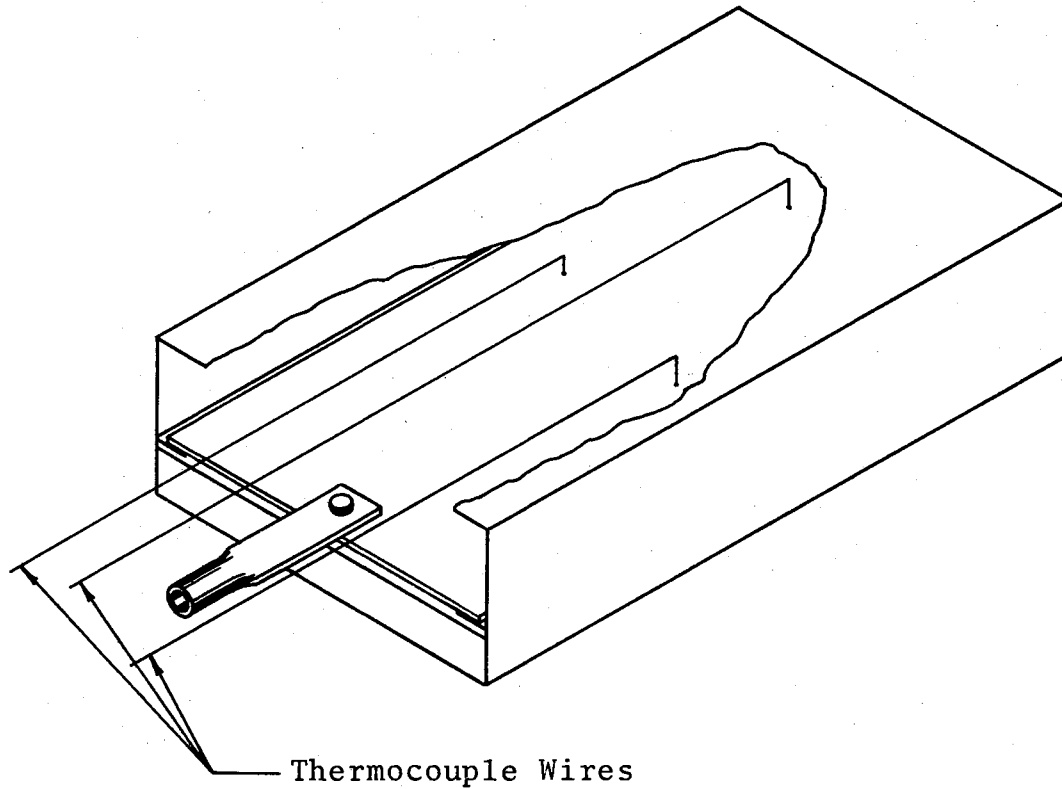
Figure 22.   Apparatus Used In Testing Temperature
Sensitive Paint

pass between the plate to which the thermocouple is attached and the blackened steel box, but the steel plate can see little more than the shield. In these circumstances, the shield exchanges heat primarily with the air and the oven coils and is at some intermediate temperature. The steel plate, however, exchanges heat with the shield and the air and is at some temperature closer to the air temperature than it would have been if the shield were not used. Also, to facilitate the absorption of heat by the shield and to minimize net radiative transport inside the shield, the entire surface area of the shield was blackened with India ink.

The following procedure was used to calibrate the thermocouples on the plate: (1) The oven temperature dial was set at a specified temperature and the oven was allowed to heat to equilibrium over a 3 hour period. (2) The thermocouples and the steel plate were placed in the shield and the entire apparatus was then introduced into the oven for another 3 hour period. During this period, readings from a Leeds and Northrup 8690 potentiometer were recorded every 15 minutes and were correlated to the temperature readings for an iron-constantan thermocouple. (3) This procedure was repeated three times at five different temperature settings over the range from $100^{0}C$ to $250^{0}C$. All three thermocouples read within $\pm 2^{0}F$ of each other and the averages of the temperatures were used as the calibration curve shown in Figure 23.
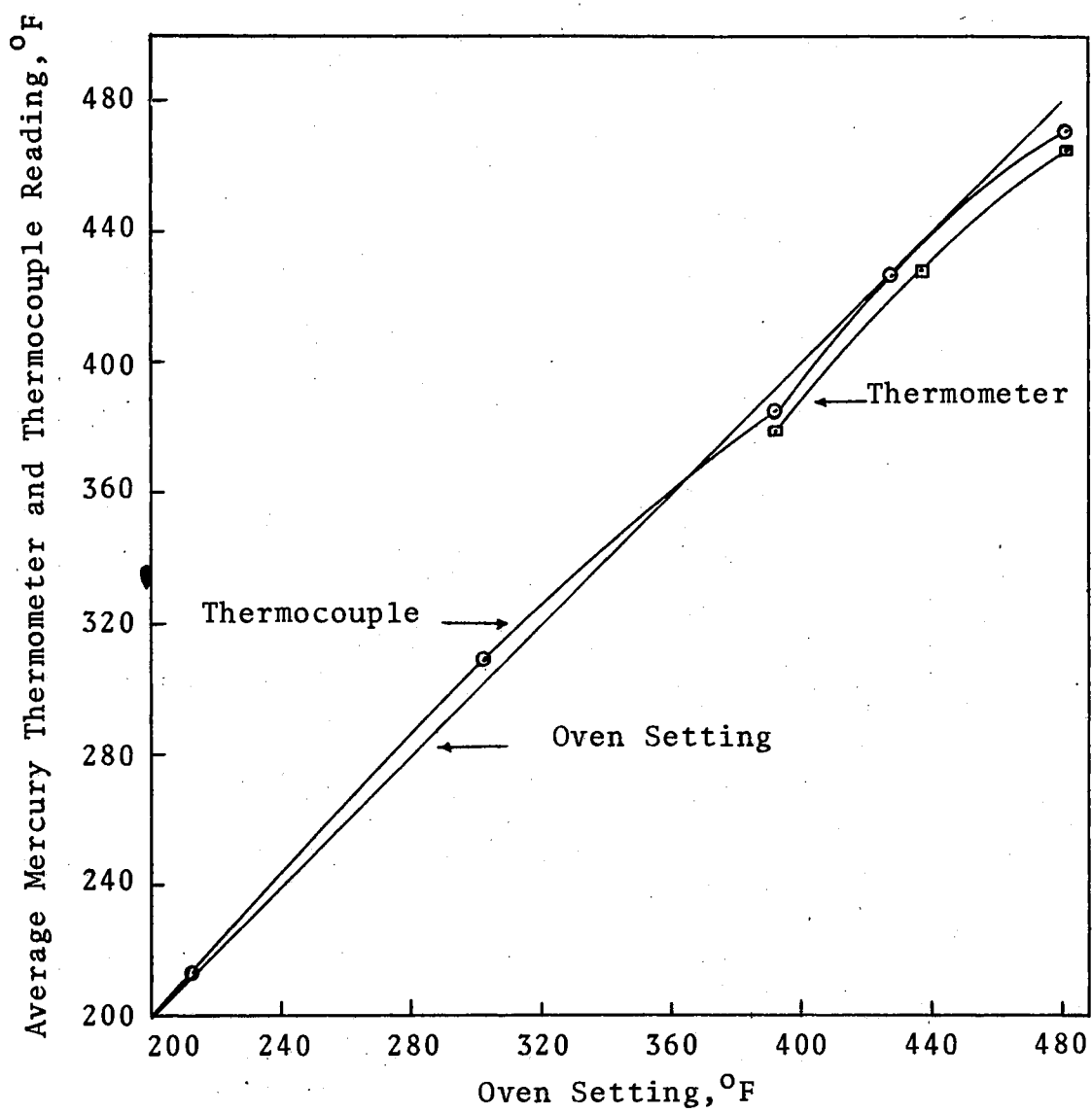
Figure 23.   Iron-Constantan Thermocouple and
             Mercury Thermometer Calibration
             Curve

One should note that to place any part of the apparatus in the oven, the oven door had to be opened thus causing a temperature drop to occur. Therefore, at this time, a thermometer to estimate this temperature drop was calibrated using the tungsten-tungsten/26% rhenium thermocouple. Both the thermometer and the tungsten thermocouple were placed in the oven through the thermometer well and were held approximately at the level of the steel plate. The averages of three repetitions at three temperatures are shown in Figure 23.

The exposure time tests were performed at oven temperature settings of 225°, 240°, and $250^{\circ}C$ and were monitored by the iron-constantan thermocouples in the plate. Since the oven did not have a window, each test at a particular oven setting was a trial and error procedure to determine the specific time at which the paint turned from a bright violet to a bright green. The following procedure was used to test the paints: (1) For each test, the oven containing the black steel box was allowed to attain thermal equilibrium over a three hour period. Also, during this interval, the paint was applied in a uniform coat on the bottom side of the 3 7/8 x 7 1/2 x 1/16 inch steel plate and allowed to dry in the atmosphere. (2) The plate was then placed in the black box in the oven and the temperature was read for each thermocouple every 1 to 2 minutes. (3) After a theorized period of exposure, the plate was removed from the oven and the paint was checked

for change of color. Regardless of whether the color
had changed or not, the paint was removed and a fresh layer
was applied to the bare metal surface and allowed to dry.
(4) If the paint had indeed changed color, additional runs
at the same oven setting were made over shorter time
intervals until the approximate elapsed time to cause a
color transition was found. Likewise, if no color change
had occurred, additional runs were made over longer
exposure periods until the approximate transition time was
found.

Due to opening the oven door to place the steel plate
in the oven, the oven temperature would drop 20-35°F
depending on the initial oven temperature. However, during
the test, the temperature would eventually level out at a
temperature near or lower than the temperature recorded
before the door was opened. Thus, one should note that
the temperature of each run is the average corrected
temperature recorded by the mercury thermometer and not the
temperature shown by the oven setting. The average temper-
atures used in the correlation are shown in Table III.

Analysis of Results

Using the manufacturer's time vs. temperature informa-
tion for the Thermindex E-94 paint shown in Figure 21, one
would suppose that at oven temperatures in excess of 165°C
(330°F) the first color change would occur in less than 5
minutes and that at temperatues in excess of 230°C (446°F),

TABLE III

COMPARISON OF OVEN SETTINGS TO ACTUAL TEST TEMPERATURES

| Run # | Oven Setting, °F | CORRECTED MERCURY THERMOMETER READINGS °F* | | | Average Test Temperature |
		Before Door Opened	After Door Closed	Average Run Temperature	
28	482	474	440	443	
29	482	466	442	421	436.5
30	482	482	460	427	
31	482	481	458	455	
32	437	442	420	421	
33	437	446	428	423	418.5
34	437	446	428	420	
35	437	444	426	410	
45	464	460	430	431	
46	464	458	430	426	429
47	464	463	432	430	

* These values are the corrected mercury thermometer readings and were corrected using Figure 21

the first color change would take place in less than 30
seconds and the second color change would take place in
something less than 10 minutes. However, from the afore-
mentioned trial and error method, the following average
oven temperatures and exposure times for the first color
change were obtained for the Thermindex E-94 paint.

Average Oven Temperature ^{o}F	Exposure Time Min.
436.5	6
429	6 1/2
418.5	7 1/2

Also the manufacturer states that the E-94 paint will begin
to change color the first time when the paint reaches $310^{o}F$
($155^{o}C$). However, during the monitored temperature tests
that have been conducted, the paint did not begin to change
color until the paint had reached $365^{o}F$. These discrep-
ancies in the results lead to testing the E-94 paint on
another metallic surface. Under the same thermal conditions,
a 1/16 inch thick aluminum plate was tested in the black
box in the oven, and in all cases, the paint turned a
brighter green in less time than did the same paint on the
steel surface.

Since the ability of the paint to change colors seems
to be a function of the metallic surface that the paint is
applied to, further analysis to determine the instantaneous
heat transfer coefficient, an estimate of the total heat
absorbed by the paint per unit area, and an estimate of the

activation energy of the reaction(s) of the paint on a
given surface was deemed necessary. Table XIII in Appendix
C indicates the runs and monitored corrected temperatures
and times for those tests which were used in this analysis.
Also, a plot of the averages of these monitored temperatures
vs. time is shown in Figure 24.

Derivation of Equations

Assuming that the thermocouple reading is a true
indication of the temperature of the paint and the plate,
then an equation to determine the heat transfer coefficient
can be obtained. The rate of heat gain from the surroundings
for $\theta > 0$ is given by

$$Q = Cp\rho V\frac{dT_p}{d\theta} = hA(T_o - T_p) \qquad (21)$$

where Cp, ρ, V, and A are the specific heat, density, total
volume, and surface area of the plate, T_p is the uniform
temperature of the plate and the paint at the instant θ,
and h and T_o are values of the unit surface heat transfer
coefficient and the average oven temperature. Transforming
the differential to a difference measurement, the instant-
aneous heat transfer coefficient can be found by

$$h = \frac{Cp\rho V}{A} \frac{\Delta T_p/\Delta\theta}{(T_o - T_p)} \qquad (22)$$
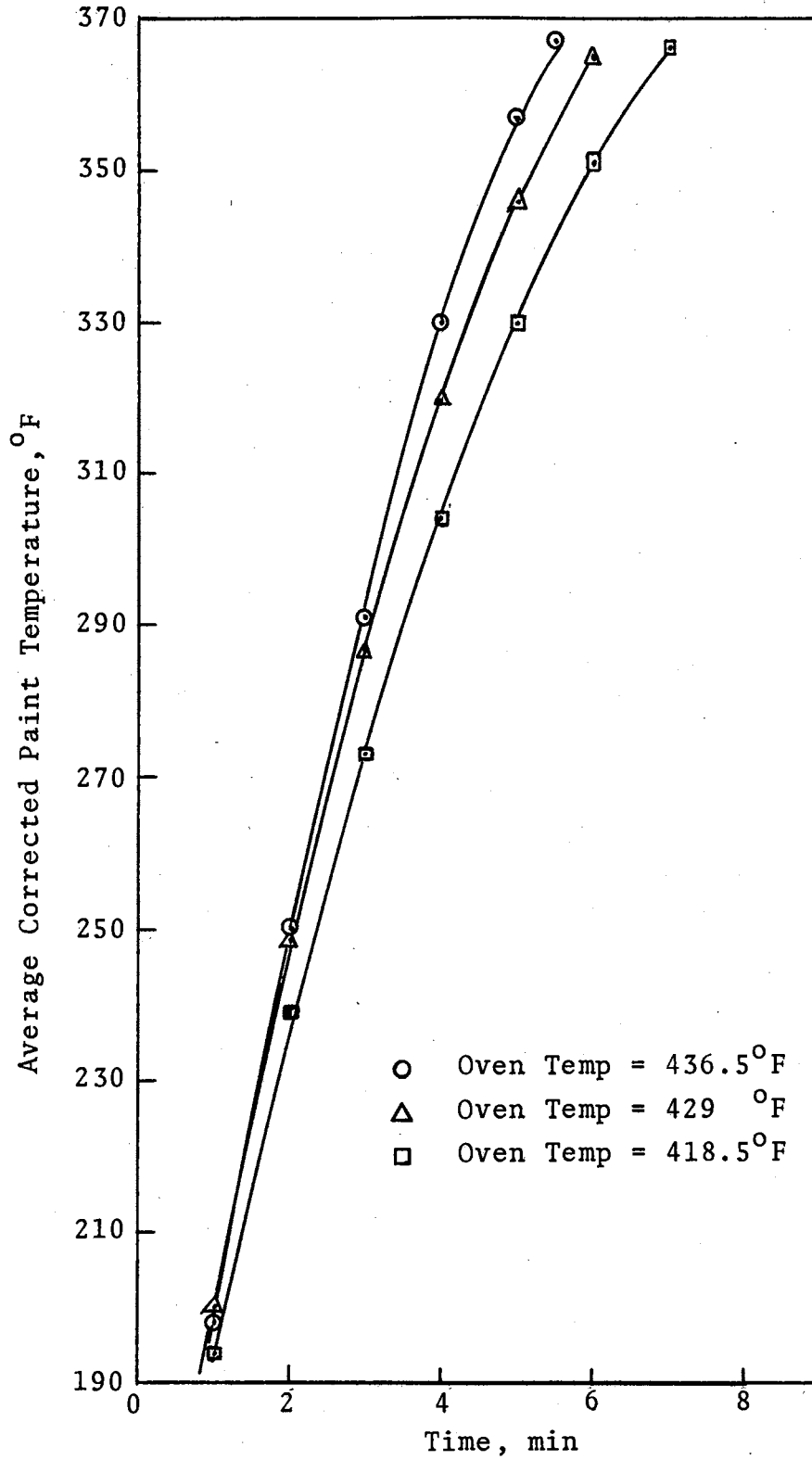
Figure 24.   Average Paint Temperatures vs.
Time for Various Average Oven
Temperatures for the E-94
Paint on a Steel Surface

Assuming that the plate is heated uniformly on both sides, then the volume to area ratio for a volume xyz becomes

$$\frac{V}{A} = \frac{xyz}{2xy} = \frac{z}{2} \tag{23}$$

where z is the plate thickness. Substituting for the volume to area ratio and using the following values for the steel plate,

Cp = .107 BTU/lb^{o}F

ρ = .284 lb/in^3 x 144 in^2/ft^2

z = 1/16 inch

the equation for h becomes

$$h = .136746 \; \frac{\Delta T_p / \Delta \theta}{(T_o - T_p)} \tag{24}$$

where $\Delta T_p / \Delta \theta$ is in units of ^{o}F/hr and $(T_o - T_p)$ is in units of ^{o}F.

Utilizing the aforementioned test data given in Table XIII in Appendix C, a plot of the average plate temperature vs. time for these tests are shown in Figure 24. Using this figure, calculations for h, the instantaneous heat transfer coefficient, were made and the results of the calculations are contained in Table IV. As one would expect, these results indicate that the instantaneous heat transfer coefficient is nearly constant for each average oven temperature but decreases as the average oven temperature decreases.

TABLE IV

CALCULATION OF INSTANTANEOUS HEAT TRANSFER
COEFFICIENT FROM FIGURE 24

Average Oven Temp, T_o ^oF	Time Min	$\Delta T_p/\Delta\theta$ $^oF/Min$	Paint Temp T_p ^oF	Heat Transfer Coefficient, h* BTU/hr ft^2 ^oF	Average Instantaneous h BTU/hr ft^2 ^oF
436.5	1	57.143	198	1.9658	
436.5	2	48.75	250	2.1447	
436.5	3	39.091	291	2.204	2.17
436.5	4	31.111	330	2.397	
436.5	5	21.053	357	2.1727	
436.5	5 1/2	18.261	367	2.156	
429	1	48.75	200	1.7466	
429	2	40.958	249	1.867	
429	3	35.714	285	2.035	1.98
429	4	30.00	320	2.2582	
429	5	21.538	346	2.1291	
429	6	14.211	365	1.822	
418.5	1	43.809	194	1.599	
418.5	2	37.60	240	1.728	
418.5	3	33.125	273	1.868	
418.5	4	28.781	304	2.062	1.81
418.5	5	21.277	330	1.973	
418.5	6	15.43	351	1.875	
418.5	7	10.345	366	1.617	

*h = $((.136746(\Delta T_p/\Delta\theta)/(T_o-T_p)) \times 60)^oF/min \ ^oF$

Returning to Equation (21) and noting that if h is assumed a constant for a given oven temperature and if the exposure time necessary for color change is known, then an estimate of the total heat absorbed by the paint and plate per unit area can be determined. If q is used to denote this rough estimate of the total heat absorbed per unit area then

$$q = \frac{Q}{A}\theta = h(T_o - T_{pa})\theta \qquad (25)$$

where h, T_o, T_{pa}, and θ are the average heat transfer coefficient corresponding to the average oven temperature, the average oven temperature, the average paint temperature, and the exposure time necessary for color change. Table V indicates that the estimate of the total heat absorbed per unit area is approximately 45.1 BTU/ft^2 when the average paint temperature is 222.5^{o}F.

Kinetics of Reaction

In order to predict how these temperature sensitive paints will perform in exposure times of less than one minute, the overall kinetics of the reaction(s), i.e. reaction rate and order, are needed. Using the aforementioned experimental data, an attempt was made to characterize an overall chemical reaction rate constant for the paint by assuming that the paint followed Arrhenius' law. From this attempt an estimate of the activation energy, E, was made.

TABLE V

CALCULATION OF THE TOTAL HEAT ABSORBED PER UNIT AREA DURING THE COLOR CHANGE OF THE E-94 THERMINDEX PAINT

Average Oven Temperature $^\circ$F	Paint Exposure Time Min	Average h_2 BTU/ft^{2}hr$^\circ$F	Initial Paint Temperature $^\circ$F	Final Paint Temperature $^\circ$F	Average Paint Temperature $^\circ$F	Total Heat Absorbed BTU/ft^2
436.5	6	2.17	75	370	222.5	46.5
429	6 1/2	1.98	75	370	222.5	44.3
418.5	7 1/2	1.81	75	370	222.5	44.5

Average total heat absorbed = 45.1 BTU/ft^2

For many reactions and in particular elementary
reactions, the reaction rate expression can be written as
a product of a temperature-dependent term and a composition-
dependent term, or

$$\text{rate} = K \cdot f(\text{composition}) \tag{26}$$

For such reactions the temperature-dependent term, the
reaction rate constant K, has been found to be well repre-
sented by Arrhenius' law:

$$K = k_o e^{-E/RT} \tag{27}$$

where k_o is called the frequency factor and E is the
activation energy of the reaction. Substituting and
rearranging, Equation (26) becomes

$$\frac{dC}{k_o \cdot f(C)} = e^{-E/RT} d\theta \tag{28}$$

Since the left hand side of the equation is independent
of temperature and it is assumed that the first color change
of the E-94 paint corresponds to a constant degree of comple-
tion of the reaction, the areas determined by integrating
the right hand side of the equation must be equal for the
different exposure time-temperature combinations. Therefore,
knowing the temperature-time profile for a given paint
exposure, and the time necessary for the first color change,
the right side of Equation (28) can be graphically integrated
for certain fixed assumed values of E/R. Thus, using the

temperature-time profile given in Figure 24 or Table XIII
in Appendix C, the E/R ratio which was determined by trial
and error and which was necessary to make the areas
approximately equal, was 28000°K. Therefore, the activa-
tion energy E is approximately equal to 55,500 calories/gm.
mole for the E-94 paint on a steel plate in an oven envir-
onment. For the three different exposure times and temper-
atures used in determining the E/R estimate, Table VI
indicates the results of the aforementioned trial and
error calculations necessary for plotting the points on
Figure 25. The area under the curves of Figure 25 are the
values for the right hand side of Equation (28) and those
areas are

Exposure Time Min.	Area 1/4 inch squares
6	67.52
6 1/2	62
7 1/2	68.24

One should note that the $e^{-E/RT}{}_p$ value at the time of color
change shown in Figure 25 is an extrapolated value. With the
apparatus used in these experiments, it was not possible to
record the paint temperature at the time of color change.

Also, due to the lack of time, evaluation of the
frequency factor and reaction order were not attempted.

TABLE VI

CALCULATIONS NECESSARY TO DETERMINE THE ACTIVATION ENERGY
OF THE THERMINDEX E-94 PAINT FOR $E/R=28000°K$

Oven Setting $°C$	Avg. Oven Temp $°F$	Time Min	T_p Paint Temp $°F$	T_p Temp $°K$	E/RT_p	e^{-E/RT_p}
250	436.5	1	198	365.2	76.7	5.04×10^{-34}
		2	250	394	71.	1.37×10^{-31}
		3	291	416.5	67.2	6.36×10^{-30}
		4	330	438.5	64.	1.86×10^{-28}
		5	357	453.5	61.9	1.54×10^{-27}
		5 1/2	367	459	61.	3.20×10^{-27}
240	429	1	200	366.5	76.5	6.62×10^{-34}
		2	249	393	71.2	1.14×10^{-31}
		3	287	416	67.2	3.60×10^{-30}
		4	320	433	64.7	8.25×10^{-29}
		5	346	447	62.6	6.25×10^{-28}
		6	365	458	61.1	2.81×10^{-27}
225	418.5	1	194	363	77.1	3.17×10^{-34}
		2	239	388	72.1	4.56×10^{-32}
		3	274	407	68.6	1.22×10^{-30}
		4	304	424	66.	2.09×10^{-29}
		5	330	438.5	64.	1.86×10^{-28}
		6	351	450	62.2	9.50×10^{-28}
		7	366	458.5	61.1	3.00×10^{-27}
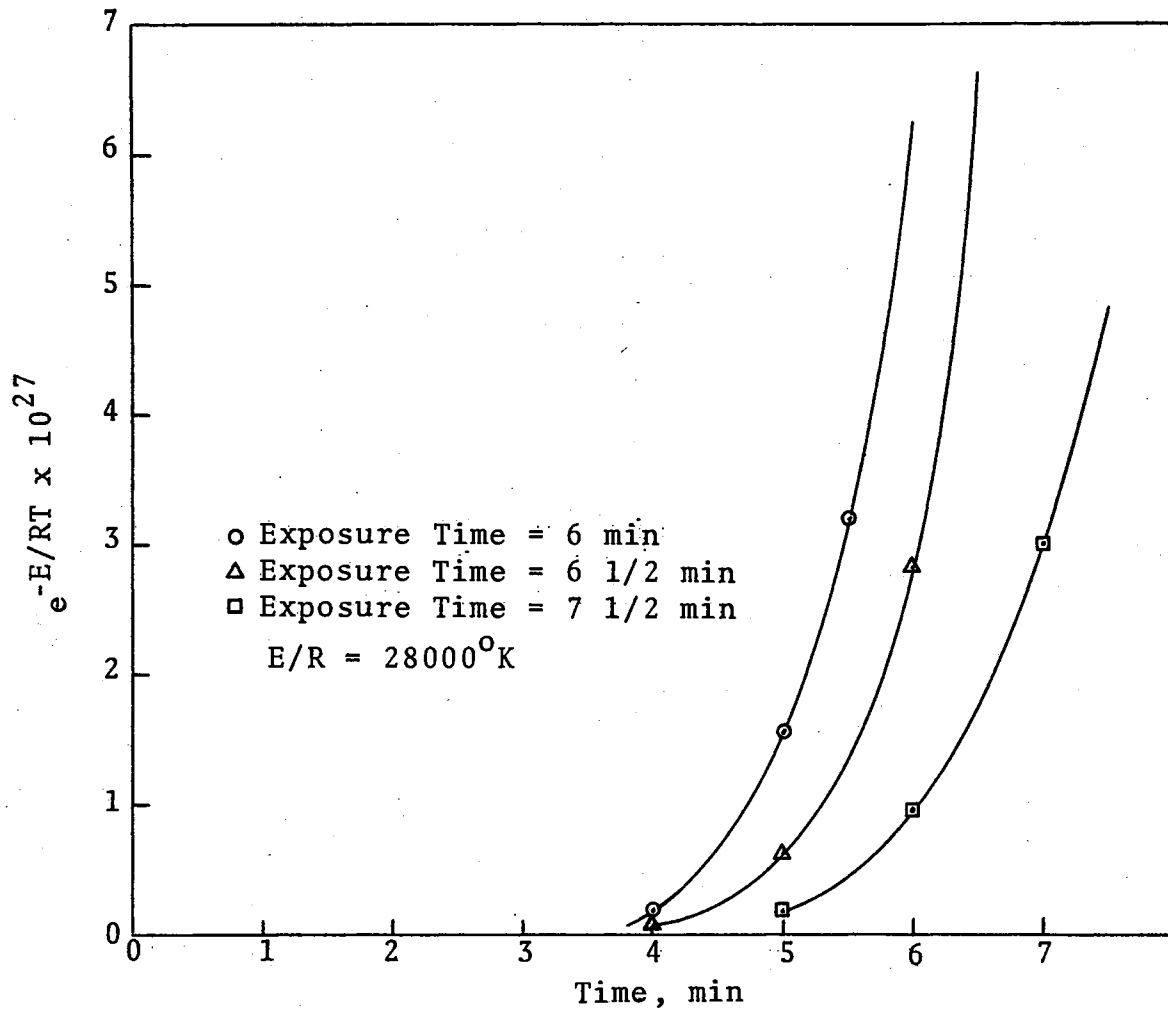
Figure 25. Equal Area Plot to Determine the Activation
Energy of the Thermindex E-94 Paint

Conclusions and Recommendations

The experimentally measured times necessary for color transition on a steel plate differ greatly from those times reported by the manufacturer. Also, in some preliminary comparison tests with an aluminum plate, it was determined that the times necessary for color transition are not the same for steel and aluminum plates.

Oven Setting ^{o}C	Paint Transition Time, Minutes	
	Steel Plate	Aluminum Plate
250	6	5
240	6 1/2	5 1/4
220	7 1/2	6

Therefore, explanation from the manufacturer is necessary to bring these results in line with those reported by the manufacturer and further testing is necessary to determine the effect of various testing surfaces.

Color transition of the paint is not a sharp change from bright violet blue to bright green as advertised, but instead changes from bright violet blue to various shades of blue green and then bright green. Therefore, judgment decisions as to the state of transition are necessary, and these judgments could easily lead to incorrect conclusions. Hence, either visual color standards are necessary or equipment capable of measuring color pigments in paint are required.

The kinetics of the reaction(s) for a given paint, along with a temperature history of the fire will enable investi-

gators to determine the amount of heat absorbed to cause a known amount of paint to change colors. Although an estimate of the activation energy for color transition was determined, more study is necessary to determine the reaction rate and order for these paints.

A simple, inexpensive method for measuring the maximum temperature in a fire is vital to the understanding of unconfined fires. Therefore, more experimentation with other temperature sensitive paints, as well as expanding experimentation to testing of Tempilabels is deemed necessary. Tempilabels, which are pressure-adhesive temperature monitors consisting of one or more heat sensitive indicators sealed under transparent heat-resistant windows, would serve as a permanent record because these tabs in contrast to paint can be removed without damage.

CHAPTER V

SUMMARY AND RECOMMENDATIONS

This study has been primarily concerned with the actual design, construction, field testing, and analysis of simple heat sensing devices for large unconfined fires. One of the instruments, the evaporative dosimeter, has been shown to be practical for application while the other instruments which were studied indicate that further testing is necessary.

The following recommendations are made concerning future work:

1. Laboratory tests should be initiated to determine the level of heat flux at which liquid entrainment occurs in the evaporative dosimeter and to determine the actual in-fire efficiency for various feasible evaporative dosimeter configurations.

2. Continued investigation is needed to further modify the melt stick dosimeter design or to discover another material with low viscosity which fits the other criteria stated in the text, or both.

3. Further testing should be done on the temperature sensitive paints in an effort to determine (1) the effect of different testing surfaces, (2) the reaction order and

frequency factor of the reaction(s), and (3) the usefulness of other indicators such as Tempilabels.

    4. Actual field testing should continue to be performed on small numbers of the modified instruments.

    5. Work should continue in other areas in hope of discovering some simplier device for measuring the heat effects of unconfined fires.

A SELECTED BIBLIOGRAPHY

1. Arpaci, V. S. Conduction Heat Transfer. London: Addison-Wesley Publishing Co., 1966.

2. Countryman, C. M. "Mass Fire Characteristics in Large Scale Tests," Fire Technology, Vol. 1, No. 4 (November, 1965), 303-317.

3. Eckert, E. R. G., and R. M. Drake, Jr. Heat and Mass Transfer. New York: McGraw-Hill Book Co., Inc., 1959.

4. Edwards, J. D., F. C. Frary, and Z. Jeffries. The Aluminum Industry. Vol. II: Aluminum Products and Their Fabrication. New York: McGraw-Hill Book Co., Inc., 1930.

5. Gallant, R. W. "Physical Properties of Hydrocarbons," Hydrocarbon Processing, Vol. 45 (March, 1966), 161-168.

6. Gallant, R. W. "Physical Properties of Hydrocarbons," Hydrocarbon Processing, Vol. 46 (April, 1967), 183-196.

7. Gallant, R. W. "Physical Properties of Hydrocarbons, Hydrocarbon Processing, Vol. 46 (May, 1967), 201-215.

8. Hodgman, C. D. Handbook of Chemistry and Physics. 33rd ed. Cleveland: Chemical Rubber Publishing Co., 1951.

9. International Critical Tables. New York: McGraw-Hill Book Co., Inc., 1933.

10. Lange, N. A. ed. Handbook of Chemistry. 10th ed. New York: McGraw-Hill Book Co., Inc., 1961.

11. McCoy, D. C. "Simple Instrumentation for Large Fires." (M. S. Thesis, Oklahoma State University, 1967.)

12. Perry, J. H. Chemical Engineers' Handbook. 4th ed. New York: McGraw-Hill Book Co., Inc., 1963.

13. Smith, W. K. Naval Weapons Center, China Lake,
         California, Private Communication, March 25, 1971.

14. Smith, W. K. Naval Weapons Center, China Lake,
         California, Private Communication, Spring, 1972.

15. Stechers, P. G. ed. The Merck Index. 8th ed. Rahway,
         N. J.: Merck and Co., Inc., 1968.

16. Thermindex Temperature Indicating Paints. New York:
         Tempil Corporation, 1970.

17. Touloukian, Y. S. ed. Thermophysical Properties
         Research Literature Retrieval Guide. 2nd ed.
         New York: Plenum Press, 1967.

APPENDIX A

TYPICAL CALCULATIONS AND DETAILED DRAWINGS

FOR THE EVAPORATIVE DOSIMETER

TYPICAL CALCULATIONS

Derivations of the total heat absorbed by a dosimeter and the total heat flow per unit area were made utilizing the following assumptions:

(1) Copper and aluminum are prefect heat conductors.

(2) Thermal expansion of dosimeter is neglected.

(3) Specific heats and heats of vaporization of the test liquids are constant.

(4) The vapor formed during the test is not superheated at any time, i.e. all heat absorbed by the dosimeter is transferred to the test liquid.

Using the assumptions above, the sensible heat absorbed by the dosimeter and the test liquid when being heated from the initial atmospheric temperature to the boiling point of the liquid is

$$Q = (W_m Cp_m + \rho_1 V_{i1} Cp_1)(T_b - T_i) \tag{29}$$

where W_m, ρ_1, V_{i1}, Cp_m, and Cp_1 are the weight of the dosimeter without the lid, the density of the test liquid, the initial volume of the test liquid, and the specific heats of the dosimeter and the test lqiuid, respectively. The specific heat of the test liquid should be evaluated at the average temperature between T_i and T_b.

If a volume V_1 of the liquid is vaporized during a test, the total heat absorbed by the dosimeter is

$$Q_t = (W_m Cp_m + \rho_1 V_{i1} Cp_i)(T_b - T_i) + \lambda_1 \rho_1 V_1 \tag{30}$$

where λ_1 is the latent heat of vaporization at the boiling point of the test liquid.

If the weight of the dosimeter is not known, then the weight term for the dosimeter can be calculated from the following equation

$$W_m = \pi \rho_m \ (R_o^2 H_o - R_i^2 H_i) \tag{31}$$

where R_o and R_i are the outside and inside radii of the dosimeter respectively and H_o and H_i are the outside and inside heights of the dosimeter with the lid not included. The dimensions necessary to make this calculation are included in the detailed drawings included in the thesis. The physical properties were taken from references (4,8,9,12) and are given below.

For Copper: $Cp = .09305 \ \text{cal/g}^oC$

   $W_m = 76.312 \ g$

   $\rho_m = 8.91 \ \text{g/cm}^3$

For Aluminum: $Cp = .214 \ \text{cal/g}^oC$

   $W_m = 133.41 \ g$

   $\rho_m = 2.71 \ \text{g/cm}^3$

For Carbon Tetrachloride: $Cp = .201 \ \text{cal/g}^oC$

   $\lambda_1 = 46.42 \ \text{cal/g}$

   $T_b = 76.8 \ ^oC$

   $\rho_1 = 1.595 \ \text{g/cm}^3$

For Water: $Cp = 1 \ \text{cal/g}^oC$

   $\lambda_1 = 538.7 \ \text{cal/g}$

$$T_b = 100^{\circ}C$$

$$\rho_1 = .995 \text{ g/ml}$$

Substituting these values into Equation (30) of this Appendix, the total heat absorbed for water and carbon tetrachloride is given in Figures 9 and 10 for the 25 ml copper dosimeter and Figures 5 and 6 for the 100 ml aluminum dosimeter.

The total heat flow per unit area is based on the theory that the best estimate of the effective heat transfer surface is the outside surface of the bottom cylinder part of the dosimeter. The air gap between the aluminum dosimeter cap and the cup acts as an insulator. This insulator prevents heat transfer from the aluminum cap to the dosimeter cup, but at the same time the air heated by the fire does transfer heat to the dosimeter cup. If the aluminum cap fits such that intimate metal to metal contact was involved then the area in question would be the surface area of the aluminum cap plus the surface area of the cup which is not covered by the cap. However, if the air was a perfect insulator and there was little circulation of the heated air under the cap, then the surface area for heat transfer would be only that surface area not covered by the aluminum cap. Therefore, since no estimate can be made of either the amount of metal to metal contact nor the insulating effectiveness or circulation of air, the total outside surface area of the dosimeter cup but not the cap is used as the estimate of the heat transfer surface area and is given by

$$A_m = \pi R_o^2 + 2\pi R_o H_o \tag{32}$$

where R_o and H_o are the outside radius of the dosimeter
and the outside height of the dosimeter cup. From the
dimensioned drawings in this Appendix, R_o and H_o equal 1/2
inch and 3 inches, respectively for the 25 ml dosimeter and
1.125 inches and 2.715 inches, respectively for the 100 ml
dosimeter. Therefore, the estimate of the heat transfer
area is .0704 ft^2 for the 25 ml dosimeter and .1607 ft^2 for
the 100 ml dosimeter. Using Figures 5, 6, 9 and 10 and the
above areas, the total amount of heat absorbed per unit area
as shown in Figures 7, 8, 11 and 12 can be determined. For
ease of calculation in units of cal. and cal/cm^2, Figures 26-
33 are included in this Appendix.

In an unconfined fire, the most important heat transfer
mechanism is convective heat transfer through air. McCoy
has shown that for low heat transfer coefficients, the heat
absorption efficiency is between .95 and 1.0 for dosimeters
with near minimum surface to volume ratios and relatively
low height to diameter ratios. Therefore, since the
approximate range of the convective heat transfer coefficient
for air is .2 - 10 BTU/hr ft^2 °F, the heat absorption efficiency
on the collected data is assumed to be 1.0 for the 25 and
100 ml dosimeters.
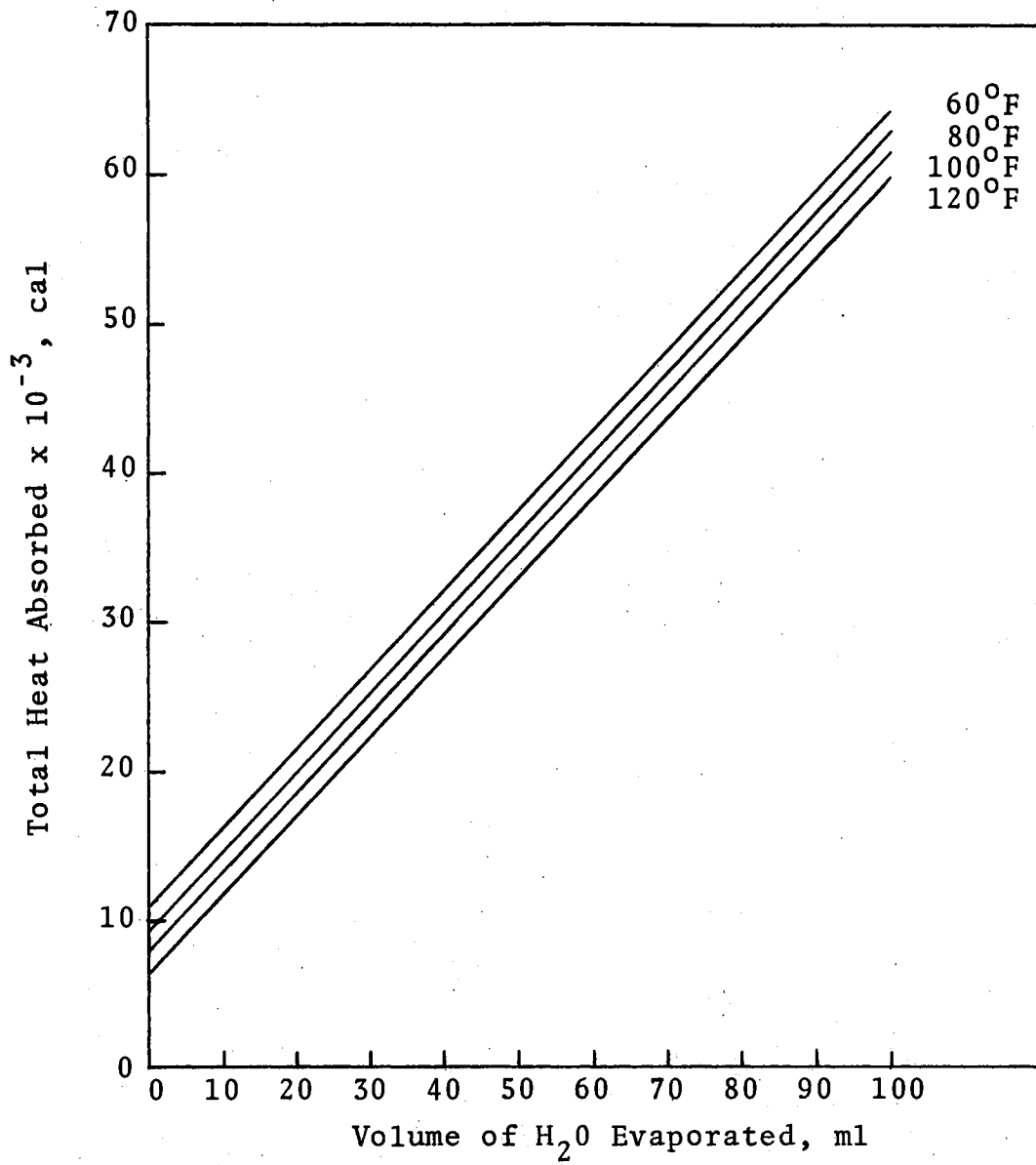
Figure 26.   Total Heat Absorbed by the Aluminum
             Dosimeter Containing 100 ml of
             Water
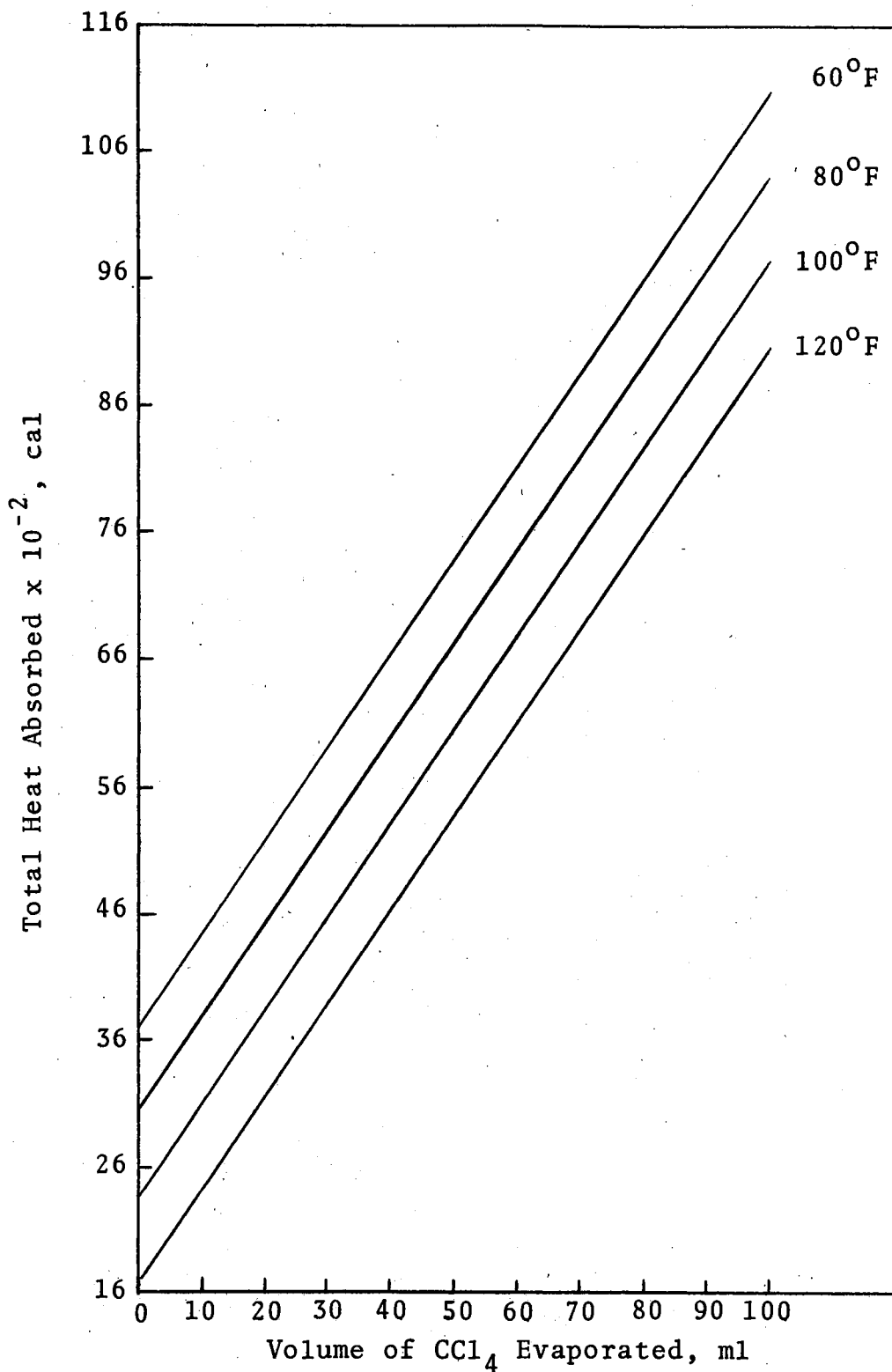
Figure 27.   Total Heat Absorbed by the
                    Aluminum Dosimeter Containing
                    100 ml of Carbon Tetrachloride
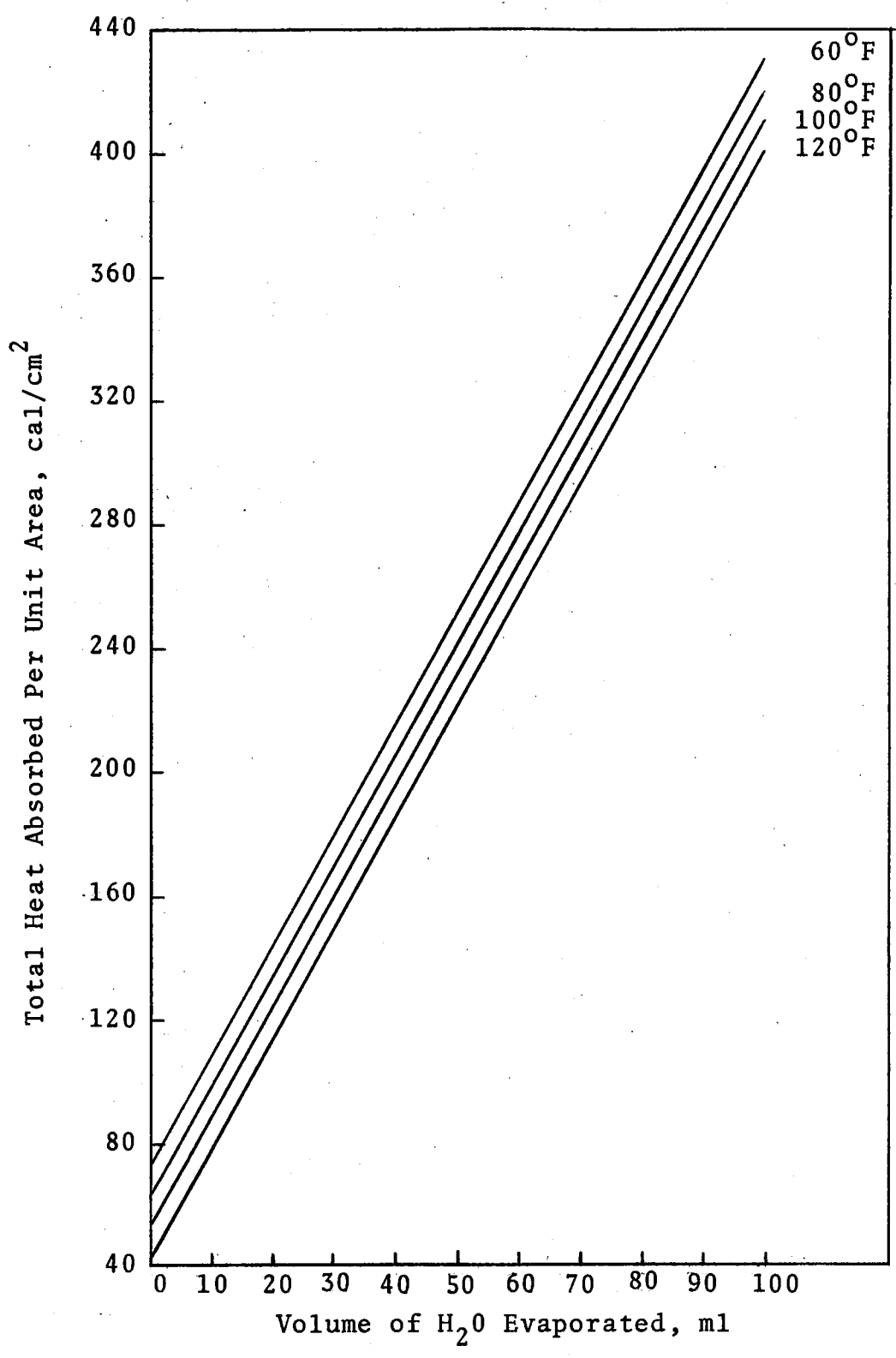
Figure 28. Total Heat Absorbed Per Unit Area
           for the Aluminum Dosimeter Con-
           taining 100 ml of Water
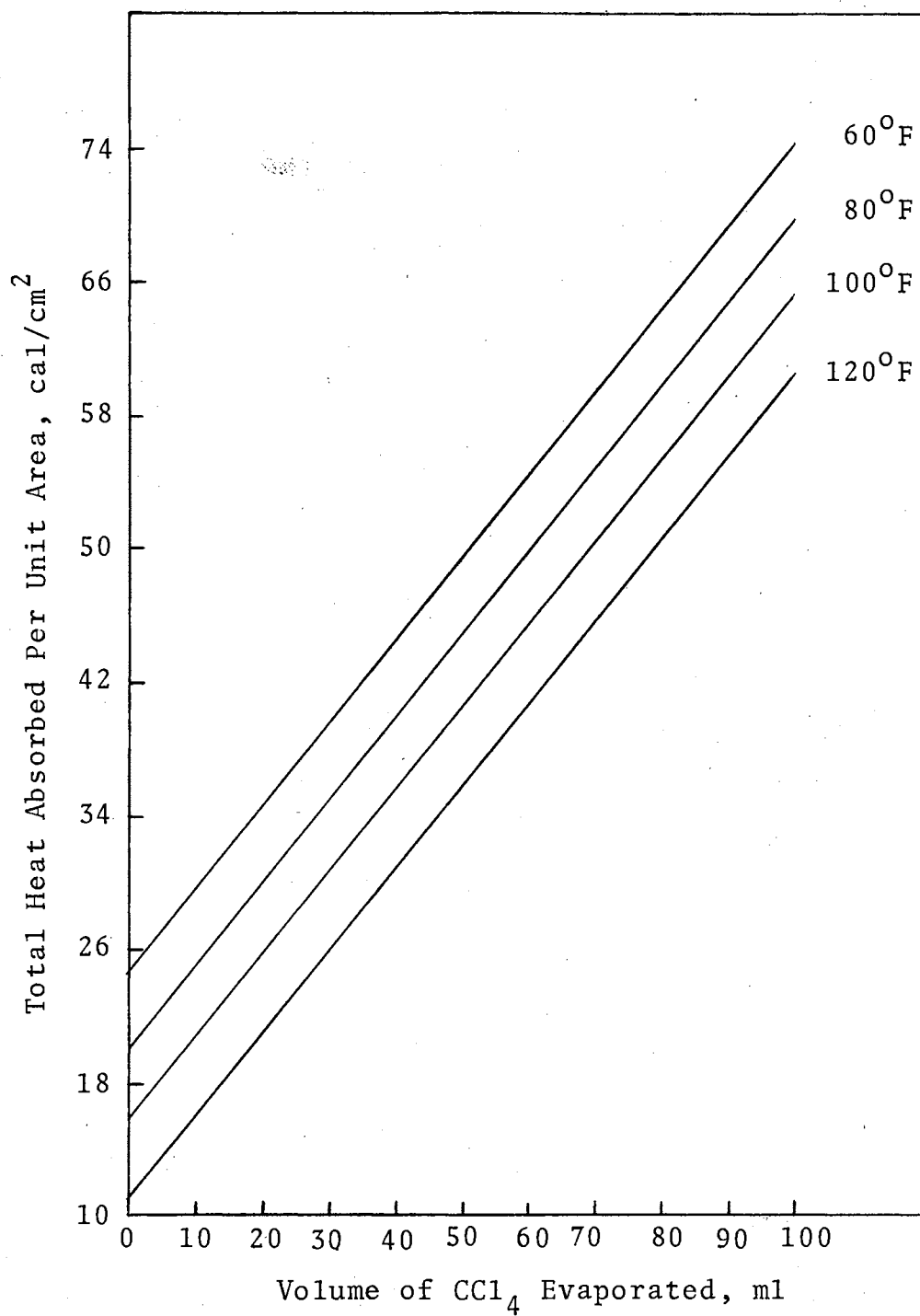
Figure 29. Total Heat Absorbed Per Unit Area
           for the Aluminum Dosimeter Con-
           taining 100 ml of Carbon Tetra-
           chloride
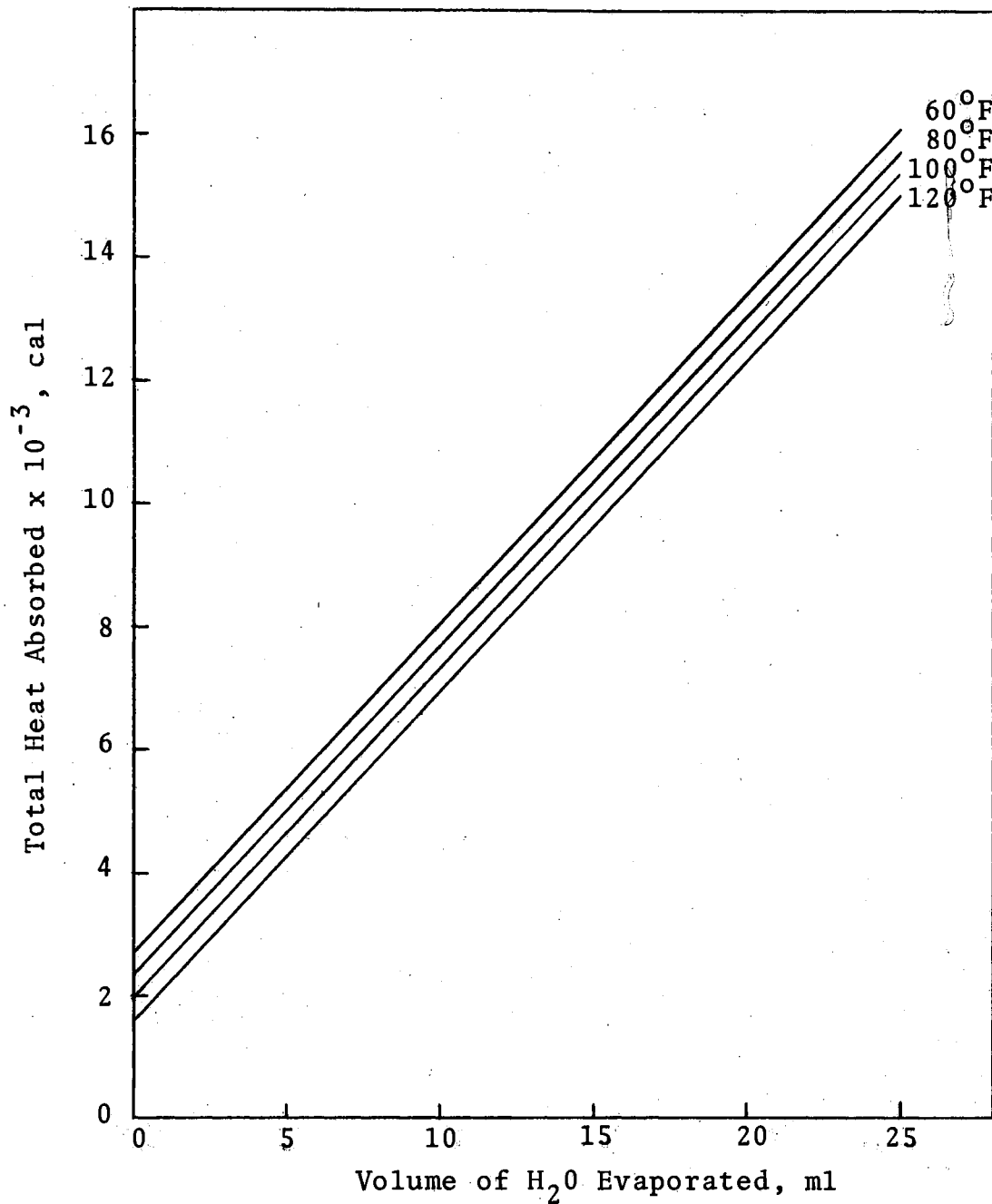
Figure 30. Total Heat Absorbed by the Copper
Dosimeter Containing 25 ml of Water
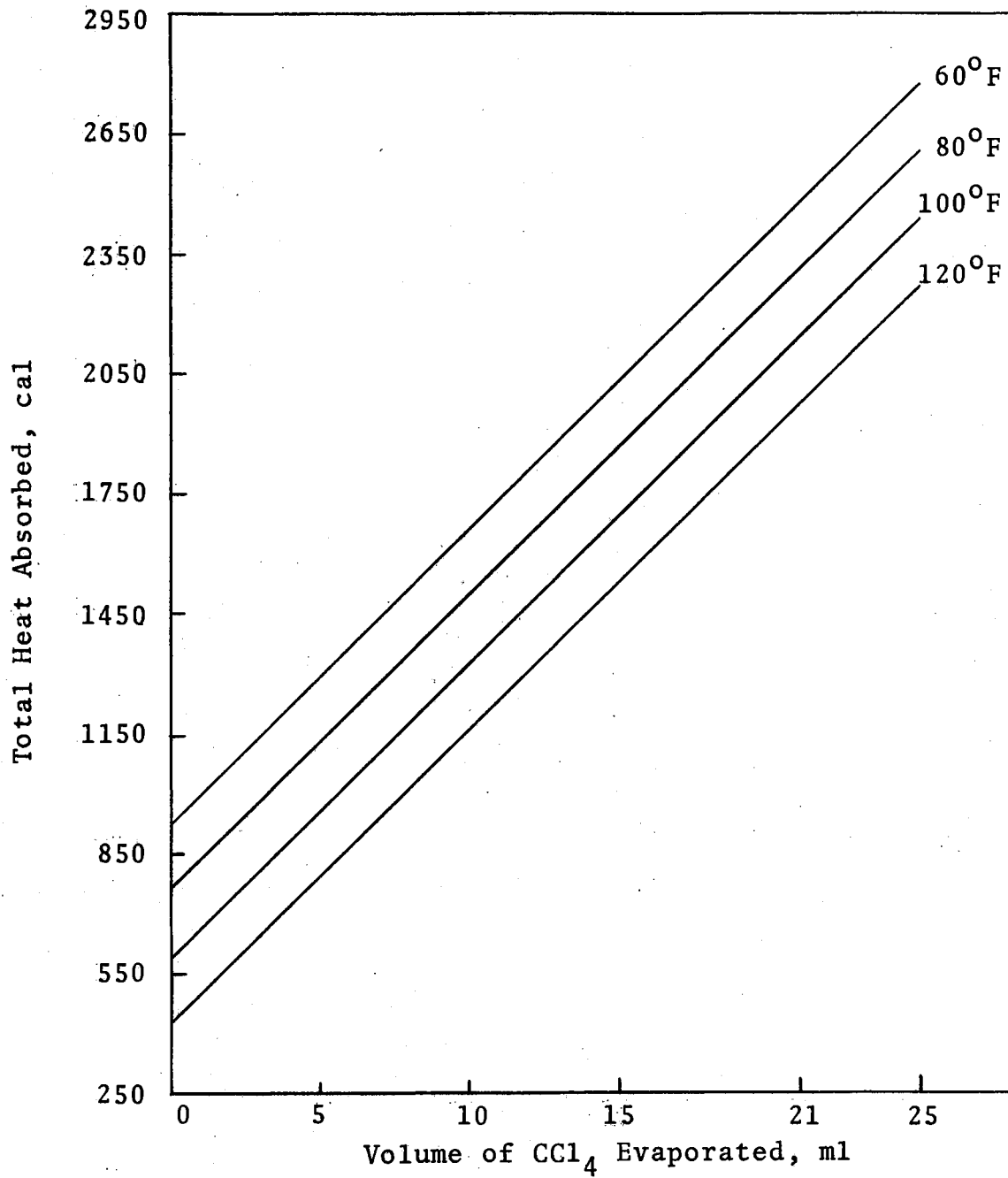
Figure 31.   Total Heat Absorbed by the Copper
Dosimeter Containing 25 ml of
Carbon Tetrachloride
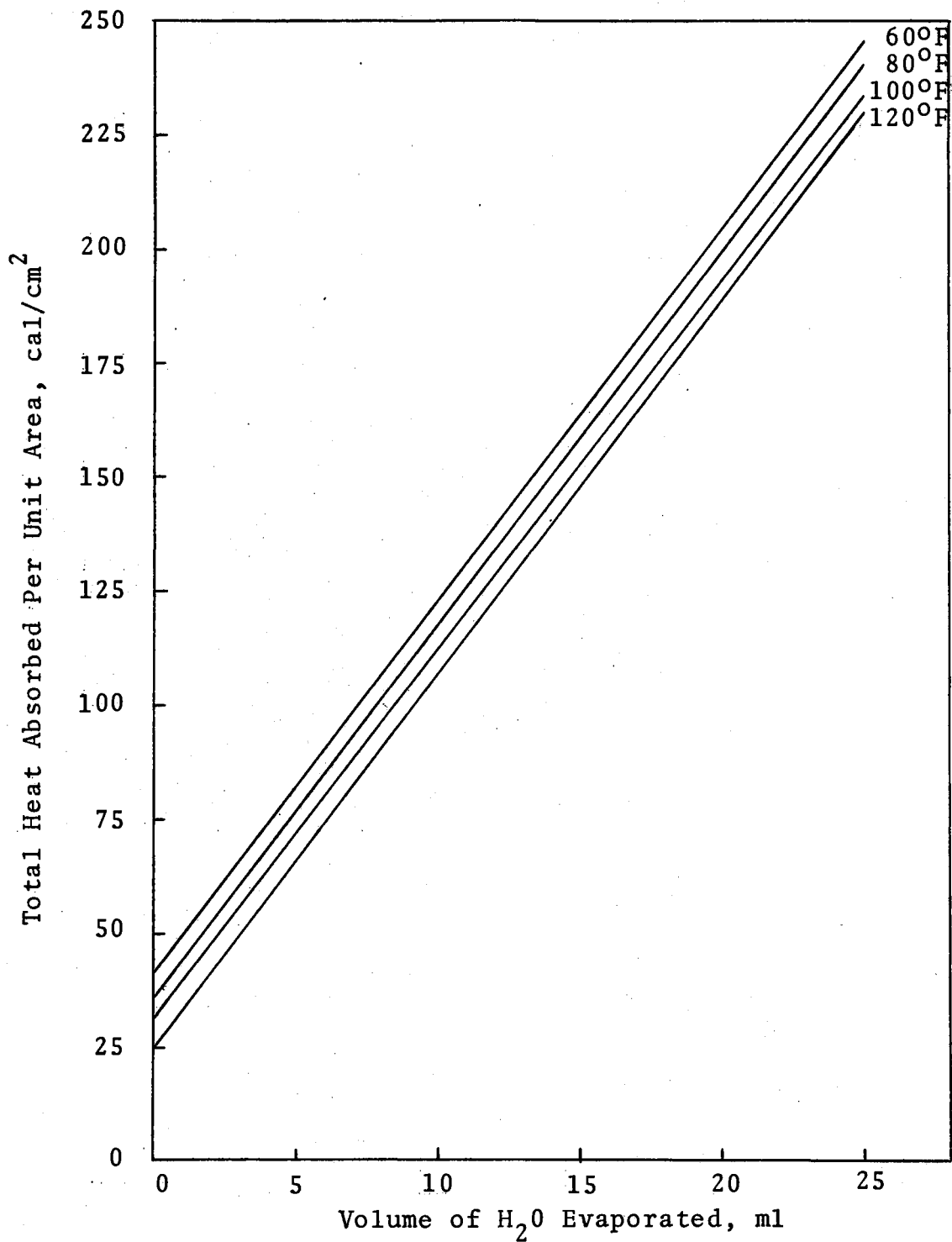
Figure 32. Total Heat Absorbed Per Unit Area for the Copper Dosimeter Containing 25 ml of Water
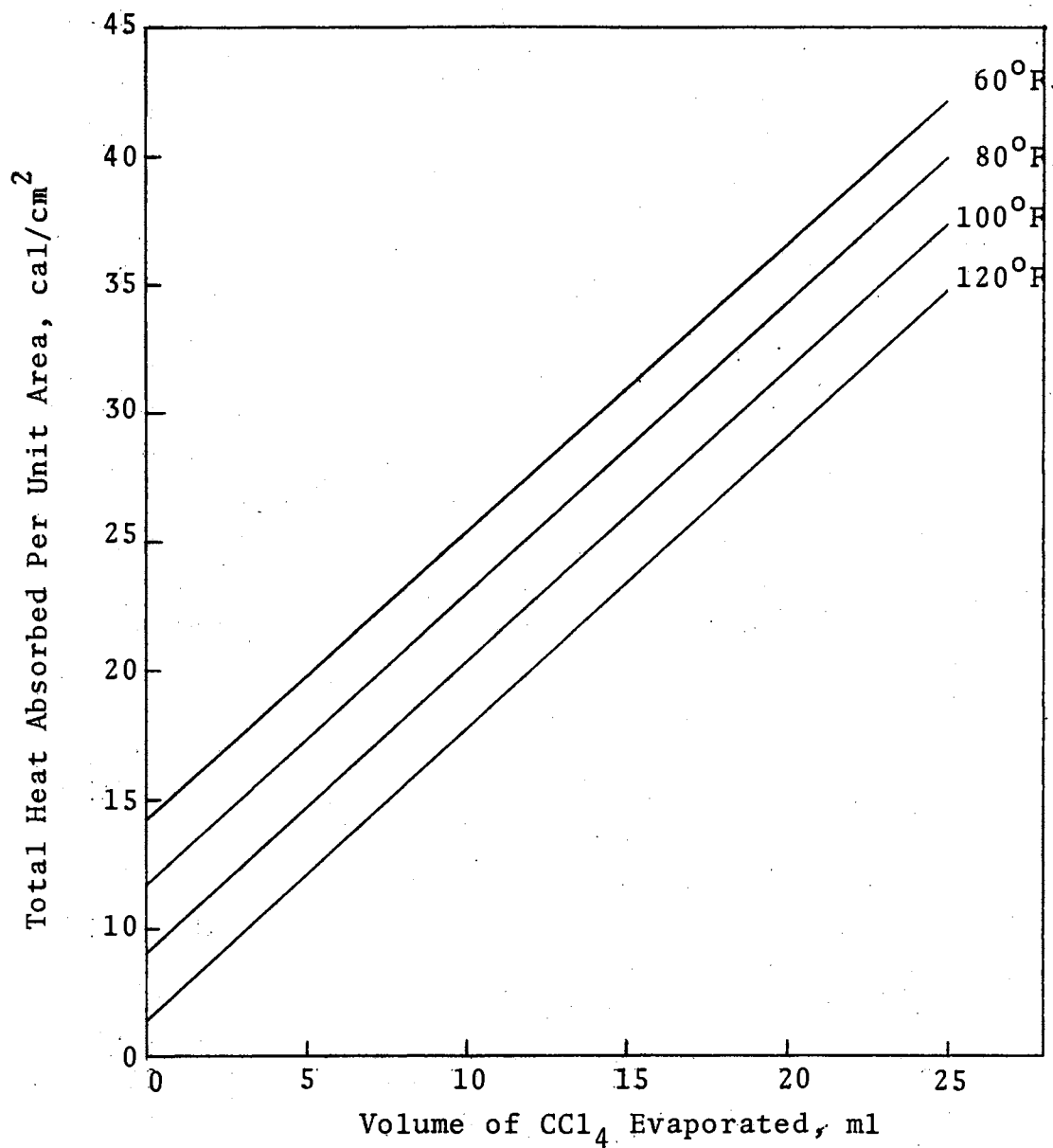
Figure 33. Total Heat Absorbed Per Unit Area For the Copper Dosimeter Containing 25 ml of Carbon Tetrachloride

TOP VIEW

SIDE VIEW

ELEVATION VIEW
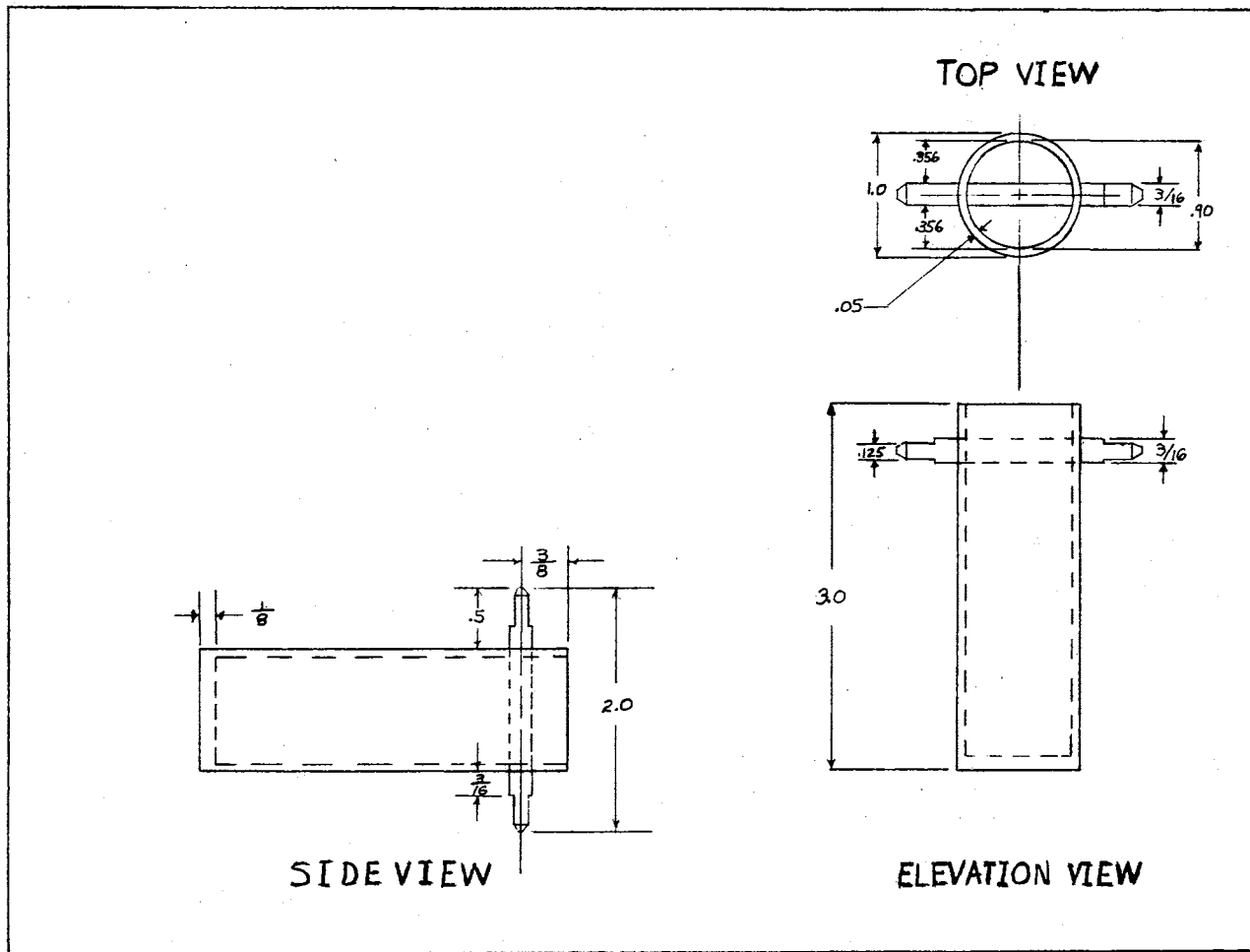
Figure 34. Detailed Dimensioned Drawing of the 25 ml Evaporative
Dosimeter Cup
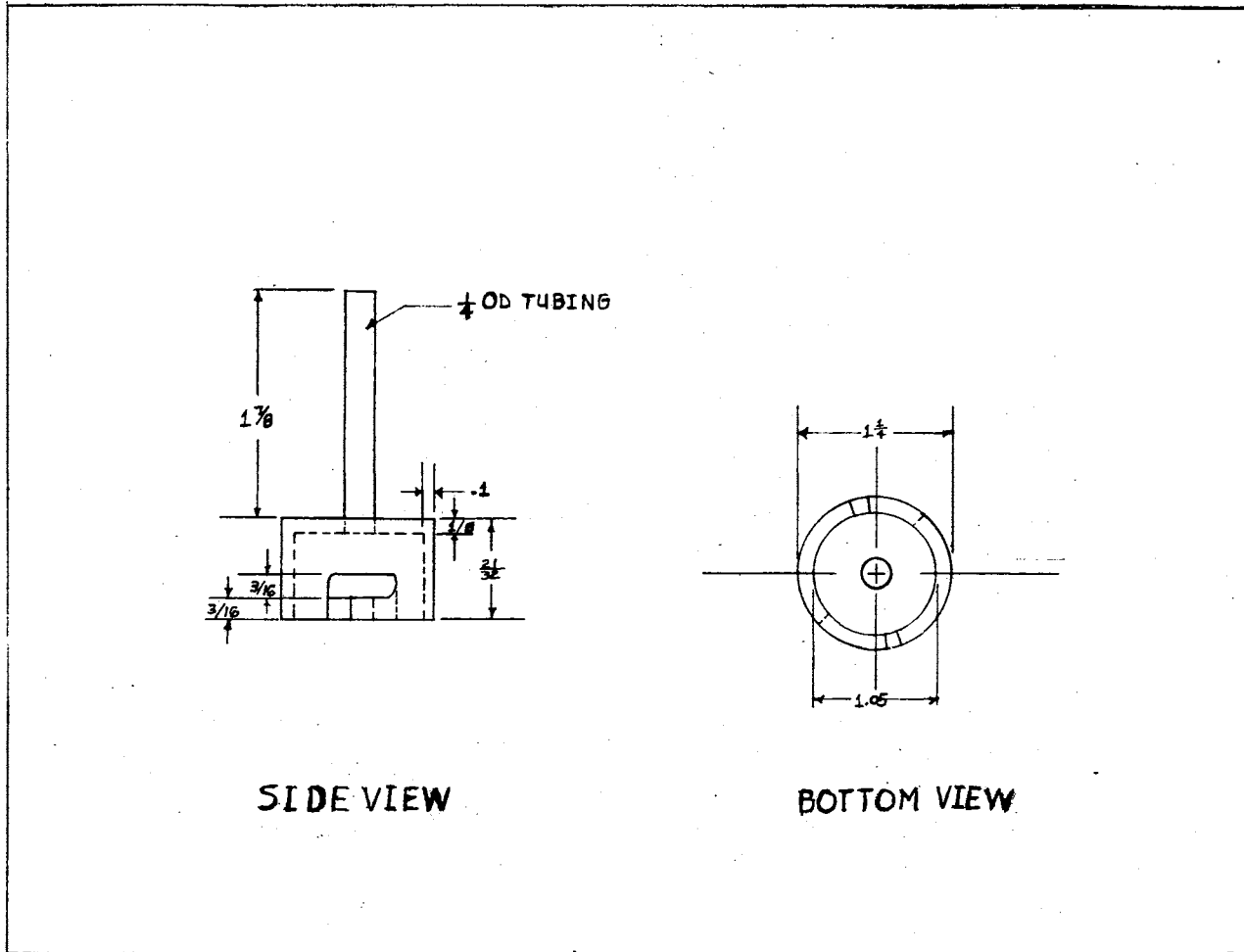
Figure 35. Detailed Dimensioned Drawing of the 25 ml Evaporative Dosimeter Cap

TOP VIEW

SIDE VIEW   FRONT VIEW
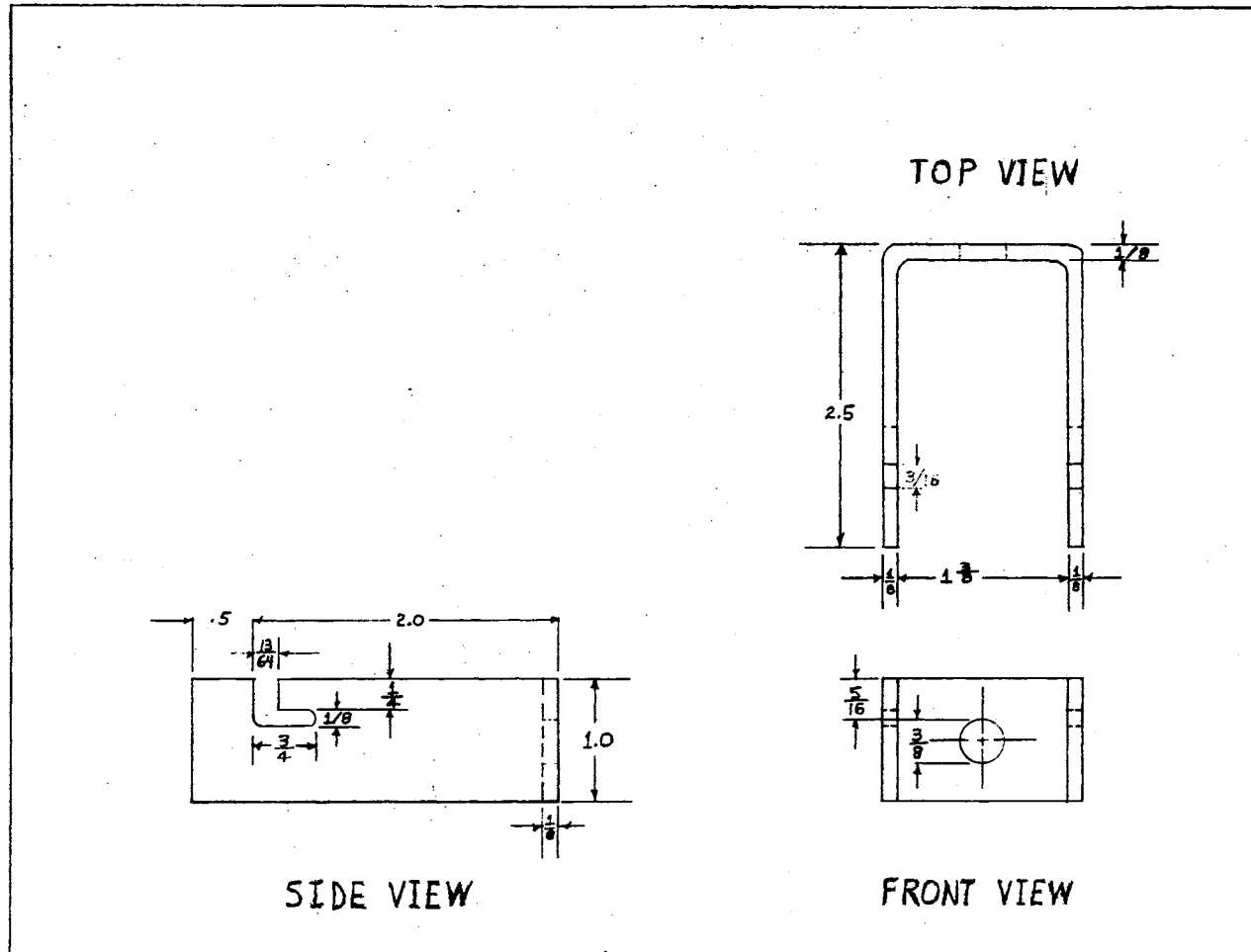
Figure 36. Detailed Dimensioned Drawing of the Hanging Rack for
            the 25 ml Evaporative Dosimeter
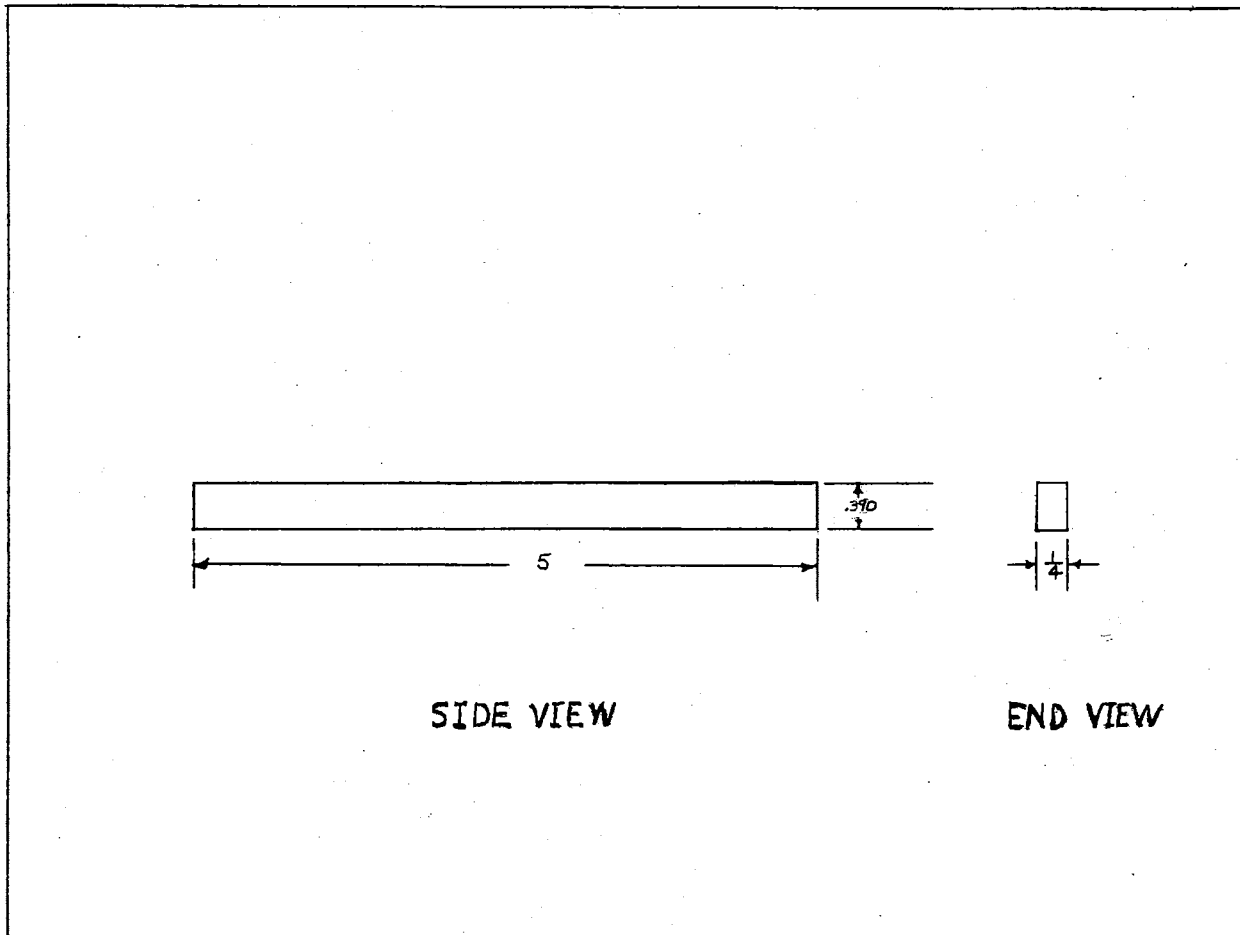
Figure 37.   Detailed Dimensioned Drawing of the Calibration Bar
for the 25 ml Evaporative Dosimeter
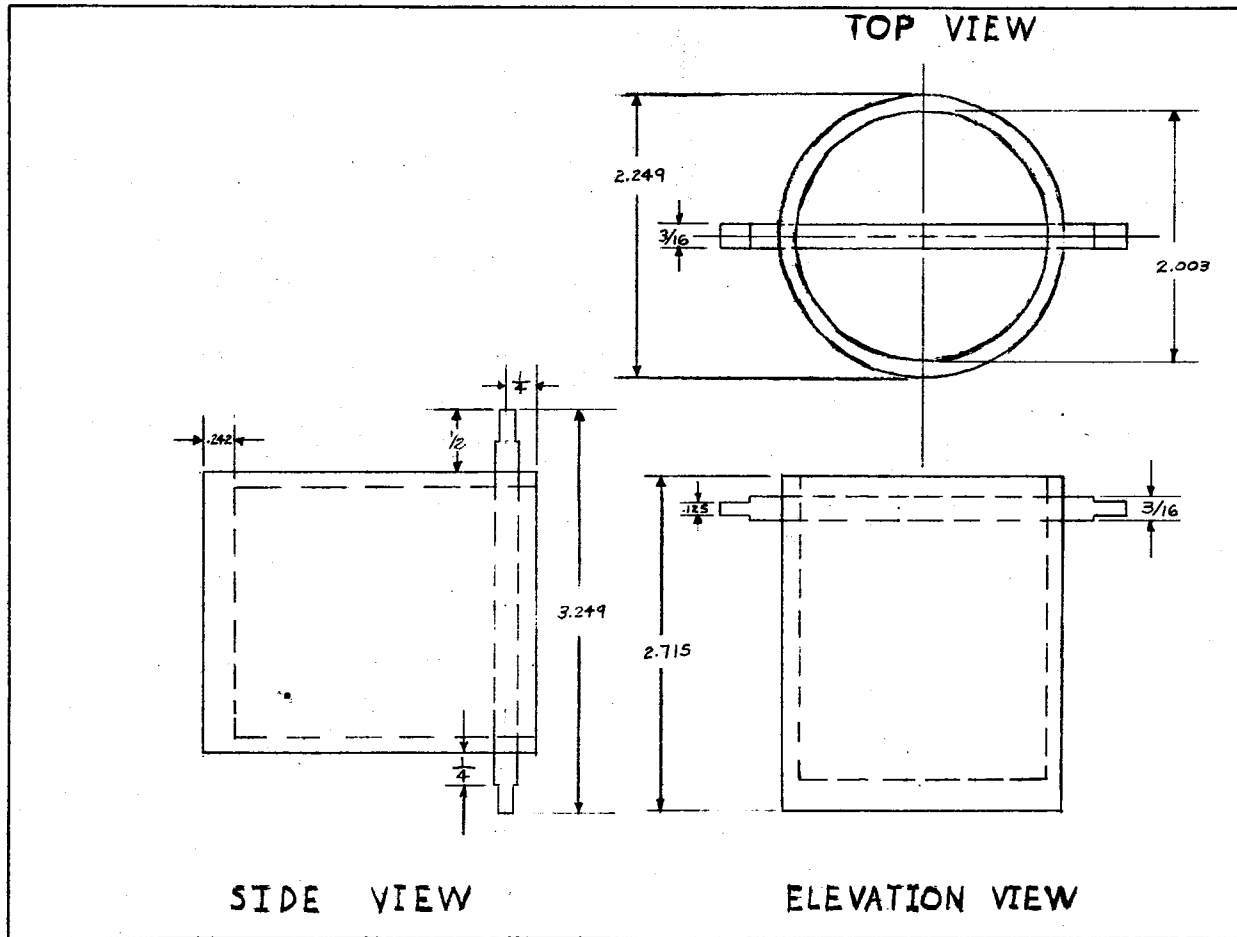
Figure 38. Detailed Dimensioned Drawing of the 100 ml
Evaporative Dosimeter Cup
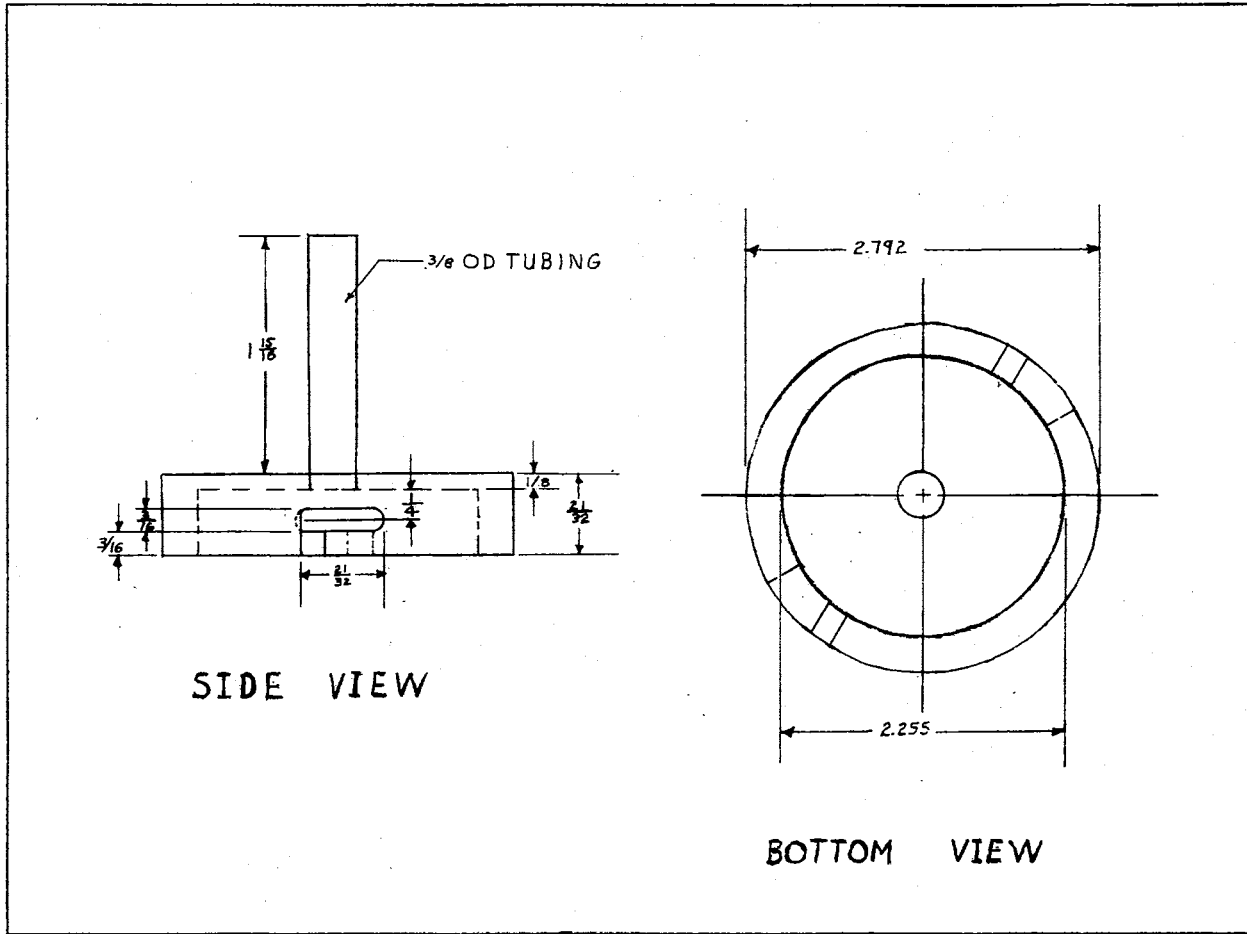
Figure 39. Detailed Dimensioned Drawing of the 100 ml
Evaporative Dosimeter Cap
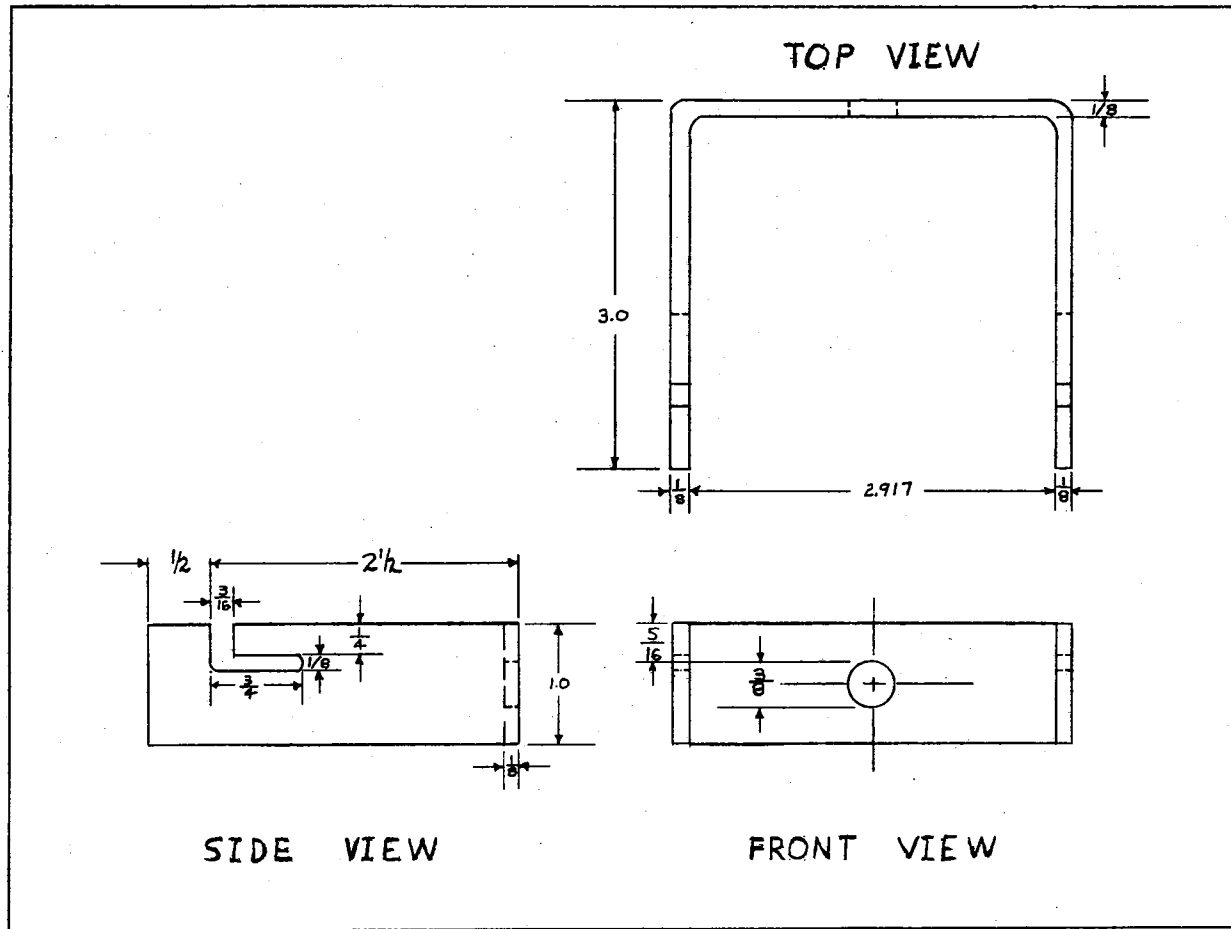
Figure 40.   Detailed Dimensioned Drawing of the Hanging Rack for
the 100 ml Evaporative Dosimeter

TOP VIEW

ROD B WILL BE THREADED
TO SCREW INTO PLATE A.
PLATE A AND RODS C AND D
WILL BE CONNECTED
BY A SCREW THROUGH
PLATE A INTO THE
RODS

ELEVATION VIEW
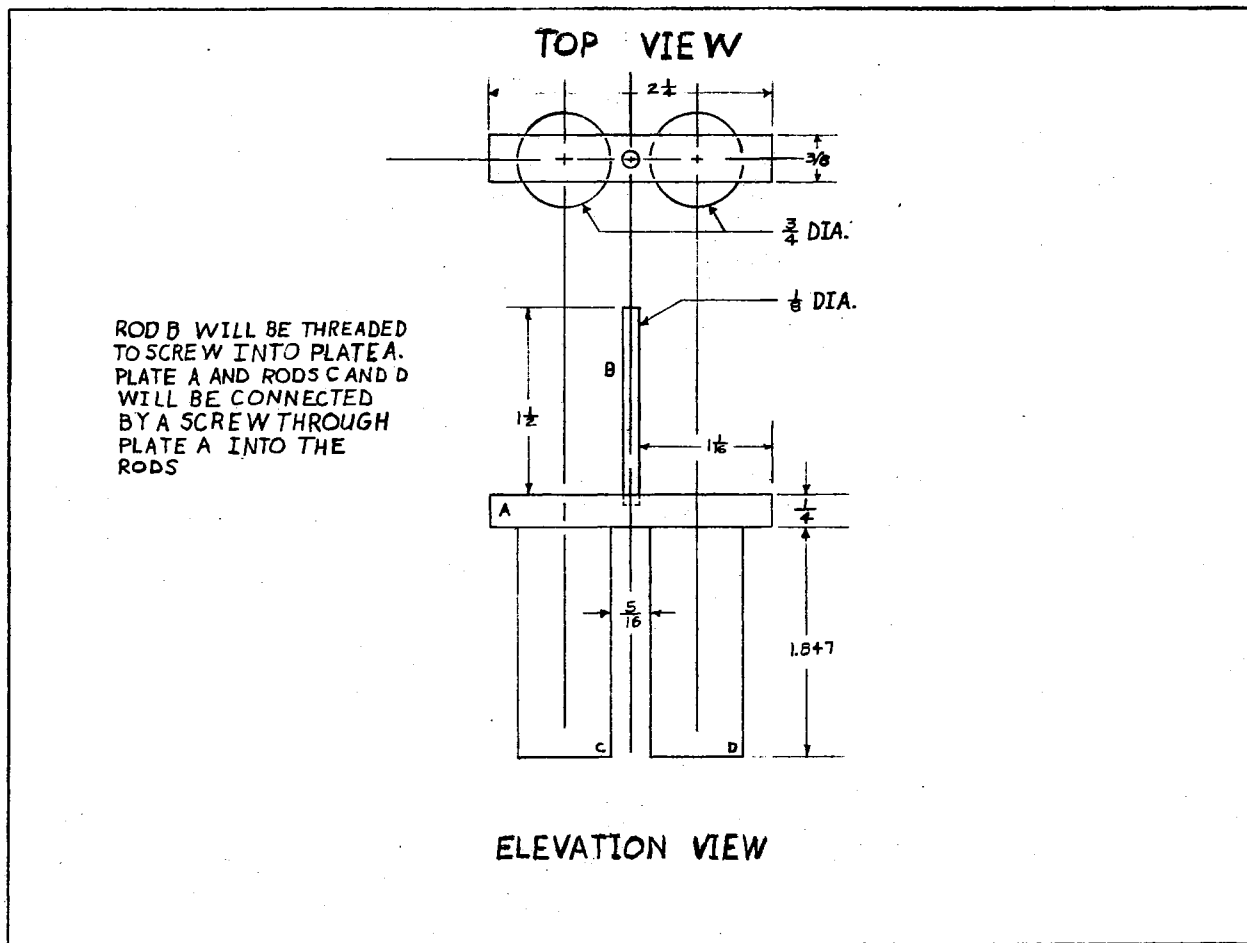
Figure 41. Detailed Dimensioned Drawing of the Calibration
Bar for the 100 ml Evaporative Dosimeter

APPENDIX B

INITIAL DESIGN DRAWINGS FOR THE FUSIBLE-ROD
INTEGRATED-HEAT FLUX METER (MELT STICK
DOSIMETER) AND TABULATED VALUES FROM
THE MELT STICK EXPERIMENT
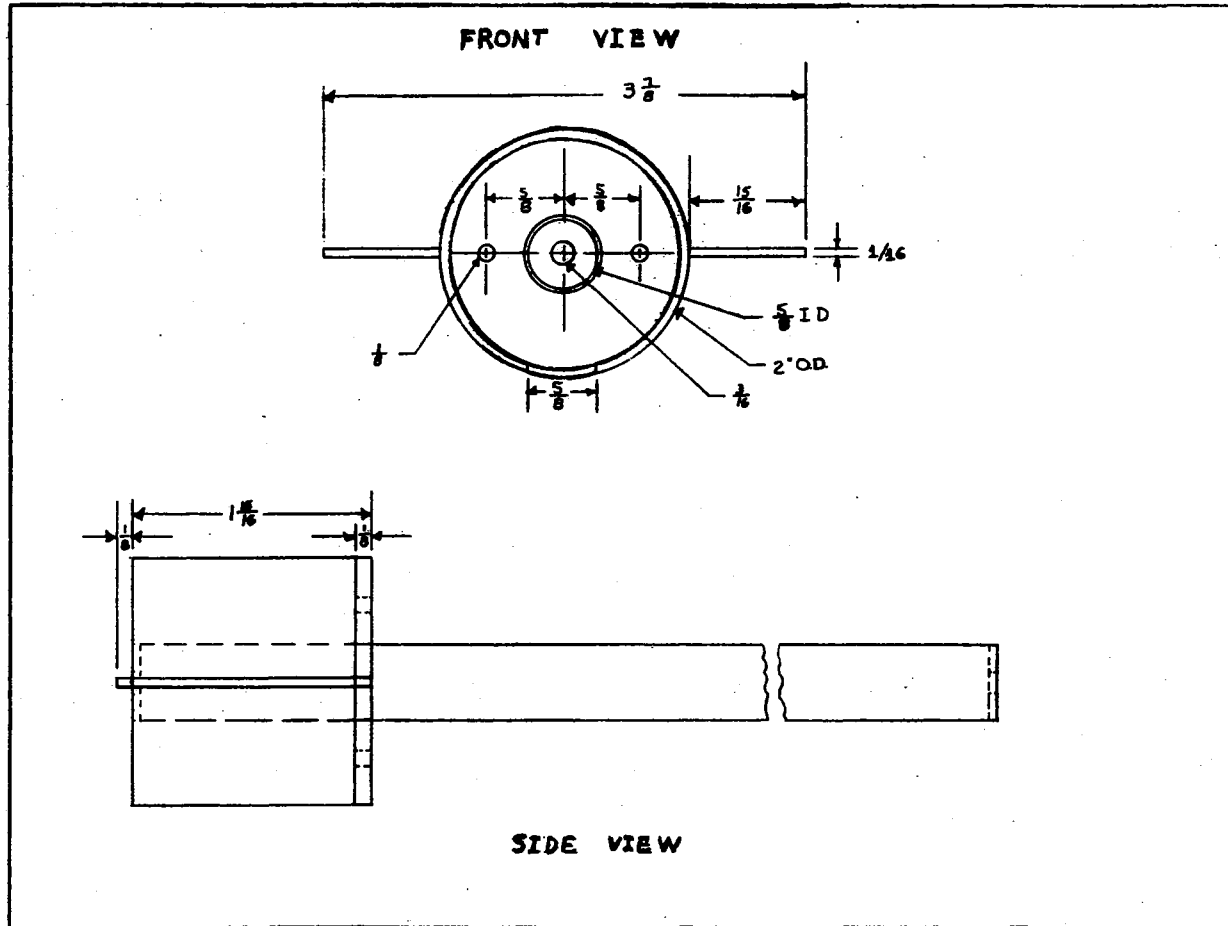
Figure 42.   Detailed Dimensioned Drawing of the Front and Side
         View of the Fusible Rod Containing Tube, and Disk
         and Material Catch Tank Connecting Mechanism
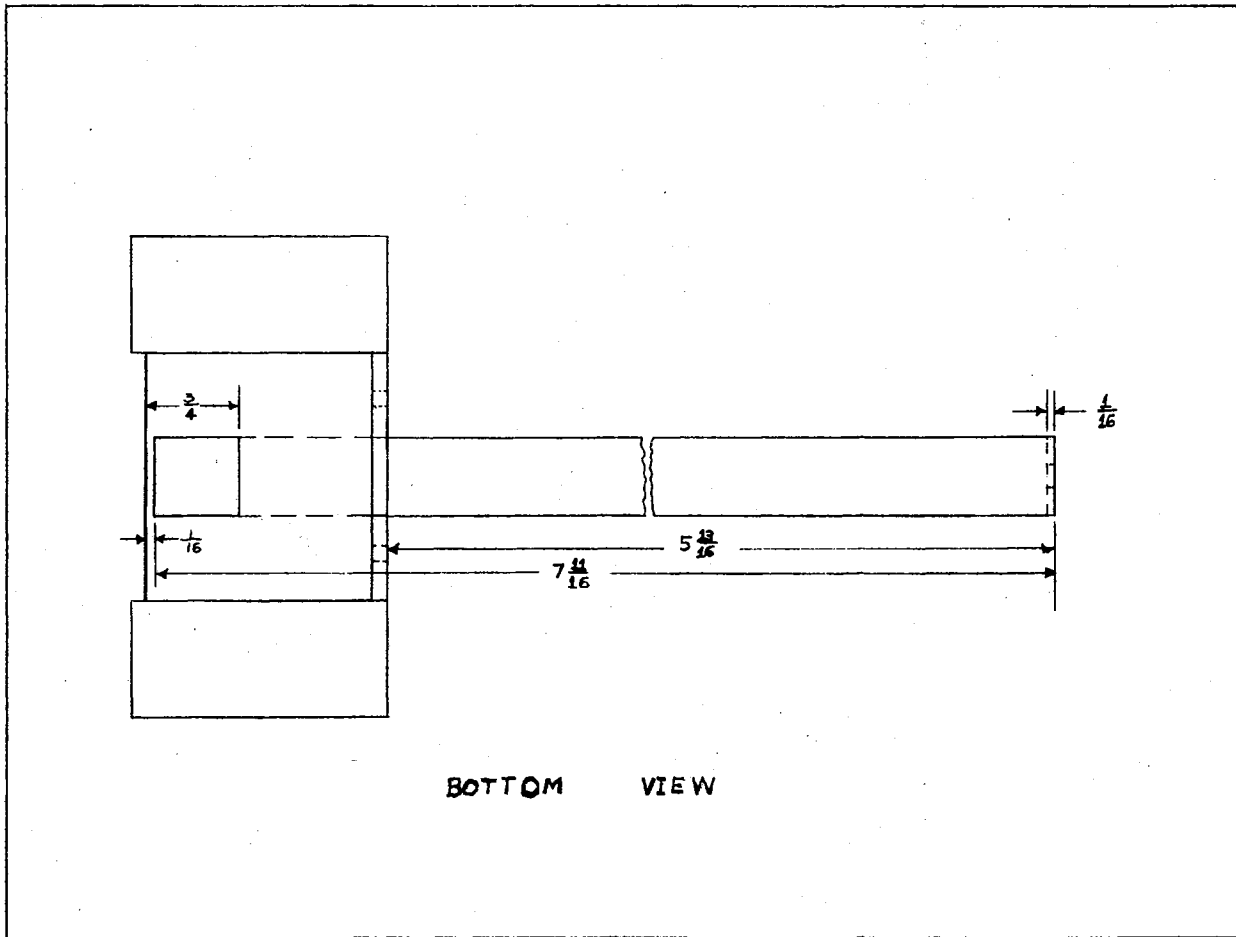
BOTTOM VIEW

Figure 43. Detailed Dimensioned Drawing of the Bottom View of
the Fusible Rod Containing Tube, and the Disk and
Material Catch Tank Connecting Mechanism

FRONT VIEW   SIDE VIEW
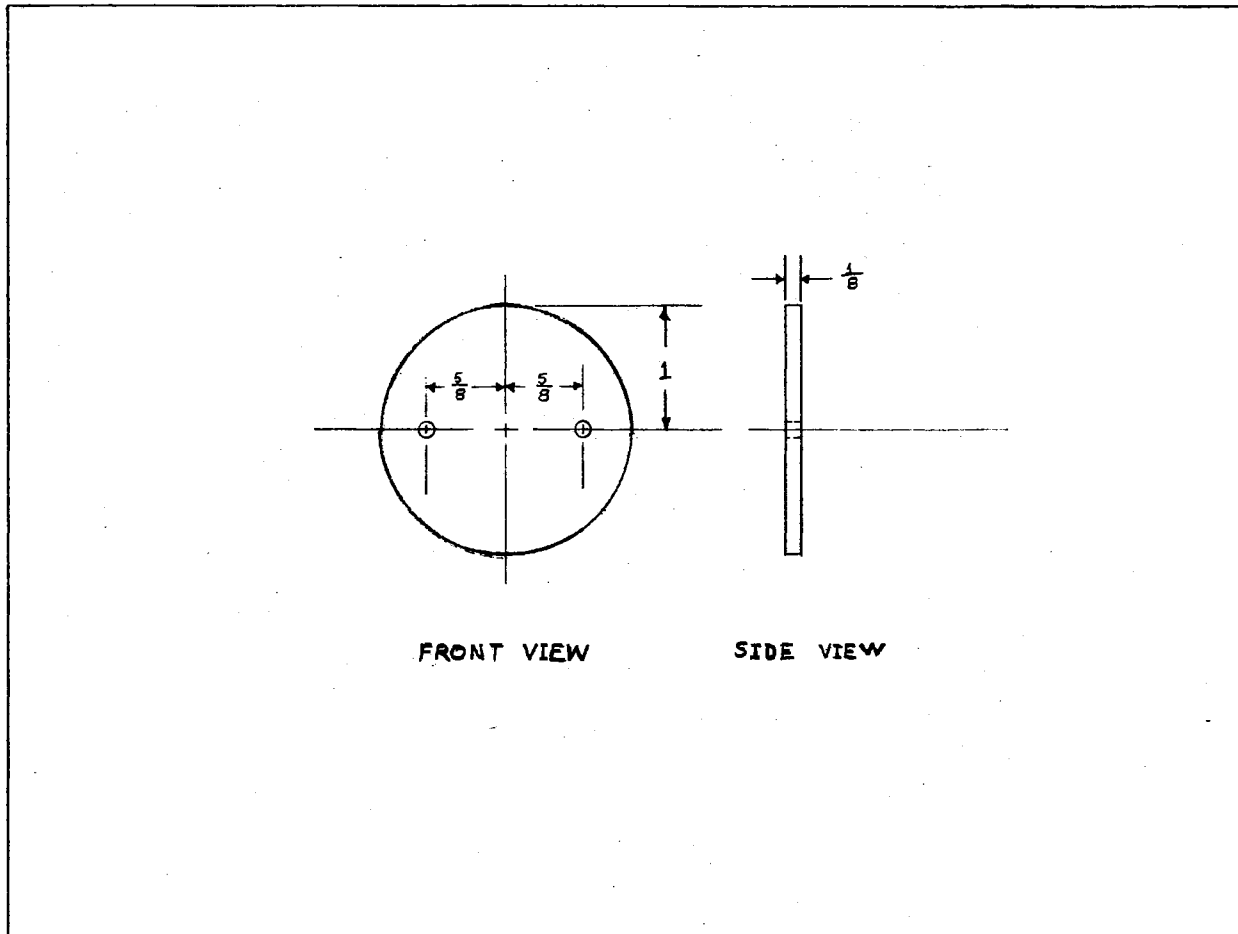
Figure 44.   Detailed Dimensioned Drawing of the Front and Side
             View of the Copper Disk

FRONT VIEW   SIDE VIEW
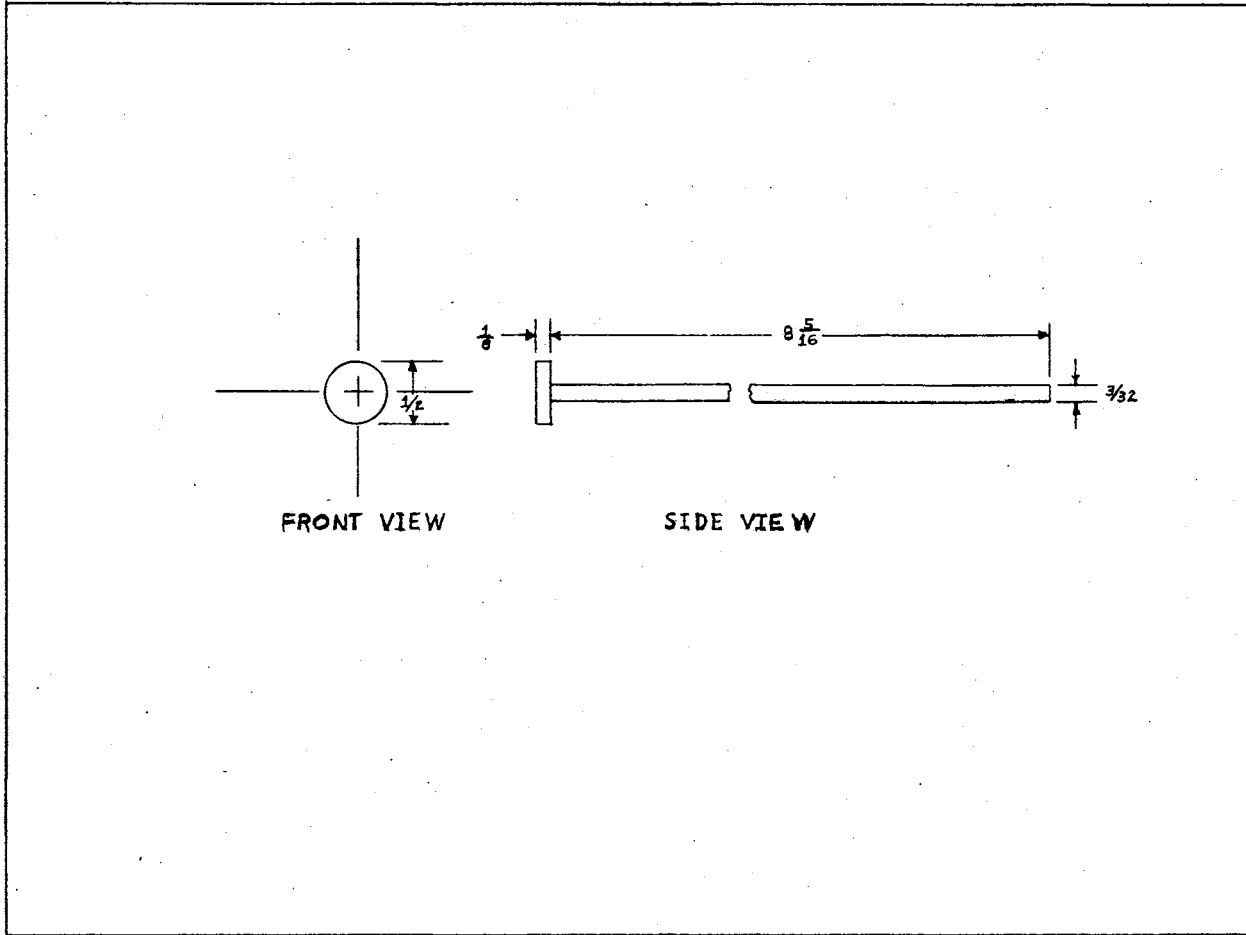
Figure 45.   Detailed Dimensioned Drawing of the Front and Side
             View of the Melt Stick Driving Rod
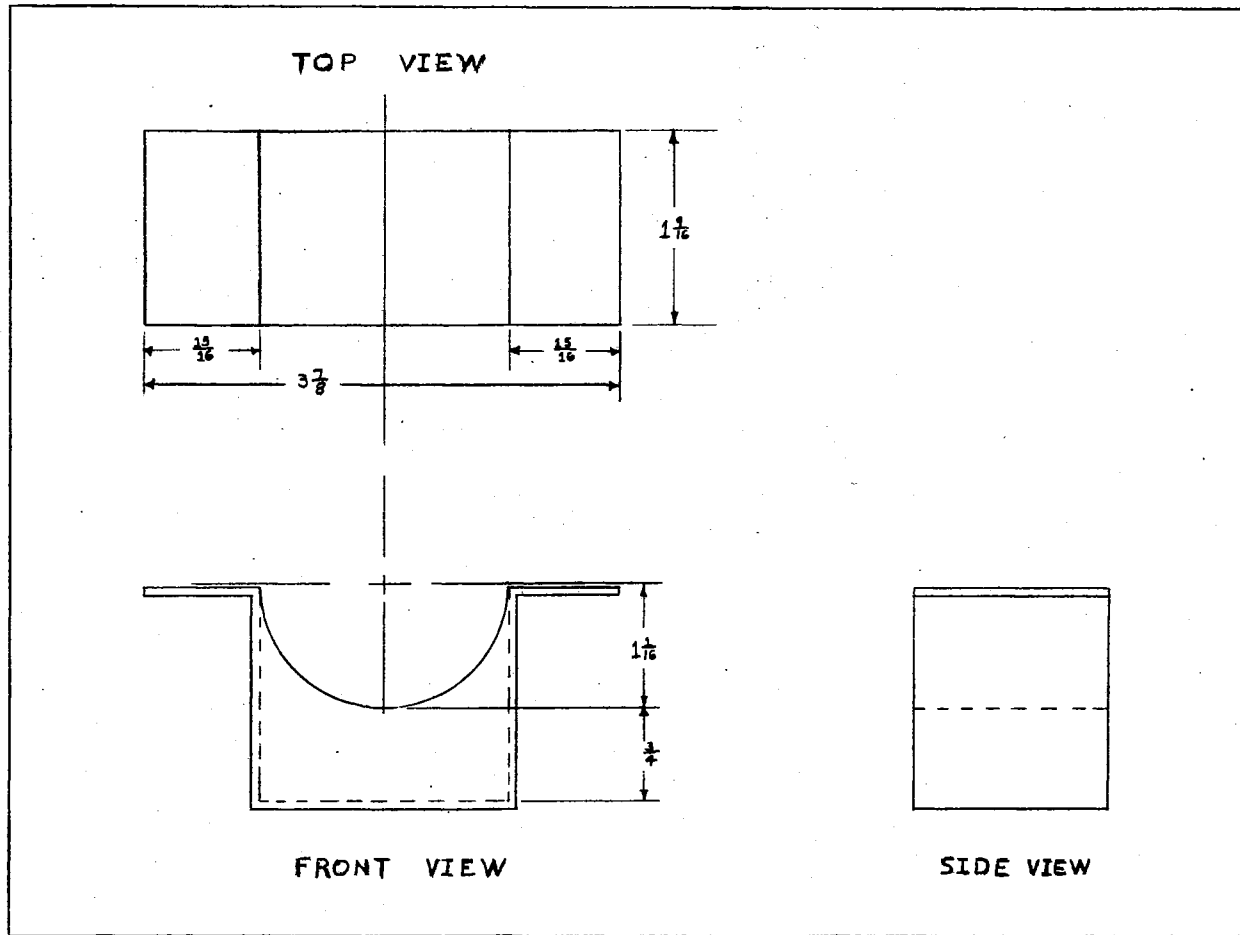
Figure 46. Detailed Dimensioned Drawing of the Material Catch Tank
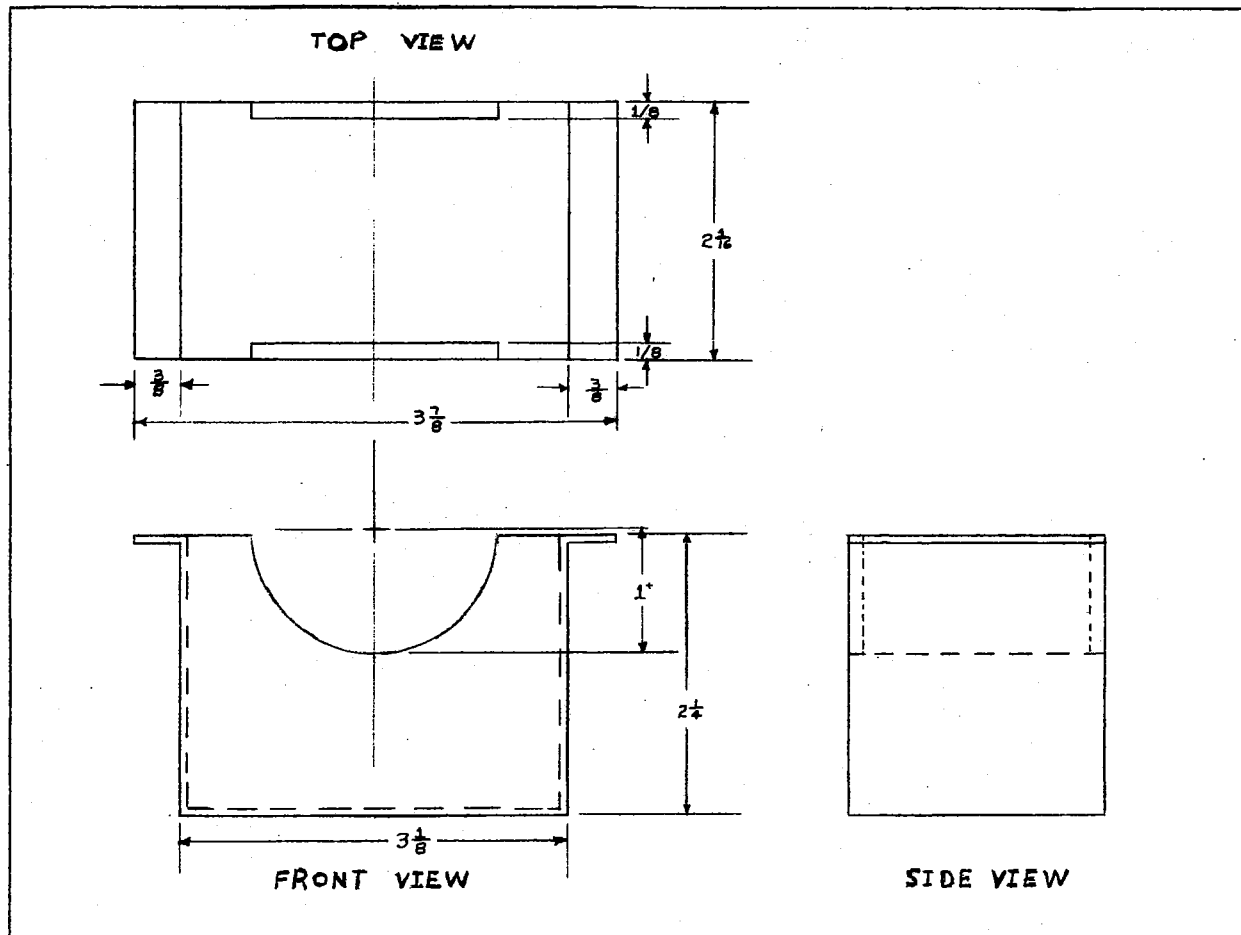
Figure 47. Detailed Dimensioned Drawing of the Outside
Covering of the Material Catch Tank

TOP VIEW

FRONT VIEW

SIDE VIEW
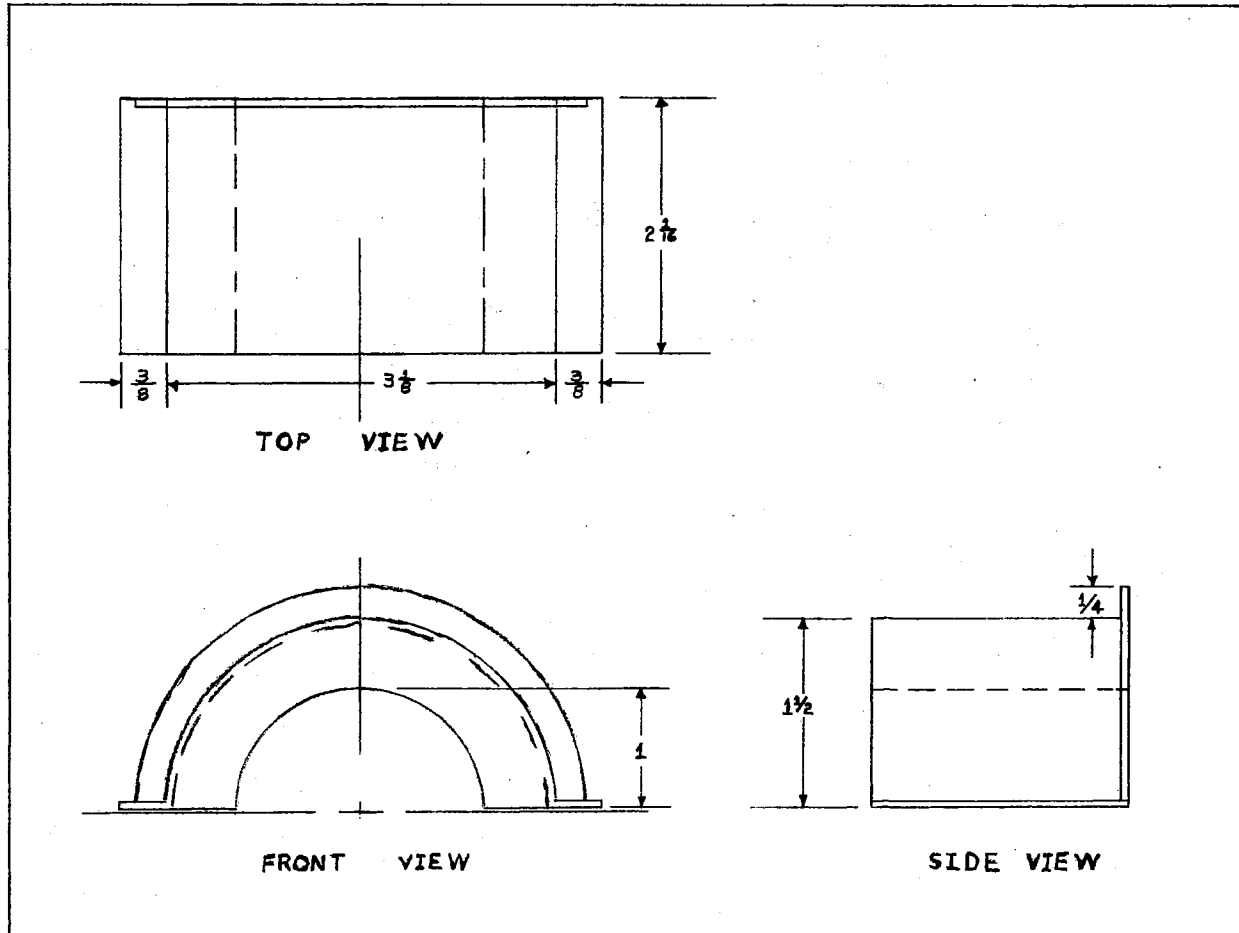
Figure 48.   Detailed Dimensioned Drawing of the Protective Cover
for the 2" OD Steel Tube

FRONT   VIEW   SIDE   VIEW
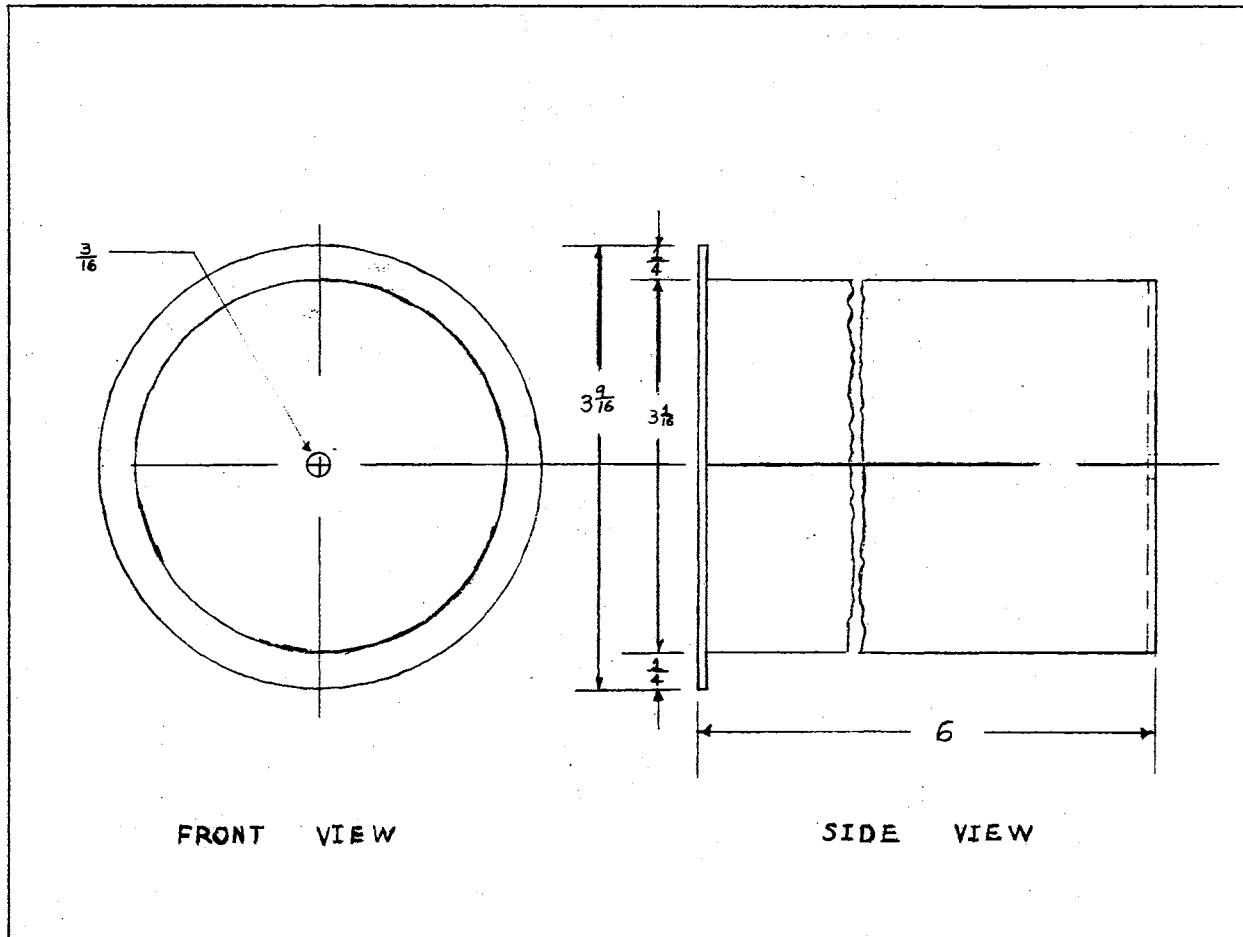
Figure 49.   Detailed Dimensioned Drawing for the Metal Covering
which Protects the Insulation Around the Fusible
Rod Containing Tube
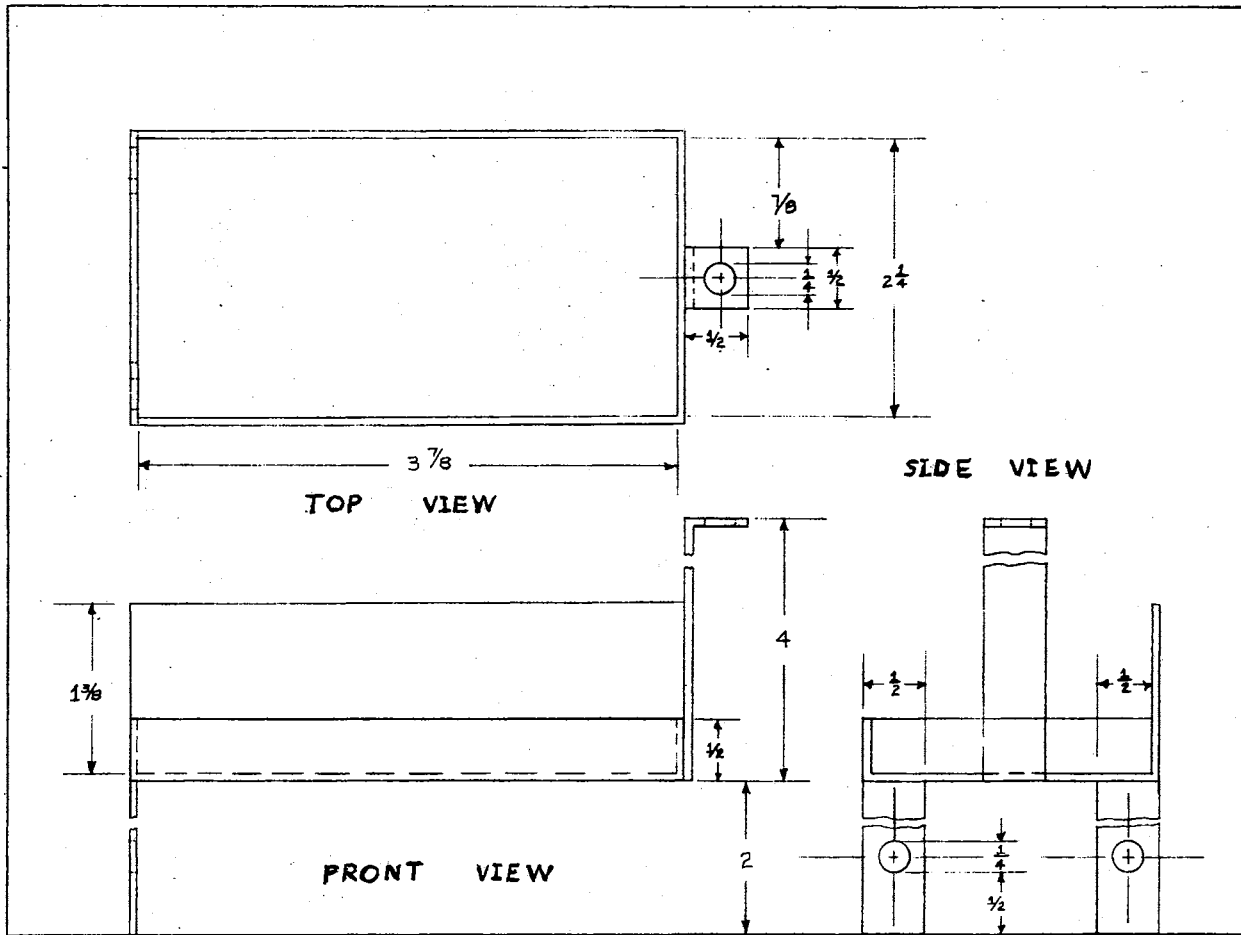
Figure 50. Detailed Dimensioned Drawing of the Major Part of
the Installation Rack
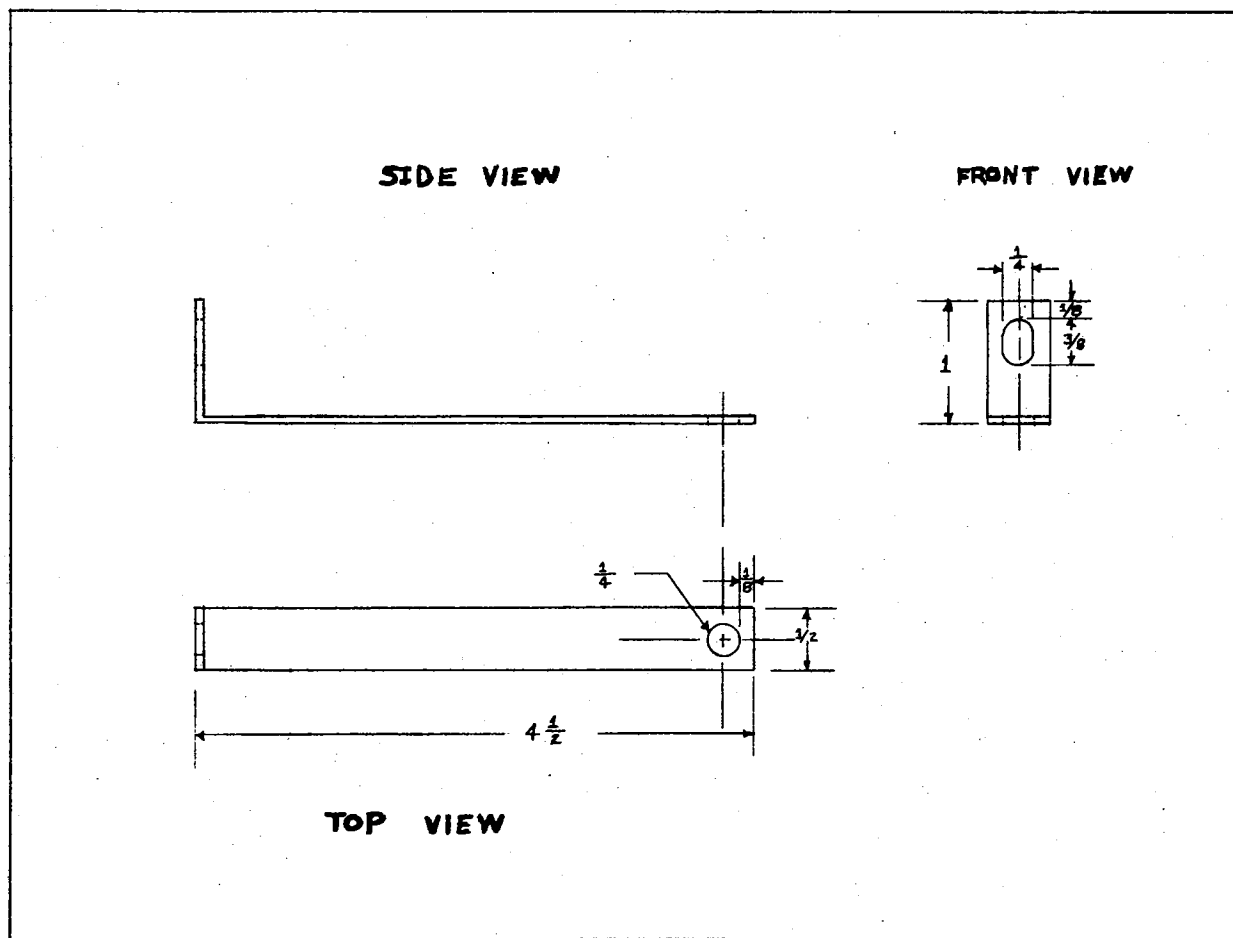
Figure 51. Detailed Dimensioned Drawing of the Bar which
             Prevents the Dosimeter from Falling from the
             Installation Rack

TABLE VII

EXPERIMENTAL AND CALCULATED DATA FOR THE COPPER DISK ON AN ASBESTOS BLOCK

Time sec	Initial Temp $^{\circ}F$	Final Temp $^{\circ}F$	T_s* $^{\circ}F$	ΔT $^{\circ}F$	ΔT $^{\circ}C$	Lamp Rate cal/cm^2	Absorbed Rate cal/cm^2	Lost Convective Rate cal/cm^2	Total Lost Convective Rate cal/cm^2
0									
2.5	87	104	95.5	17	9.44	2.5	2.5	0	0
5.0	104	117	110.5	13	7.22	2.5	1.916	.584	.584
7.5	117	131.5	124.25	14.5	8.06	2.5	2.317	.363	.947
10.0	131.5	147	139.25	15.5	8.61	2.5	2.285	.215	1.162
12.5	147	160	153.5	13	7.22	2.5	1.916	.584	1.746
15.0	160	175	167.5	15	8.33	2.5	2.21	.29	2.036
17.5	175	189	182	14	7.78	2.5	2.063	.437	2.473
20.0	189	204	196.5	15	8.33	2.5	2.21	.29	2.763
22.5	204	218	211	14	7.78	2.5	2.063	.437	3.200
25.0	218	233	225.5	15	8.33	2.5	2.21	.29	3.490
27.5	233	247	240	14	7.78	2.5	2.063	.437	3.927
30.0	247	261	254	14	7.78	2.5	2.063	.437	4.364
32.5	261	275	268	14	7.78	2.5	2.063	.437	4.801
35.0	275	290	282.5	15	8.33	2.5	2.21	.29	5.091
37.5	290	304.5	297.25	14.5	8.06	2.5	2.137	.363	5.454
40.0	304.5	318	311.25	13.5	7.5	2.5	1.99	.51	5.964
42.5	318	330	324	12	6.67	2.5	1.769	.731	6.695

*T_s = average of initial and final temperatures

TABLE VIII

TABULATED VALUES FOR CURVE II OF FIGURE 15

Time sec	Initial Temp °F	Final Temp °F	T*s °F	ΔT °F	ΔT °C
0					
2.5	87	104	95.5	17	9.44
5	104	113	108.5	9	5
7.5	113	125	119	12	6.66
10	125	137.5	131.25	12.5	6.94
12.5	137.5	149	143.25	11.5	6.38
15	149	158	153.5	9	5
17.5	158	167	162.5	9	5
20	167	177	172	10	5.55
22.5	177	186.5	181.75	9.5	5.28
25.0	186.5	194.5	190.5	8	4.44
27.5	194.5	202.5	198.5	8	4.44
30	202.5	210	206.25	7.5	4.17
32.5	210	218	214	8	4.44
35	218	225	221.5	7	3.89
37.5	225	233	229	8	4.44
40	233	240	236.5	7	3.89
42.5	240	247	243.5	7	3.89
45	247	254	250.5	7	3.89
47.5	254	260	257	6	3.33
50	260	266	263	6	3.33
52.5	266	274	270	8	4.44
55	274	280	277	6	3.33
57.5	280	286	283	6	3.33
60	286	291	288.5	5	2.78
62.5	291	297	294	6	3.33
65	297	303	300	6	3.33
67.5	303	309	306	6	3.33
70	309	315	312	6	3.33
72.5	315	320	317.5	5	2.78
75	320	326	323	6	3.33

* T_s = average of initial and final temperatures

TABLE IX

CALCULATED DATA FOR THE REGULAR DOSIMETER ASSEMBLY USING TABULATED
VALUES FROM TABLE VIII AND FIGURE 16

Time sec	Lamp Rate cal/cm^2	Absorbed Rate cal/cm^2	Total Lamp Rate cal/cm^2	Total Absorbed Rate cal/cm^2	Total Convective Rate cal/cm^2	Total Rate by Conduction cal/cm^2	Interval Rate by Conduction cal/cm^2
0							
2.5	2.5	2.5	2.5	2.5	0	0	0
5	2.5	1.3265	5	3.8265	.54	.6335	.6335
7.5	2.5	1.7887	7.5	5.5952	.81	1.0948	.4613
10	2.5	1.8424	10	7.4375	1.04	1.5224	.4276
12.5	2.5	1.695	12.5	9.1325	1.30	2.0675	.5451
15	2.5	1.3265	15	10.459	1.75	2.791	.7235
17.5	2.5	1.3265	17.5	11.7855	1.95	3.7645	.9735
20	2.5	1.474	20	13.2595	2.24	4.5005	.7360
22.5	2.5	1.4002	22.5	14.6597	2.47	5.3668	.8663
25	2.5	1.179	25	15.8387	2.65	6.5113	1.1445
27.5	2.5	1.179	27.5	17.0177	2.85	7.6323	1.121
30	2.5	1.1054	30	18.1231	3.05	8.827	1.1947
32.5	2.5	1.179	32.5	19.3021	3.25	9.948	1.121
35	2.5	1.0317	35	20.3338	3.45	11.216	1.268
37.5	2.5	1.179	37.5	21.5128	3.65	12.337	1.121
40	2.5	1.0317	40	22.5445	3.85	13.6055	1.2685
42.5	2.5	1.0317	42.5	23.5762	4.05	14.8738	1.2683
45	2.5	1.0317	45	24.6079	4.23	16.1621	1.2883
47.5	2.5	.8843	47.5	25.4922	4.4	17.6078	1.4457
50	2.5	.8843	50	26.3765	4.57	19.0535	1.4457
52.5	2.5	1.179	52.5	27.5555	4.87	20.0745	1.021

TABLE IX (Continued)

Time sec	Lamp Rate cal/cm^2	Absorbed Rate cal/cm^2	Total Lamp Rate cal/cm^2	Total Absorbed Rate cal/cm^2	Total Convective Rate cal/cm^2	Total Rate by Conduction cal/cm^2	Interval Rate by Conduction cal/cm^2
55	2.5	.8843	55	28.4398	4.96	21.6002	1.5257
57.5	2.5	.8843	57.5	29.3241	5.11	23.0659	1.4657
60	2.5	.7369	60	30.061	5.21	24.729	1.6631
62.5	2.5	.8843	62.5	30.9453	5.35	26.2047	1.4757
65	2.5	.8843	65	31.8296	5.5	27.6704	1.4657
67.5	2.5	.8843	67.5	32.7139	5.72	29.0661	1.3957
70	2.5	.8843	70	33.598	6.0	30.402	1.3359
72.5	2.5	.7369	72.5	34.3351	6.29	31.875	1.473
75	2.5	.8843	75	35.219	6.85	32.9306	1.0556

TABLE X

CALCULATED HEAT TRANSFER COEFFICIENTS DURING COOLING FOR THE
COPPER DISK ON THE ASBESTOS BLOCK

Time 1 sec	Temp 1 ^{o}F	Time 2 sec	Temp 2 ^{o}F	ΔT ^{o}F	$\Delta T/\Delta \theta$ $^{o}F/sec$	T_{s}^{*} ^{o}F	$T_{s}-T_{\infty}$ ^{o}F	Heat Transfer Coefficient BTU/hr ft$^{2} {}^{o}F$
50	333	60	327	6	.6	330	243	4.831
60	327	70	321	6	.6	324	237	4.953
70	321	80	315	6	.6	318	231	5.082
80	315	90	307	8	.8	311	224	6.987
90	307	100	300	7	.7	303.5	216.5	6.325
100	300	110	294	6	.6	297	210	5.589
110	294	120	287	7	.7	290.5	203.5	6.73
120	287	130	281	6	.6	284	197	5.959
130	281	140	275	6	.6	278	191	6.146
140	275	150	268	7	.7	271.5	184.5	7.423
150	268	160	262	6	.6	265	178	6.594
160	262	170	256	6	.6	259	172	6.825
170	256	180	250	6	.6	253	166	7.071
180	250	190	245	5	.5	247.5	160.5	6.095
190	245	200	240	5	.5	242.5	155.5	6.291
200	240	225	227	13	.52	233.5	146.5	6.944
225	227	250	218	9	.36	222.5	135.5	5.198

* T_{s} = average of initial and final temperatures

TABLE XI

CALCULATED HEAT TRANSFER COEFFICIENTS DURING COOLING FOR THE REGULAR DOSIMETER ASSEMBLY

Time 1 sec	Temp 1 °F	Time 2 sec	Temp 2 °F	ΔT °F	$\Delta T / \Delta \theta$ °F/sec	T_S^* °F	$T_S - T_\infty$ °F	Heat Transfer Coefficient BTU/hr ft^2°F
80	333	90	305	28	2.8	319	232	23.61
90	305	100	282	23	2.3	293.5	206.5	21.79
100	282	110	264	18	1.8	273	186	18.93
110	264	120	248	16	1.6	256	169	18.52
120	248	130	234.5	13.5	1.35	241.25	154.25	17.12
130	234.5	140	223.5	11	1.1	229	142	15.16
140	223.5	150	214	9.5	.95	218.75	131.75	14.11
150	214	160	205	9	.9	209.5	122.5	14.37
160	205	170	197	8	.8	201	114	13.73
170	197	180	190	7	.7	193.5	106.5	12.86
180	190	190	184.5	5.5	.55	187.25	100.25	10.73
190	184.5	200	179	5.5	.55	181.75	94.75	11.36
200	179	210	175	4	.4	177	90	8.69
210	175	220	171	4	.4	173	86	9.10
220	171	230	168	3	.3	169.5	82.5	7.11
230	168	240	165	3	.3	166.5	79.5	7.38
240	166	250	163.5	2.5	.25	164.25	77.25	6.33

* T_S = average of initial and final temperatures

TABLE XII

CALCULATION DATA FOR THE FLUX LOST TO CONDUCTION DURING COOLING
FOR THE REGULAR DOSIMETER ASSEMBLY

Time 1 sec	Time 2 sec	$\Delta Temp/\Delta \theta$ $^\circ$F/sec	Cooling Flux BTU/hr ft^2	$T_s - T_\infty$ $^\circ$F	Convective Flux BTU/hr ft^2	Conduction Flux BTU/hr ft^2	Conduction Flux as % of Cooling Flux
80	90	2.8	5477.85	232	1430.28	4047.57	73.89
90	100	2.3	4499.66	206.5	1273.07	3226.59	71.71
100	110	1.8	3521.48	186	1146.69	2374.79	67.44
110	120	1.6	3130.2	169	1041.89	2088.31	66.72
120	130	1.35	2641.11	154.25	950.95	1690.16	63.99
130	140	1.1	2152.01	142	875.43	1276.58	59.32
140	150	.95	1858.56	131.75	812.24	1046.32	56.30
150	160	.90	1760.74	122.5	755.21	1005.53	57.11
160	170	.80	1565.1	114	702.81	862.29	55.09
170	180	.70	1369.46	106.5	656.57	712.89	52.06
180	190	.55	1076.00	100.25	618.04	457.96	42.56
190	200	.55	1076.00	94.75	584.13	491.87	45.71
200	210	.4	782.55	90	554.85	227.70	29.09
210	220	.4	782.55	86	530.19	252.36	32.25
220	230	.3	586.91	82.5	508.61	78.30	13.34
230	240	.3	586.91	79.5	490.12	96.79	16.49
240	250	.25	489.10	77.25	476.25	112.85	2.63

APPENDIX C

TABLE OF DATA POINTS

TABLE XIII

EXPERIMENTAL TIME VS. TEMPERATURE FOR THE
E-94 PAINT ON A STEEL SURFACE

Run #	Time, Min	Corrected Plate Temp^{o}F	Average Plate Temp^{o}F	Average Oven Test Temp^{o}F
28	1	207		436.5
29	1	190		
30	1	196		
31	1	197	198	
28	2	256		
29	2	240		
30	2	256		
31	2	249	250	
28	3	296		
29	3	280		
30	3	295		
31	3	292	291	
28	4	333		
29	4	316		
30	4	336		
31	4	332	330	
28	5	360		
29	5	344		
30	5	363		
31	5	360	357	
28	5 1/2	370		
29	5 1/2	356		
30	5 1/2	373		
31	5 1/2	370	367	
45	1	199		429
46	1	199		
47	1	202	200	
45	2	250		
46	2	248		
47	2	249	249	
45	3	288		
46	3	288		
47	3	285	287	
45	4	322		
46	4	320		
47	4	318	320	
45	5	348		
46	5	346		
47	5	344	346	
45	6	365		
46	6	365		

TABLE XIII (Continued)

Run #	Time, Min	Corrected Plate Temp°F	Average Plate Temp°F	Average Oven Test Temp°F
47	6	364	365	
32	1	202.3		418.5
33	1	189		
34	1	196.3		
35	1	187	194	
32	2	239		
33	2	237		
34	2	240		
35	2	239	239	
32	3	274		
33	3	274		
34	3	276		
35	3	274	274	
32	4	302		
33	4	304		
34	4	304		
35	4	305	304	
32	5	328		
33	5	331		
34	5	330		
35	5	331	330	
32	6	348		
33	6	351		
34	6	352		
35	6	352	351	
32	7	368		
33	7	365		
34	7	365		
35	7	366	366	

VITA

Michael Holt Nash

Candidate for the Degree of

Master of Science

Thesis: AN EXPERIMENTAL STUDY WITH SIMPLE INSTRUMENTATION
FOR LARGE FIRES

Major Field: Chemical Engineering

Biographical:

Personal Data: Born in Pawhuska, Oklahoma, August 8,
1947, to Oren Russell and Clara H. Nash.

Education: Graduated from Pawhuska High School,
Pawhuska, Oklahoma, in May 1965; received the
degree of Bachelor of Science in Chemical
Engineering at Oklahoma State University,
Stillwater, Oklahoma, in January, 1970; completed
requirements for the Master of Science Degree in
Chemical Engineering at Oklahoma State University
in July, 1972; completed requirements for the
Master of Business Administration at Oklahoma
State University in July, 1972.

Professional Experience: Employed by Pan American
Petroleum Corporation, Oklahoma City, Oklahoma,
as a petroleum engineer during the summer of 1969;
employed by Union Carbide Corporation, Houston,
Texas, during the summer of 1970 as a process
engineer.

Membership in Scholarly or Professional Societies:
Beta Gamma Sigma, Phi Eta Sigma, Sigma Tau,
Omega Chi Epsilon, and an Affiliate member of the
American Institute of Chemical Engineers.